National Technical University of Athens
School of Naval Architecture & Marine Engineering

Diploma Thesis

Elastohydrodynamic Analysis and Comparative Study of Oil and Water Lubricated Marine Journal Bearings

Georgios Branikas

Examination Committee Members:
Supervisor: Christos I. Papadopoulos, Associate Professor NTUA
Lambros Kaiktsis, Professor NTUA
George Papalambrou, Associate Professor NTUA

Athens, 2023

Εθνικό Μετσόβιο Πολυτεχνείο
Σχολή Ναυπηγών Μηχανολόγων Μηχανικών

Διπλωματική Εργασία

Ελαστοϋδροδυναμική Ανάλυση και Συγκριτική Μελέτη Ναυτικών Ακτινικών Εδράνων Λιπασμένα με Λάδι και Νερό

Γεώργιος Μπρανίκας

Μέλη Εξεταστικής Επιτροπής
Επιβλέπων: Χρήστος Ι. Παπαδόπουλος, Αναπληρωτής Καθηγητής ΕΜΠ
Λάμπρος Καϊκτσής, Καθηγητής ΕΜΠ
Γεώργιος Παπαλάμπρου, Αναπληρωτής Καθηγητής ΕΜΠ

Αθήνα, 2023

Contents

List of Figures

List of Tables

Acknowledgments

The completion of my Diploma Thesis leads to my graduation from the School of Naval Architecture and Marine Engineering of NTUA and I would like to express my appreciation to everyone whose support strengthened my efforts.

Words cannot express my gratitude to my professor and supervisor, Dr. Christos Papadopoulos, for being an excellent educator and mentor, and offering me all the necessary guidance and tools to complete the present thesis. I am also grateful to all my professors and faculty members who generously provided knowledge and expertise during my studies at NTUA. Also, I would like to thank Georgios Rossopoulos, PhD candidate, for his help, insight and excellent collaboration during this project. Thanks should also go to my classmates and friends for their help, support and all the unforgettable memories.

Lastly, I would be remiss in not mentioning my family, my parents, and brother. Their support during all the years of my studies is invaluable. Their belief in me has kept my spirits and motivation high throughout this effort.

Abstract

Mechanical systems, designed to transfer energy or transform one form of energy to another in order to perform work, can be traced back to ancient civilisations. Engineers throughout history aim to achieve technological advancements, perfecting the operation of machines and augmenting their efficiency. In mechanical systems friction is a primary cause of energy loss. The successful, efficient and safe operation of modern ships requires the operation of a series of mechanical systems, one of the main being the propulsion system, where substantial friction losses arise. An integral part of the propulsion system is the shafting arrangement, where hydrodynamic journal bearings are crucial components. The operation of the propulsion plants and the consequent rotation of the shafts require the support of radial loads from journal bearings. This is accomplished with the development of a thin lubricant film between the shaft and the journal bearing bush liner. The hydrodynamic film supports the shaft weights avoiding metal to metal contact, thus contributing to significant reduction of friction forces and material wear. Furthermore, a major part of the shafting arrangement is the stern tube bearing system which supports the weight of the tail shaft as well as that of the overhang propeller and the transient hydrodynamic loads which arise from its operation.

The present Diploma Thesis investigates the operation of marine hydrodynamic oil and water lubricated journal bearings using computational tools developed at the Division of Marine Engineering, Machine Elements and Tribology Lab of NTUA. In particular, an in-house solver is utilised to perform numerical simulations of bearings, by solving the well known Reynolds differential equation. The existing algorithm is extended, using a plane strain hypothesis model, to include the deformation of the bush liner of the bearings simulated. Essential part of the present study is the validation of the extended model. This process requires data derived from appropriate experimental studies, and needs to be carried out for both water and oil lubricated bearings. Hydrodynamic lubrication in the lubricant domain between the shaft and the bearing bush corresponds to a calculated pressure field which is compared with experimental measurements. Subsequent to the validation process is the investigation of the effect of the extension to the simulations' results. In order to highlight this effect, the operation of bearings with different liner configurations and under a series of shaft rotational speeds is simulated and appropriate comparisons are presented.

The validated extended algorithm is utilized for the simulation of two stern tube bearing systems. Two pairs of journal bearings, one pair of oil lubricated bearings and one water lubricated, each pair consisting of the aft and the forward bearing of a ship, are modeled and simulated. The geometrical and operational parameters are set in accordance with relevant regulations and requirements, as well as engineering manuals of commercial makers and actual ships. The simulations are carried out for an array of operating conditions in order to gain insight on the differences, the similarities and the overall performance of the systems.

Σύνοψη

Μηχανικά συστήματα, σχεδιασμένα να μεταφέρουν ή να μετατρέπουν ενέργεια από μία μορφή σε άλλη για την παραγωγή έργου, μπορούν να εντοπιστούν από την αρχαιότητα. Ιστορικά οι μηχανικοί στοχεύουν στην δημιουργία τεχνολογικών επιτευγμάτων, στην τελειοποίηση μηχανών και στην βελτίωση της αποδοτικότητας τους. Σε μηχανικά συστήματα η τριβή αποτελεί πρωτεύοντα λόγο απώλειας ενέργειας. Η επιτυχημένη, αποδοτική και ασφαλής λειτουργία των σύγχρονων πλοίων απαιτεί τη λειτουργία μίας σειράς από μηχανικά συστήματα, εκ τα οποία ένα από τα βασικότερα είναι το σύστημα πρόωσης, όπου προκαλούνται σημαντικές απώλειες τριβής. Ένα κύριο μέρος του συστήματος πρόωσης είναι το αξονικό σύστημα, όπου υδροδυναμικά ακτινικά έδρανα εκτελούν ρόλο υψηλής σημασίας. Καθώς, η λειτουργία των εγκαταστάσεων πρόωσης και η συνδεδεμένη περιστροφή των αξόνων απαιτούν τη στήριξη φορτίων από έδρανα. Αυτό επιτυγχάνεται με την ανάπτυξη ενός λεπτού λιπαντικού φιλμ μεταξύ του άξονα και του εδράνου. Το υδροδυναμικό φιλμ συμβάλλει στην σημαντική και απαραίτητη μείωση των δυνάμεων τριβής και φθοράς υλικού. Επίσης, ένα βασικό μέρος του αξονικού συστήματος είναι τα έδρανα χοάνης πλοίου που υποστηρίζει το βάρος του άξονα, της προπέλας καθώς και τα μεταφερόμενα από τη λειτουργία φορτία.

Η παρούσα διπλωματική εργασία ερευνά τη λειτουργία ναυτικών υδροδυναμικών ακτινικών εδράνων που λιπαίνονται με λάδι και νερό, χρησιμοποιώντας εργαλεία που έχουν παραχθεί στο Εργαστήριο Στοιχείων Μηχανών και Τριβολογίας του Τομέα Ναυτικής Μηχανολογίας του Ε.Μ.Π. Συγκεκριμένα, χρησιμοποιώντας επιλυτή του εργαστηρίου εκτελέστηκαν αριθμητικές προσομοιώσεις με βάση τη λύση της γνωστής διαφορικής εξίσωσης Reynolds. Ο υπάρχων αλγόριθμος επεκτείνεται, με τη χρήση ενός μοντέλου υπόθεσης τάσης-παραμόρφωσης πεδίου, ώστε να συμπεριλάβει την παραμόρφωση του χιτωνίου των μοντελοποιημένων τριβέων. Βασικό κομμάτι της μελέτης αποτελεί η επικύρωση του επεκταμένου μοντέλου. Η διαδικασία αυτή απαιτεί δεδομένα προερχόμενα από κατάλληλες πειραματικές μελέτες, και χρειάζεται να εκτελεστεί για έδρανα που χρησιμοποιούν ως λιπαντικό μέσο νερό αλλά και για έδρανα λαδιού. Η υδροδυναμική λίπανση στο πεδίο μεταξύ άξονα και χιτωνίου αντιστοιχεί σε υπολογιζόμενο πεδίο πίεσης, το οποίο συγκρίνεται με πειραματικές μετρήσεις. Επακόλουθη στη διαδικασία επικύρωσης είναι η μελέτη της επιρροής της επέκτασης στο αποτελέσματα των μοντελοποιήσεων. Προκειμένου να διαφωτιστεί αυτή η επιρροή, μοντελοποιείται η λειτουργία εδράνων με διαφορετικές σχεδιάσεις χιτωνίων και κάτω από διαφορετικές ταχύτητες περιστροφής, και πραγματοποιούνται κατάλληλες συγκρίσεις.

Ο επικυρωμένος αλγόριθμος χρησιμοποιείται για τη μοντελοποίηση δύο συστημάτων εδράνων χοάνης πλοίου. Δύο ζευγάρια ακτινικών εδράνων, ένα ζευγάρι λαδιού και ένα νερού, κάθε ζευγάρι αποτελούμενο από το πρυμναίου και το πρωραίο έδρανο, σχεδιάζονται και μοντελοποιούνται. Οι σχεδιαστικοί και λειτουργικοί παράγοντες καθορίζονται σύμφωνα με σχετικούς κανονισμούς και απαιτήσεις, καθώς και μηχανολογικούς οδηγούς κατασκευαστών και πραγματικές εφαρμογές πλοίων. Οι μοντελοποιήσεις ολοκληρώνονται για μια σείρα λειτουγικών καταστάσεων ώστε να σχηματισθεί πληρέστερη εικόνα σχετικά με τις διαφορές, τις ομοιότητες και τη γενική συμπεριφορά των συστημάτων.

Introduction

The power required for the propulsion of a marine vessel is generated form its main engine, and transmitted to the propeller causing its rotation and subsequently the flow of water. Ship navigation is achieved as a result of the total induced force and the operation of the steering gear. Crucial to this procedure, described above in a simplified manner, is the shafting system. The axis of the propeller transmits the power and receives the axial driving force, journal bearings (stern tube, line and crankshaft bearings) are required for the support of radial shaft loads, while the main engine thrust bearing transmits axial loads to the ship's structure.

Through the years, the demands of the maritime industry and engineering breakthroughs have led to the increase of power density in marine propulsion plants. From a machine design standpoint, increased power capabilities translate to higher loads. Hydrodynamic journal bearings are components integral to smooth power transmission, as they are designed to carry loads in different operating conditions. In shipbuilding, the role of journal bearings is critical to the synergy of the stiff shafting system and the flexible hull structure, while their operation needs to be efficient from a mechanical and an economical aspect. Therefore, it is useful and constructive to assess the operating characteristics and performance parameters of hydrodynamic journal bearings by experimental or computational means. The main function of these mechanical elements is to offer support through a thin film of lubricant generated between the sliding surfaces and at the same time minimize friction and wear. In tribological analysis, hydrodynamic lubrication theory is employed in order to mathematically describe and calculate with high accuracy the operating behavior of journal bearings. Models and software packages can be utilized to predict the key parameters of journal bearing tribological behavior under different operating conditions, to facilitate the material or lubricant selection process and test possible new technological improvements. Depending on a series of factors, such as required accuracy, calculation time, computational power, study stage and researcher proficiency, different methods and tools can be used.

During the last decades, various studies have been published regarding hydrodynamic journal bearings, this accumulation of scientific data has led to progress in their tribological behavior and operating performance. At the same time, demands for economic and environmental efficiency in the maritime industry keep growing, conforming with goals and regulations set by the United Nations and International Maritime Organization. Moreover, IMO has adopted measures to reduce emissions of greenhouse gases from international shipping by 50% by 2050 compared to 2008 levels. Additionally, a follow-up program has been approved, its focus is on blueprinting mechanisms aiming to reduce the carbon intensity of the maritime industry. Sustainable, zero pollution ships are the target the industry is striving for, and a holistic effort to enhance shipbuilding and ship operation practices is required. At the moment oil lubricated shafting systems are the industry standard for commercial ships. Since zero emissions and pollution translate to elimination of oil leakage, unregulated discharge of oil and improvement of energy efficiency in the broader sense, the optimization of such systems is required in order to minimize the ship's environmental impact.

An alternative to oil lubricated shaft bearings is water lubricated systems. Advancements in polymer materials, condition-based monitoring tools and corrosion prevention techniques have established water lubricated shaft bearing systems as a technically equivalent and, to a great extent, an environmentally sustainable solution compared with a sealed oil-lubricated system. This type of journal bearing can significantly decrease the usage of lubricating oil in the shaft bearing system, and subsequently slash down the lubrication costs. To that matter, it is proper to note that the lubricant costs are part of the operating expenses of the ship and, depending on the type of charter party,

are usually covered by the ship owner or operator. The reduction of these expenses offers an additional reason for ship owners to explore water lubricated bearings as an option in comparison with the more common oil lubricated arrangements. Also, as per IACS (International Association of Classification Societies) the requirements regarding water and oil lubricated propeller shaft and tube shaft arrangements are clear and with documented implementation. Additionally, the withdrawal and survey rules of water lubricated bearings are comparable to those of oil lubricated, while the interval periods and extension requirements are the same. While oil lubricated journal bearings remain the industry's dominant choice, further analysis and development can lead to optimized solutions. Furthermore, through comparative studies with water lubricated bearings, in regular and extreme operating conditions, a more reliable framework for shaft bearing arrangement selection is established.

Literature Review

Over the past decades, a plethora of studies has been conducted around rotor dynamic systems. Through the examination of such systems, it is evident that bearing support analysis plays a key role in the accuracy and completeness of the studies' results. The flexibility of bearing support, the film dynamic coefficients and the journal bearing lubrication problem constitute the main elements of the existing literature. In addition, shaft tilting, bending, journal misalignment and bearing deformation and wear have great effect on rotor dynamic behaviour. A review of the existing literature is necessary in order to set the goals of this study and the framework of the present study.

The fluid film bearing analysis methods have advanced during the past decades. Furthermore, analytical solutions and the mobility method charts and maps were used with main objective the calculation of forces and journal motion. These methods were later supplemented by numerical solutions focusing on pressure and gap distributions and concerning a variety of designs (grooves, pockets, crowning, waviness, etc.). In the following years, more work taking into account Reynolds boundary conditions, elastic and thermal deformation was presented. To the present day, a variety of methods and computational tools has been developed including finite difference and finite element methods, Computational Fluid Dynamics and elastohydrodynamic (EHD)-thermoelastohydrodynamic (TEHD) analysis. Setting the goals of this study an overview of the existing literature, past articles and studies is considered fundamental.

The mobility method is broadly used for numerical applications concerning crankshafts and connecting rod bearings. A typical example of its application can be found in the article by J. F. Booker [1], in which he used this method to approach the solution of the lubrication analysis problem of dynamically loaded journal bearings. This method is characterised by its speed, simplicity and computational accuracy, but its main drawback originates from the assumption of circumferential symmetry. Furthermore, the application of this method aims at predicting the motion of a journal centre under arbitrary loading using bearing characteristics inferred from models or experimental data, neglecting, however, cases of journal misalignment and special inlet geometry (e. g. oil grooves and oil holes).

Extensive research involving journal bearings has been reported in the field of elastohydrodynamic (EHD) and thermoelastohydrodynamic (TEHD) analysis. These studies analyse bearing lubrication while taking into account elastic structural deformation and thermal effects. Computational algorithms are used in conjunction with finite element or linear superposition models in order to obtain solutions for functions as film pressure and film thickness. For instance, Goenka and Oh in [2] asses the effects of deformation on the operating characteristics of a connecting rod bearing by applying the Newton-Raphson method to the nonlinear system resulting from the coupling of the Reynolds equation and elasticity equations. In general, these methods are computationally intensive but the rapid increase of computational power in recent years reinforced their use in a variety of applications. Nikolakopoulos, Papadopoulos and Kaiktsis in [3] presented a bearing optimization procedure where the EHD analysis is coupled with objective functions and a genetic algorithm, based on the Pareto dominance principle, in order to create a tool for limiting the range of independent variables in EHD journal bearing design. While, in [4] Charipotopoulos et al performed a computational fluid dynamics (CFD) investigation of the tribological characteristics of parallel and quasi-parallel slider bearings operating under TEHD regime. These type of methods find application in comparative studies, as shown in [5] where Fillon, Kuznetsov and Glavatskih compare the effect of liner materials on journal bearing characteristics using a numerical THD model. The main aim of other works is to develop tools, that facilitate the optimazation of the bearing design process. A notable example

is presented by Rossopoulos et al in [6], where optimum designs for single and double slope stern tube bearings are determined and compared. This was achieved by developing tools to calculate the operational parameters performance characteristics of bearings and the utilization of a general purpose optimizer.

Other studies focus on the subject of the dynamic characteristics of fluid film bearings. A wide range of approaches has been developed regarding the journal bearing flexibility problem. In the past the research focused on experimental techniques for the determination of the dynamic coefficients, while in the latter years, the increase of computational power proved to be a valuable tool to the development of methodologies for the numerical calculation of these coefficients. In addition, as reported in papers by Lund [7], [8] and Kostrzewsky and Flack [9] inaccuracies can be observed in the experimental values of the dynamic coefficients, in comparison to numerical results. These divergences were justified by the fact that the dynamic characteristics cannot be measured directly but are derived from other measurements, which are often dependent on test conditions, and by the challenges in acquiring accurate measurements. As explained by Jang and Lee in [10] the basic elements of the proposed numerical approaches can be identified in two fundamental methods. The first one is termed as the physical perturbation method, and it is based on the differentiation of the bearing forces with respect to finite displacements and velocities of the bearing centre, for the calculation of the stiffness and the damping coefficient respectively. The main drawback of this method is that it is computationally intensive. The other method, is the mathematical perturbation method as presented in the classic article [11] by Lund and Thomsen. Moreover, the fluid film stiffness and damping coefficient were calculated by coupling the finite element method and the perturbed Reynolds equation. In their article [12] Ebrat et al presented a journal bearing hydrodynamic analysis of the oil film dynamic characteristic based on a finite difference formulation. The calculation of the oil film pressure distribution and the bearing dynamic stiffness and damping matrices was generated through a perturbation approach on the Reynolds equation. The effects of local bearing structural deformation (EHD) and journal tilting and bending are taking into account as the bearing dynamic characteristics are based on perturbations of each node of the oil film domain. The results of the proposed method were validated with numerical results from the literature.

Studies incorporating models with more than two degrees of freedom demonstrate results of greater accuracy and address journal misalignment and structural deformation effectively. Journal bearing misalignment can be generated by a number of different factors and their combinations. Main causes are manufacturing and assembling errors, deflection of the shaft, thermal distortion during operation, and asymmetric bearing loading according to Pafelias and Broniarek, who in their paper [13] studied the effect of misalignment on the performance of a bearing through the calculation of its dynamic coefficients. P. G. Nikolakopoulos and C.A. Papadopoulos in their article [14] also study the effects of misalignment in journal bearing but also take into account the caused wear, they investigate the friction coefficient and the variation in power loss of the rotor bearing system as a function of wear depth and misalignment angles. In general, wear occurs in journal bearings when their surface comes in contact with the rotor. Operating conditions as is high load and temperature, low angular viscosity or low velocity cause the reduction of the systems load bearing capacity and as a result the two parts come in contact and wear is induced. Shaft misalignment is also one of the most common causes of wear. A well-known model was proposed by Dufrane et al [15] (used in [16] and [3]), in which the film thickness is defined in the worn and the non-worn region of the bearing and are depended on the starting and final points of the worn regions. This model is used again in [17] by Papanikolaou et al where the effect of wear in journal bearings is investigated through the alternation of the dynamic coefficients.

The operational characteristics of water lubricated bearings have been studied through experimental and computational models similar to those of oil lubricated bearings described above. For example,

in [18] by Litwin and Olszewski, numerical and experimental simulations are conducted and the characteristics of water lubricated bearings with different bush materials (metal-bronze, polymer and rubber) are compared. The results offer a great insight on the behavior of the bearings during start-up and stop operation, their lubrication regimes and characteristics during operation. While in [19], Zhang et al study side by side water and oil lubricated plain journal bearings, using CFD simulations. Moreover, their main target is to compare their operational characteristics focusing on the load capacity of the bearings, and calculating the length ratio of water and oil lubricated bearings which work under the same conditions and loads.

Goals of the Present Study

The goal of the present thesis is to calculate the performance characteristics and study the operational behavior of water and oil lubricated journal bearings. This is achieved through the completion of numerical simulations concerning bearings of varying design parameters, subjected to different operational conditions. The numerical simulations depend on the solution of the Reynolds differential equation, which is carried out using a solver developed at the section of Marine Engineering, Machine Elements and Tribology Lab of NTUA.

In an effort to acquire results of increased accuracy, an extension, based on a plane strain hypothesis, is going to be added to the modeling software. Moreover, by adding this extension, the elastic deformation of the journal bearing bush will be factored into the simulations. The results, derived from the extended model, are going to be validated with findings from past studies for both oil and water lubricated hydrodynamic bearings. Using a series of comparative models, defined by an array of operational and geometric parameters, the results of the extended model will be juxtaposed to the ones obtained by the original algorithm. Subsequently, appropriate simulations will be carried out, in order to determine the effect journal bearing design parameters, such as liner material or thickness, and operating conditions, for example rotational speed, have on performance characteristics. Additionally, a comparative case study will be carried out concerning water and oil lubricated ship shaft bearings, operating under normal, misaligned and different loading conditions.

With its completion, this project will highlight the importance of the liner material selection and design process, by offering findings concerning the influence liner compliance has on the calculations of bearing characteristics. Apart from the effects of the bush, a series of operating factors, different conditions as well as designs will be examined. These simulations are going to be completed side by side for water and oil lubricated bearings, and the analysis of the corresponding results will offer insight to the differences, advantages and disadvantages of the behavior of these types of bearings. This thesis aims to achieve its goals and make them comprehensible for engineers and technically skilled professionals, by presenting a coherent framework in the area of hydrodynamic lubricated journal bearings and marine shaft systems.

1 Lubricants

Lubricants are interposed between two surfaces in order to control friction, enhance the smoothness of their relative motion and to prevent damage, thin layers of gas, liquid and solid materials can be created to achieve lubrication in different applications. Fundamental information about lubricants is a necessary part of this study. The principal physical properties of lubricants, the composition of oils and greases and their marine applications are presented in this chapter, using a range of literature ([20], [21], [22]) and other mentioned in the following sections).

1.1 Physical Properties

The fundamental physical properties of a lubricant can be used to understand its behaviour and predict its performance in different operations. There are many parameters that describe the different physical properties of oils which can be found in literature. In this part of the present study the most frequently specified parameters are presented.

1.1.1 Viscosity

In lubrication, oil viscosity is considered an integral parameter as different oils exhibit different viscosities. This property, of a liquid or a gas, results from its resistance to shear forces and hence to flow. It corresponds to the measurement of flow resistance for a liquid or a gas. The detailed interpretation of viscosity results using the Newton formulas concerning laminar fluid flow between a moving and a fixed one. Between these two surfaces the fluid layers move at different velocities for different distances from the fixed surface. If for a distance y the fluid layer velocity is v, it becomes $v + dv$ for a distance equal to $y + dy$. Then the shear stress is given by:

$$\tau = \eta \frac{\theta u}{\theta y}$$

and η is known as the coefficient of viscosity, or the dynamic viscosity. To form this equation, the assumption that there is a proportional coefficient between the shear stress and the velocity gradient is required. This assumption is confirmed experimentally for a wide range of fluids and it leads to the segregation of fluids to Newtonian and non-Newtonian. Moreover, when the previous equation between the shear stress and the velocity gradient applies to a fluid it is called Newtonian, when this relationship is more complicated (i.e., non-linear with the velocity gradient), under severe operating conditions or with specific fluids, the fluid is considered as having non-Newtonian behaviour. Common dynamic viscosity units are the Poise [P] and the centipoise [cP] and the SI unit Pascal-second [Pas]. Their relationship is as follows:

$$1 \text{ P} = 100 \text{ cP} = 0.1 \text{ Pa s}$$

The ratio of dynamic viscosity to fluid density equals to kinematic viscosity ν:

$$\nu = \frac{\eta}{\rho y}$$

The SI kinematic viscosity unit is the [m^2/s] and the Stoke [St] and centistoke [cSt] are also commonly used. Their relationship is as follows:

$$1\ \text{St} = 100\ \text{cSt} = 0.0001\ [\text{m}^2/\text{s}]$$

The operating temperature affects at a high rate the viscosity of lubricating oils, so it consequently affects the lubricant film thickness. The importance of knowing the relation between the viscosity and the temperature of a lubricant is evident from an engineering perspective. The oil viscosity at a specific temperature can be either calculated from the viscosity-temperature equations or obtained from the viscosity-temperature American Society for Testing Materials (ASTM) chart. The ASTM chart (D341) is widely used and is derived from Walther's equation:

$$log_{10}log_{10}(\nu + b) = a - log_{10}T$$

Where:

v : kinematic viscosity [cSt]
T : temperature [K]
b : constant approximately equal to 0.6
a, c : coefficient depending on the lubricant

This relationship shows that the curve viscosity versus temperature, using logarithm for abscissa and Log Log for ordinate, is a straight line. This graphic, has been standardised by ASTM. Such a chart allows for a given oil to determine its viscosity at a given temperature if it is known for two other temperatures.

The kinematic viscosity evolution according to temperature corresponds to the lubricating oil quality, this relationship is shown through a factor called Viscosity Index (VI). Oils with high VI are less affected by temperature changes than oils with low VI. This index is used to compare the oil of interest with two reference oils that display a significantly different behaviour in temperature sensitivity. Pennsylvania paraffinic oils have excellent temperature behaviour and were given VI value of 100 at 100 Â°F. On the other hand, Gulf Coast naphthenic oils displayed great viscosity difference when the temperature was altered and they were given VI value of 0 at 100 Â°F. The index for an oil of interest is calculated using the following equation:

$$VI = \frac{L - U}{L - H} \cdot 100$$

Where:

L : the viscosity of a naphthenic oil (VI=0) at 40Â°C
H : the viscosity of a paraffinic oil (VI=100) at 40Â°C
U : the viscosity of oil of interest at 40Â°C

Using viscosity index (VI) improver additives and higher-quality base oils, this viscosity index is increasing and can be greater than 100. That is why a new viscosity index has been defined and named VI_E:

$$VI_E = \frac{10^N - 1}{0.00715} + 100$$

Where:

$$N = \frac{log_{10}H - log_{10}U}{log_{10}V}$$

and

V : the viscosity of oil of interest at 100Â°C

Pressure also affects the viscosity of lubricants. The viscosity of most of oils is increasing with pressure and although there is a number of attempts to develop a formula to accurately describe the relationship between pressure and viscosity of lubricants, some are best applicable to low and moderate pressures while others to higher values. This phenomenon is critical for the operation of rolling element bearings and gears. The best known equation to calculate the viscosity of a lubricant at moderate pressures is the Barus equation:

$$\eta_p = \eta_0 \cdot e^{ap}$$

Where:

η_p : the viscosity at the pressure p of concern [Pa s]

η_0 : the atmospheric viscosity [Pa s]

a : the slope of the natural logarithm of dynamic viscosity versus pressure

The International Standards Organisation Viscosity Grade (ISO VG) was introduced in 1975 and represents the lubricants's kinematic viscosity at 40 Â°C (104 Â°F).

1.1.2 Density and Specific Gravity

Density is another oil characteristic, important in engineering calculations and useful for lubricant selection and identification. Specific gravity or density is used as a crude oil indicator as it gives an approximation of the amount of gasoline and kerosine present in the crude. Specific gravity is defined as the ratio of the mass of a given volume of oil (and any other liquid) at temperature t_1 to the mass of an equal volume of pure water at t_2. Density is defined as the mass per volume. A commonly used factor is the API unit (American Petroleum Institute), it is calculated as:

$$API = \frac{141.5}{s} - 131.5$$

Where:

s : the specific gravity at 15.6 Â°C (60 Â°F)

1.1.3 Specific Heat

Specific heat is one of the most important thermophysical properties of lubricants. It expresses the amount of heat necessary to raise the temperature by one unit per unit of mass and varies linearly

with temperature. The following formula can be used for an approximate calculation of specific heat:

$$C_p = \frac{1.63 + 0.0034\theta}{\sqrt{s}}$$

Where:

C_p : the specific heat [kJ/kg·K]
θ : temperature [Â°C]
s : the specific gravity at 15.6 Â°C (60 Â°F)

1.1.4 Thermal Conductivity

Thermal conductivity of a material is a measure of its ability to conduct heat, this property is another important indicator of lubricant thermal behaviour. Thermal conductivity also varies linearly with the temperature and is the coefficient k represented in Fourier's law of conduction:

$$q = -k\frac{dT}{dx}$$

The following equation is commonly used for an approximate calculation of thermal conductivity:

$$k = \frac{0.12}{s} \cdot (1 - \frac{1.667 \cdot \theta}{10^4})$$

Where:

k : thermal conductivity [W/m·K]
θ : temperature [Â°C]
s : the specific gravity at 15.6 Â°C (60 Â°F)

1.1.5 Thermal Diffusivity

Thermal diffusivity is a parameter which is derived from properties already defined. Thermal diffusivity results as the ratio of thermal conductivity to density and specific heat heat capacity and expresses the temperature propagation into the solids. As described the calculation formula is:

$$\chi = \frac{k}{\rho \cdot C_p}$$

Where:

χ : thermal diffusivity [m^2/s]
k : thermal conductivity [W/m·K]
ρ : density [kg/m^3]
C_p : the specific heat [kJ/kg·K]

1.1.6 Oxidation Stability

Oxidation stability is the resistance of a lubricant to molecular breakdown or rearrangement at elevated temperatures in the ordinary air environment. The rate of oxidation depends on the degree of oil refinement, temperature, presence of metal catalysts and operating conditions. In general, oxidation of the oil takes place at much lower temperatures than thermal degradation.

1.1.7 Thermal Stability

Thermal stability is the property of a lubricant that expresses its resistance to molecular breakdown or rearrangement at elevated temperatures in the absence of oxygen. Even without the presence of oxygen, some oils decompose above a certain temperature and break down to methane, ethane and ethylene. Thermal stability can be improved by the refining process, but not by additives and usually synthetic oils have better thermal stability than mineral oils.

1.1.8 Temperature characteristics

Temperature characteristics are factors that limit the temperature range over which the lubricant can be used, therefore play a significant role in the procedure of selecting a lubricant. Operating at a non-designed temperature can lead to undesirable effects that affect not just the lubricant, but can also lead to damage of the lubricated equipment. Degradation or decomposition of oil can be caused by thermal decomposition and oxidation, also other damages like corrosion can be caused by the acidity of oxidised oils. The most important thermal properties of a lubricant are its pour point, flash point, volatility, oxidation and thermal stability, surface tension, neutralisation number and carbon residue. These parameters play important roles in the smooth operation of lubricated equipment as they describe a lubricant's behaviour and set different limits and ranges.

1.2 Lubricant Formulation and Composition

Lubricant formulation is defined as the mixing of chemical substances with the purpose of composing a mixture, usually fluid or semisolid, able to separate a tribopair and limit the force necessary to accommodate their relative motion. An efficient lubricant achieves the required level of friction and wear rates while maintaining these standards in spite of degradation. Different kinds of lubricants are used for different applications depending on the operational and financial requirements. Another important factor is the oil additives which constitute 5% of a typical lubricant, while 95% is its base stock. Categorisation of lubricants can be done according to different base stocks: biological, mineral and synthetic. Sources of biological oils can be: vegetable and animal, these oils are suitable in applications where the risk of contamination must be limited, for example food industries. In 1988 the American Petroleum Institute (API) introduced grouping of base oils in their API 1509 publication. This base oil differentiation consists of five Base Oil Groups:

Group I: Base oils with less than 90 % saturates which leads to poorer oxidation resistance and shorter operational life, more than 0.03 % sulphur, viscosity in the range of ISO VG 80 to 120 and restricted temperature range

Group II: Hydrogen-treated base oils, with more than 90 % saturates (better ageing properties), less than 0.03 % sulphur and viscosity in the range of ISO VG 80 to 120

Group III: Base oils with more than 90 % saturates, less than 0.03 % sulphur, viscosity greater than ISO VG 120 and improved low temperature operating capability (around -20 Â°C)

Group IV: Polyalphaolefin oils with similar properties as mineral oils but more uniform from a molecular perspective, with relatively good high temperature oxidation resistance and good low temperature flow characteristics

Group V: all other base oils (except vegetable oils) not included in groups I to IV, such as: phosphate ester, polyalkylene glycol, polyolester, silicone, biodegradable lubricants, and also blends of various base oils.

In the context of this study a brief presentation of sources, formulation considerations and manufacture of mineral, synthetic oils and greases is considered useful.

1.2.1 Mineral oils

Mineral oils are considered liquid by-products or hydrocarbon fluids derived from the distillation of petroleum crude oil, which is mined in various parts of the world. They are the most commonly used lubricants with certain advantages and disadvantages depending on the application.

Mineral oil base fluids consist largely of carbon and hydrogen (hydrocarbons), but may also contain smaller amounts of sulphur, oxygen, and nitrogen compounds. Mineral oil fluids with viscosity properties suitable for lubricants have carbon numbers in the C20-C40 range. Because of the large number of different molecular structures possible in this carbon number range, compositions are described by major hydrocarbon classes. The main mineral oil compositions are: Paraffins, Isoparaffins, Aromatics, Naphthenes, and Olefins. Paraffins, isoparaffins, and naphthenes are saturated hydrocarbons; aromatics are the only unsaturated structures in mineral oil base fluids, as olefins are generally

removed during the manufacturing process. Based on this, there are three basic chemical forms of mineral oil: paraffinic, naphthenic, aromatic, oils are distinguished based on the relative proportions of these components. The presence of different types of molecules determines some of the physical properties of the lubricants, i.e. pour point, viscosity index, pressure-viscosity characteristics, etc. The fundamental differences between mineral oils are based on chemical forms but two other factors of equal importance are sulphur content and viscosity. Sulphur content in mineral oils varies, depending on the source of the crude oil and the refining process. Small amounts of sulphur in the oil are desirable to give good lubrication and oxidation properties, while too much sulphur is detrimental to the performance of the machinery. It has been demonstrated, for example, that a small percentage, between 0.1% to 1%, of natural sulphur content ensures reduced wear, while excessive amounts can accelerate corrosion. Mineral oils can also be classified by viscosity, which depends on the degree of refining. For commonly used mineral oils, viscosity varies from about 5 [cS] to 700 [cS].

The manufacture or refining of mineral oil base fluids from petroleum crude consists of up to five basic steps:

1. distillation
2. deasphalting
3. solvent or hydrogen processing
4. solvent or catalytic dewaxing
5. hydrogen or clay finishing

These steps ensure that the finished product meets the performance and quality requirements of the finished lubricant formulation. The refiner will select the crude oil and utilise a combination of processes to economically refine mineral oils with the desired properties.

1.2.2 Synthetic Oils

Synthetic oils, which consist of chemical compounds, are developed as substitutes for mineral oils. Synthetic oils differ from petroleum-based oils in that they are not found in nature, but are manufactured chemically and have special properties that enhance performance or accommodate severe operating conditions. Because they are manufactured, many of their properties can be tailored for specific needs through the choice of starting materials and reaction processing. The development and use of synthetic oils gradually increased as more operations required oils with specialised characteristics. Some of the negative effects of mineral oils as well as their limitations, for example their temperature and pressure ranges of operation, are prohibited in many specialised applications such as gas turbine engines. There are three basic types of synthetic lubricant:

- synthetic hydrocarbon lubricants
- silicon analogues of hydrocarbons
- organohalogens

Each type of synthetic lubricant has unique characteristics and all have limitations that should be understood. Such things as compatibility with other lubrication systems and mechanical components (seals, sealants, paints, clutches, etc.), behaviour in the presence of moisture, lubricating qualities, and overall economics should be analysed carefully for each type of synthetic lubricant under consideration for a given application. There is a variety of processes and techniques involving the manufacture of the different categories and subcategories of synthetic oils. Their basic elements can be described and differentiate its category's manufacturing procedure. In most cases synthetic hydrocarbon lubricants are produced from low molecular weight hydrocarbons which are derived from the â□□cracking' of petroleum. The process of cracking is performed in order to reduce the range of molecules present in the oil. Through the application of high pressures and catalysts large complex molecules present in the oil are decomposed to more simple, smaller and more uniform molecules. The low molecular weight hydrocarbons are then polymerised under carefully controlled conditions to produce fluids with the required low volatility and high viscosity. Halogenated lubricants are also manufactured on a large scale; these are appropriate for low temperatures or where there is an extreme fire risk. These lubricants are made from ethylene and halogen compounds in a process of simultaneous halogenation and polymerisation within a solvent. Organohalogens and silicones are produced using catalysts. Organohalogens are manufactured by reacting hydrocarbon gas, i.e. methane and hydrogen chloride, under pressure and temperatures of about 250Â°C or more in the presence of a catalyst such as alumina gel or zinc chloride. Silicones, on the other hand, are produced from methyl chloride which is reacted with silicon in the presence of copper catalysts at 380Â°C to form dimethyl-silicon-chloride. Secondary treatment with hydrochloric acid causes the removal of the chloride radicals to form a silicone. After neutralising and dewatering the original stock the polymerisation of silicones is then induced by alkali, resulting in the finished product.

1.2.3 Greases

Grease is a stable emulsion of fluid, thickener, and additives, usually applied as a lubricant in moving equipment where a fluid lubricant would run out. Grease is defined by the consensus organisation ASTM International as a semi-fluid to solid product of a dispersion of a thickener in a liquid lubricant. The dispersion of the thickener forms a two-phase system and immobilises the liquid lubricant by surface tension and other physical forces. Other ingredients imparting special properties are often included. Grease is composed of three major ingredients:

- base oil: to provide lubrication
- thickener: to maintain a solid to semifluid state
- additives: to provide special properties

Most lubricating oils can be used as the base oil of grease; mineral oils and synthetic oils with viscosity values from 10 to 170 mm^2/s at 40 Â°C are typically used. The type of base oil governs the major properties of grease (i.e., oiliness or boundary lubrication ability, heat resistance, oxidation stability, low temperature property, compatibility with rubber and resin, etc.). Typical thickeners include metal soaps complex soaps, diurea, and polyurea. The thickener forms a three dimensional network that provides grease with its solid to semifluid property by retaining the base oil. The amount of thickener governs the consistency of grease. Further, it has recently been understood that thickeners possess their own lubricating effects, which must be taken into account when choosing

the composition of grease. A variety of additives are used to provide grease with specific properties. Most are to the same as those used in lubricating oil, such as oiliness improvers, friction modifiers, extreme pressure additives, anti-wear agents, viscosity- index improvers, oxidation inhibitors, and rust preventive agents. Further, solid lubricants are successfully used because the consistency of grease prevents sedimentation.

1.3 Marine Propulsion Systems Lubricants

A frame of reference concerning lubricants used in marine applications is necessary in this study, hence an overview is presented in this chapter. Marine service varies from recreational outboard engines to heavy-duty diesel engines for large ships and inland marine operations. Oils for recreational marine use in smaller vessels may be formulated for two or four-stroke cycle gasoline engines depending on the fuel in use. Larger vessels, merchant ships, and ocean-going ships in general, require lubrication for the main engine but also for a series of machinery (e.g. bearing, stern tubes, deck machinery, steering gear, turbo chargers), these lubricants are heavily influenced by the type of fuel used and the design of the engines themselves. Examining marine lubricants a review of the different categorisations, requirements and elements is made using a collection of literature sources ([23], [24])

1.3.1 Categorisation of Marine Lubricants

Generally, ocean-going ships are powered by two types of diesel engines: low speed two-stroke diesel engines and medium speed four-stroke diesel engines. A differentiation can be made between three types of marine engine lubricants. Moreover, cylinder oil and system oil is used in low-speed two-stroke crosshead engines and trunk piston engine oil in medium-speed four-stroke engines.

Typically, cylinder oils have short operational life, have to meet viscosity grade of ISO VG 220 (SAE 50) and are usually formulated with an alkalinity reserve of 70 BN for engines operated with high-sulphur heavy fuel oil, while a 40-50 TBN cylinder oil is often employed for low-sulphur fuels. A high viscosity grade is required to provide sufficient lubrication at high pressures, high liner temperatures of the 230 °C range and low speeds, a strong oil film needs to be sustained between the cylinder liner and the piston rings. In addition, the lubricant has to be sufficiently stable from an oxidation and thermal perspective to prevent formation of deposits by thermal decomposition and oxidation and nitration of the lubricant, so a high alkalinity reserve is required. Another important requirement is satisfactory wear performance, to achieve the desired levels in low speed engines all factors have to optimised, including the engine design, the operations, and the lubricant quality, in order to minimise corrosive wear, abrasive wear, and mechanical wear in the engine.

System oils in low speed two-stoke engines have different functions, including piston cooling and the lubrication of different types of bearings, the crosshead guide in the crankcase and of other machinery. The oil viscosity needs to meet the ISO VG 100 (SAE 30) viscosity specification. It needs to provide good bearing performance, which means apart from proper viscosity, the oil has to be clean and provide rust and oxidation protection. To prevent deposit formation in the piston cooling space, the system oil needs to demonstrate sufficient thermal and oxidation stability. The oil should have a mild alkaline reserve to neutralise condensing acids. A typical BN of a system oil is around 5 BN. Furthermore, system oils require good demulsibility and should provide corrosion protection against salt water contamination.

At the same time, typical desired properties of trunk piston engine oils are viscosity grades of the ISO VG 100-140 (SAE 30-40) range and the alkaline level varies from 12 to 50 BN depending on the sulphur content of the fuel and the oil consumption of the engine.Like other crankcase engine oils, the main role of marine trunk piston engine oils is to lubricate the engine, to control piston deposits, to protect bearings, and to provide good anti-wear performance. Marine medium speed oils

also need to provide good filterability and enable proper purification, good balanced water shedding properties and fuel compatibility.

Following the previous categorisation of marine lubricants on the basis of different uses and engine types, it is noted that lubricants can be differentiated in terms of a variety of their functions and characteristics. For example, lubricants of marine propulsion systems and ships in general can be classified in two groups: loss lubricants and closed-system lubricants. With many pieces of lubricated equipment being exposed (i.e. wire rope lubricant), a large percentage of loss lubricant is unavoidably discharged into the environment. Closed-system lubricants, in contrast, are directed into a waste disposal process and recycled either thermally (i.e. by burning) or materially (i.e. by processing treatment). It is highlighted that closed-system lubricants can also be released into the environment (i.e. through a seal or hose failure). Lubricants can also be classified according to their different applications: hydraulic fluids, bearing lubricants, gear oils, engine oils, greases, solid lubricants, and specific fluids for applications such as compressors, well control line fluids, cutting fluids. Another worth mentioning differentiation can be made according to environmental characteristics: biodegradability, toxicity, and propensity to bioaccumulate in organisms.

1.3.2 Lubrication Environment

Marine lubricants have some unique requirements, compared to lubricants in other applications. The fundamental properties of lubricants, such as viscosity, high oxidation stability, high thermal stability, anti-wear behaviour have already been described, and in the context of this study some other essential properties of marine lubricants are highlighted:

- Water Separability: A very important oil property, as water condensation in ship machinery is a common phenomenon. To keep the oil in good condition, marine engines are equipped with purifiers to remove water contamination and impurities from the oil.
- Corrosion Protection: Corrosion and rust can be induced by contaminants like sea water and sulphuric acids. Therefore alkaline additives are used to condensed acids and protect the exposed machinery.
- Oil Filterability: As marine oils are contaminated with substances as oxidation and nitration products, soot particles, partially combusted fuel, and calcium salts, purification is taking place to remove these contaminants. To achieve the right conditions and assure the filtration of the contaminants, marine lubricants are enriched with a calculated ratio of detergents and dispersants.
- Shear Stability: Lubricants are subjected to mechanical (shear) stress and, consequently, thermal stress. This causes a reduction of oil viscosity and creates a need for additives of high molecular weight.
- Fuel Compatibility: Marine fuel oil contains contaminants. which along with fuel oil and its combustion products, can contaminate lubricating oils and cause serious problems in in some machine elements. Lubricating oils must be designed and chosen in such way that such contaminants are dispersed and filtered. An examination of the usage of fuel oils with different sulphur levels reveals another important aspect of the importance of fuel and lubricating oil compatibility. Moreover, the sulphur cap imposed globally in 2020, corresponds to 0.5 % sulphur in fuel used globally and 0.1 % in ECAS. It has been observed that if low sulphur fuel

is used in combination with high BN oils, higher amounts of deposits are formed in machine elements (i.e. piston crowns). As the low concentrations of sulphur content lead to excessive alkalinity supply. Bringing the supply of the alkalinity in balance with the fuel sulphur content and adjusting the oil feed rate resolves the problem in most cases.

It is evident, that to achieve the desired lubricating performance oil additives are essential. Additives are vital to improving the performance of the base oil. They are used to enhance the natural properties of the base oil, such as viscosity, and extend its operational range, examples are extreme pressure (EP) additives for bearings and gears. In addition, additives can act on the surfaces of the mechanical components enhancing the system's function. Additives can be used to enhance the performance of the equipment and protect it from contaminants and wear causing phenomena. A differentiation of lubricant additives can be made on the basis of their function in marine applications as follows:

Table 1: Lubricant Additives and Corresponding Functions.

Wear and friction improvers	Absorption or boundary additives Anti-wear additives Extreme pressure additives
Viscosity improvers	
Anti-Oxidants	Metal deactivators Radical inhibitors Peroxide decomposers
Corrosion control additives	Corrosion inhibitors Rust inhibitors
Contamination control additives	Mild dispersants Over-based dispersants
Pour point depressants	
Foam inhibitors	

1.3.3 Environmentally Acceptable Lubricants

Mineral oil-based lubricants are toxic to aquatic life, persistent and present a greater remediation challenge in comparison with lighter petroleum products. The poor biodegradability of mineral oils poses an environmental hazard and the degree of persistence depends on the type of hydrocarbons in the oil and its main physical properties. The notion of degradability and biodegradability conveys the meaning of the breaking down of complex, and possibly toxic material into simple and common forms, in which the elements carbon, hydrogen and oxygen exist or are simply associated. Since the decade of 1980 environmentally friendly lubricants are used increasingly, while organisations and agencies, such as the Environmental Protection Agency, the European Committee for Standardisation and the International Maritime Organisation, issue regulations regarding criteria for lubricants' usage. Environmentally friendly lubricants biodegrade faster and are less toxic than mineral oils and many do not bioaccumulate, they constitute a sufficient and competing alternative to hydrocarbon mineral oil-based products. Synthetic oils have a large part to play in offering environmentally acceptable lubricants (EAL), with superior performance characteristics than mineral oils. There is a variety of S synthetic EAL base oils with different compositions and characteristics. In all applica-

tions, the different benefits and limits of its lubricant must be taken into account in. A categorisation of EAL synthetic oils based on their composition can be made as follows [25]:

Table 2: Synthetic EAL base oil comparisons.

Base Types	ISO 15380	Characteristics
Polyglycols [PAGs]	HEPG (hydraulic oil environmental polyalkylene glycols)	Highly hygroscopic, water cannot be drained out Equipment corrosion issues Do not mix with mineral-based oils Recommend full system filling of flushing oil Poor compatibility, seals, hoses, paint, paper filters Higher density, sink, lower pump suction pressures
Synthetic Hydrocarbons [PAOs]	HEPR (hydraulic oil environmental polyalphaolefins)	Low base oil viscosity Requires viscosity improvers Viscosity must be regularly monitored Limited shear stability Can be blended with esters to achieve biodegradability
Unsaturated synthetic esters	HEES (hydraulic oil environmental ester synthetic)	Poor oxidation stability Poorer thermal stability, increase in viscosity High risk of hydrolysis Poor low temperature properties Poorer water separation properties Limited life
Saturated synthetic esters	HEES (hydraulic oil environmental ester synthetic)	High oxidation resistance Very good shear stability Good low temperature flow No lacquering Good demulsibility Life time fill potential

2 Journal Bearings

A journal bearing is composed of a shaft operating inside a stationary or rotating/oscillating sleeve (or bushing). Journal bearings are the most common and simple type of radial bearings and are used in a plethora of applications. Naturally, their design and performance parameters are interconnected with the bearing material and dynamic behaviour. The main role of journal bearings is the support of radial loads but their role extends to other functions. Minimisation of wear, fatigue resistance, absorption and damping of vibrations impulses or sudden force variations constitute some examples. For these objectives to be achieved, the presence of lubricants is required. In this part of the present study, the main aspects of the operational framework of journal bearings are examined and presented.

2.1 Principles of Operation

As mentioned above, journal bearings hold the radial position of the rotor in rotating machinery, transmitting the weight and radial forces from the rotor to the stationary structure. In marine propulsion systems, the radial load of the propulsion shaft is supported by the bearings, which at the same guide a smooth transmission of torque from the engine to the propeller.

The rotating shaft is separated with the bushing by the created lubricant film. In different applications journal bearings may be lubricated with a fluid lubricant, grease, or gas, or even a solid lubricant. Lubricant is supplied to the system and channeled to the bearing sleeve this fundamental action is completed through distinct features and configurations, such as inlet holes, axial, circumferential and helical grooves. In other words, a journal bearing obtains its capacity to support an applied load through the resulting eccentric position of the shaft when subjected to rotation. A journal, under load, shifts its location to an eccentric position inside the bearing (sleeve) that houses the shaft. The pressure field created through eccentric rotation of the journal balances the change in momentum in the convergent-divergent sections of the fluid film hosted in the clearance between the journal and the sleeve.

Journal bearings can be differentiated on many groups based on variety of factors, one way, is based on the type of lubrication that takes place in the bearing. Moreover, a journal bearing may be a hydrodynamic bearing designed to have a full lubricant film or a partial lubricant film. It may be a hydrostatic bearing with the fluid pressure provided by an external source, or a hybrid bearing that uses both hydrostatic and hydrodynamic pressures. Hydrodynamic journal bearings have the most applications and are widely used in power generation operations. Usually, a significant amount of lubricant is required and the friction coefficient during startup process is inevitably high, especially when the startup and stop processes takes place under an applied load, as the hydrodynamic lubrication film is developed above a value of rotation speed and may become turbulent above a certain speed limit. This type of phenomena are examined in the next chapters of this study but it is important to introduce the different lubrication regimes in journal bearings as follows:

- Hydrodynamic Lubrication: The relative rotational speed of the two surfaces surpasses a limit and hydrodynamic pressure allows their separation by the lubricant. Constant supply of lubricant is required but with no need for inlet pressure.

- Hydrostatic Lubrication: A fluid under pressure is used to support loads and separate the surfaces. Pressure generated externally is required in systems of hydrostatic lubrication. Application of a load compensation mechanism using restrictors or flow control devices ensures that a stable fluid film continues to separate the two surfaces under a range of applied loads and operating speeds.
- Elastohydrodynamic Lubrication: This type of lubrication is a mode of hydrodynamic lubrication in which hydrodynamic action is augmented due to surface elastic deformation and lubricant viscosity increases because of high pressure.
- Boundary Lubrication: The formation of thin adherent films can be observed in the absence of a hydrodynamically generated fluid films. This regime can be caused due to small bearing surface, low rotational speed, inadequate amount of lubricant or high applied load.
- Solid-film Lubrication: Solid lubricants can be used in applications where conditions do not allow the usage of fluid, for example in cases of excessive heating.

In the present study, the lubrication conditions of the journal bearings studied correspond to hydrodynamic and elastohydrodynamic lubrication, and are analysed in the next chapters.

2.2 Journal Bearing Geometry

The geometry of a journal bearing results from its design. Plain circular bearings are useful for general analyses and definition of fundamental characteristics. Over the years a series of bearings deigns have been developed for different applications and requirements. Besides plain sleeve cylindrical bearings other design examples are: multi-lobe, elliptical, pressure dam, offset split and tilting-pad bearings. In addition, supply arrangements range from a simple inlet hole to axial, circumferential and helical grooves for efficient distribution. The structural geometry of a journal bearing is shown in Figure 1 [26].

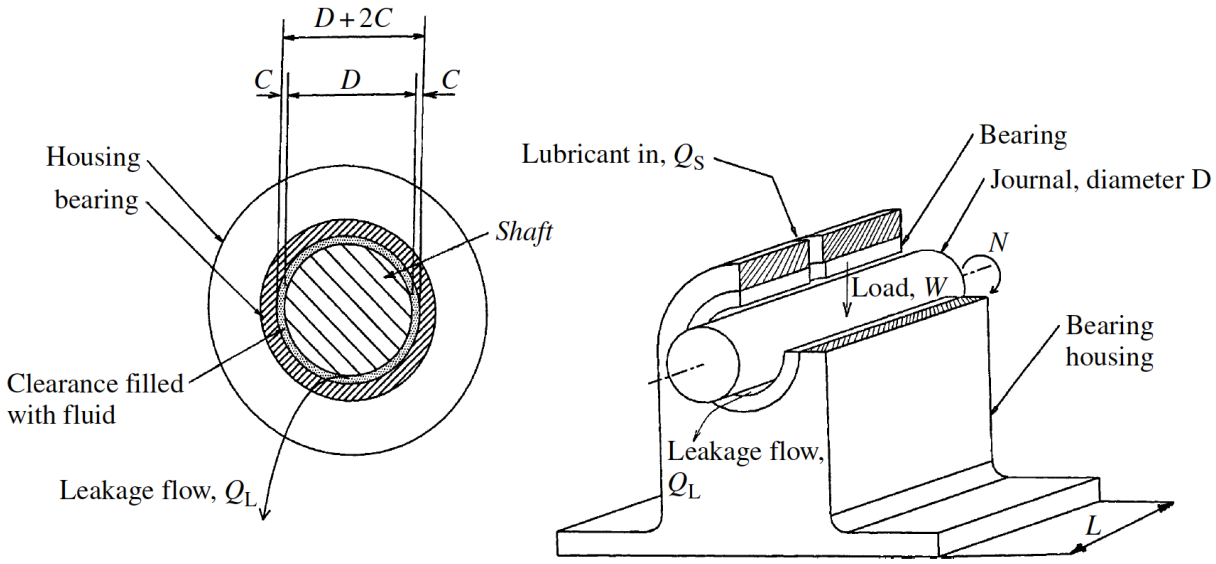

Figure 1: Journal bearing structural geometry and nomenclature.

During the start-up process the shaft begins its motion, and with the the support of the created fluid film it assumes a position. The steady state of the shaft corresponds to a position in the bearing clearance circle with specific coordinates. This state is depicted in a cross section figure of a journal bearing.

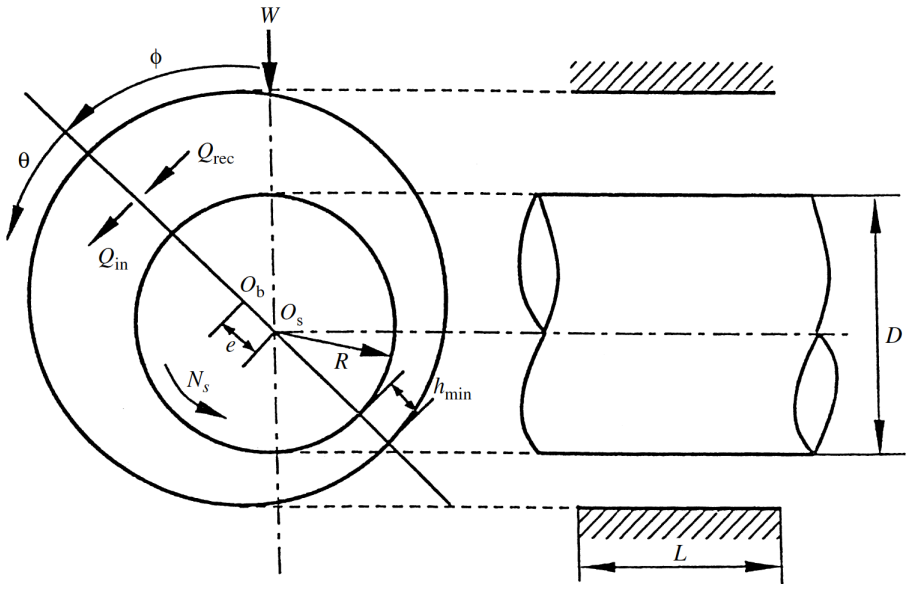

Figure 2: Cross section of a journal bearing.

The geometrical quantities depicted in the previous figures describe the geometry of the bearing and are defined as follows:

D: journal diameter
c: radial bearing clearance
Q_l: lubricant leakage flow
O_b: bearing centre
W: applied load
h_{min}: minimum oil film thickness
φ: angle of the line of centres and the perpendicular axis
θ: circumferential coordinate angle defined by the line of centres
R: journal radius
L: bearing length
Q_s : lubricant inlet flow
O_s: journal center
N_s: rotor angular velocity
e: eccentricity

Taking a closer look at the geometry of the journal an equation for the film thickness can be expressed as follows:

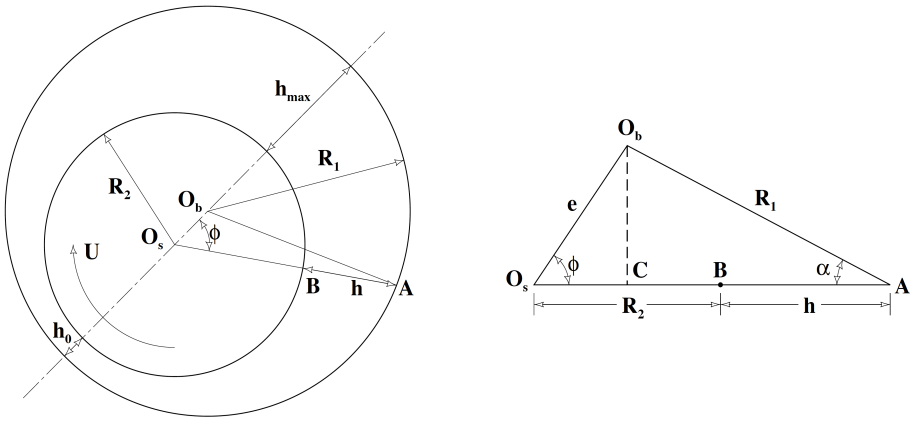

Figure 3: Film thickness geometry.

Where:

$$O_sA = O_sW + CA = O_sB + BA \quad \text{or} \quad O_sA = e \cdot cos\theta + R_1 \cdot cosa = R_2 + h$$

$$\text{thus:} \quad h = e \cdot cos\theta + R_1 \cdot cosa - R_2$$

$$\text{apllying the sine rule:} \quad \frac{e}{sina} = \frac{R_1}{sin\theta} \quad \text{and since:} \quad sin^2a + cos^2a = 1, \frac{e}{R_1} << 1$$

$$\text{result is:} \quad cosa = \sqrt{1 - (\frac{e}{R_1})^2 \cdot sin^2\theta} \approx 1 \quad \text{and with proper substitution:}$$

$$h = c + e \cdot cos\theta = c \cdot (1 + \epsilon \cdot cos\theta) \quad \text{with:} \quad c = R_1 - R_2 \quad \text{and the eccentricity ratio:} \quad \epsilon = \frac{e}{c}$$

The above equation describes the film thickness geometry with an accuracy of 0.1%.

2.3 Bearing Materials

Most journal bearings consist of two or more layers. Usually one or more bearing materials are used on the inner diameter and a higher-strength material (normally steel) on the outer diameter. As presented in [27] and [28], the parameters for the selection of materials are listed below:

- Compatibility and Friction: Shaft-to-bearing contact (absence of fluid film) and the brief operation of the bearing in the partial or boundary lubrication regimes lead to friction losses. In order to minimise these losses, a low sleeve and shaft friction coefficient is needed. The lower the friction and wear rates are during these events, which usually occur during startup and shut down, the more compatible the journal and bearing materials are as a pair.
- Conformability: Expresses the ability of the sleeve material to conform to potential shaft imperfections and misalignment.
- Embeddability: As contaminants may appear in the fluid film, this property is used to express the ability of the material to embed these foreign particles.
- Fatigue Strength: Bearings are subjected to high cyclic loads, consequently it is important that the materials used resist failure due to fatigue cracking.
- Cavitation Erosion Resistance: Cavitation erosion is caused by rapidly decreasing oil film pressure in specific regions and speeds.
- Corrosion Resistance: Due to oil acidity and oxidation, some bearings materials may be subject to corrosion.
- Thermal Conductivity: Heat, either generated in the bearing or entering through the shaft or housing, is dissipated proportionately with the thermal conductivity of the bearing material.
- Cost and Manufacturing: The process of choosing the bearing material is affected by the cost and availability of the materials and the manufacturing methods. Under every set of conditions all bearing materials issues involve a compromise, trading one property for another in the correct balance to achieve sufficient performance. This process includes limits on manufacturing costs and capabilities.

The successful functionality of a journal bearing is ensured with a combination of layers and materials. As mentioned, each layer serves a different purpose, and different properties are required. For cost-effectiveness and simplicity purposes steel and cast iron are often used in bearing structural parts, while silver and zinc also find limited use. A variety of materials is used to compromise the inner layers. A review of the most common materials is presented:

White metals or Babbitt materials are tin and lead-based alloys and are widely used in bearings. These softer metals are used to form the metal contact surface of the bearing shell, overlaying a stronger steel support shell. Attractive attribute of the babbitt layers is that they exhibit combinations of high conformity and embeddability.

Copper-based (copper-lead alloys, leaded bronzes, and non-leaded bronzes) materials find application in highly loaded steel-backed bearings (i.e. crankshaft, stern tube, engine small end rod bushings).

Aluminum-based lining materials are often used in bearings in lightly loaded positions and applications in general. They offer several advantages, including a good combination of strength and sliding properties, but their usage is limited due to their restricted fatigue strength (specific loads demonstrate a limit in the range of 55-70 MPa).

Coatings are added to bimetal bearings forming bearings known as ”trimetal”. Usually applied to copper-base linings, coatings are used to meet high performance requirements. Overlays for journal bearings are categorised as electrodeposited or sputtered according to the way they are applied, while polymer base coatings also find applications. Trimetal bearings are considered more versatile than bimetal bearings and augment properties of the bearing. For example, sputtered aluminum-tin overlays are applied to bronze and aluminum linings for improved resistance in wear and fatigue, electroplated lead-tin-copper and lead-indium overlays are commonly used and offer corrosion resistance, strength and wear resistance.

Non-metallic and composite materials are often used in steel-backed bushings where the usage of lubricants is limited, as a substitute for white metal. Materials that find common application as bearing linings include rubber, polymers, elastomers and a variety of composite materials (PTFE-polytetrafluoroethylene, phenolics, nylon, ceramic).

2.4 Design and Performance Parameters

The study of journal bearings coincides with the evaluation of their important design and performance parameters. In fluid film bearings the hydrodynamic pressure is calculated by the solution of the Reynolds equation, as it is analysed in the next chapter. Knowing the fundamental geometric characteristics, operating conditions and pressure profile of a journal bearing the evaluation of its design and performance characteristics is uncomplicated. The most important parameters are presented in this section using a range of bibliography ([26], [28], [29]).

2.4.1 Load Capacity

In hydrodynamic journal bearings, load capacity is affected by a series of factors such as: the bearing type, geometry, materials and operating conditions (speed, lubricant flow rate and temperature). The load capacity of a journal bearing is interconnected with the oil-film formation, minimum thickness, and operating temperature.

The total load that can be supported with hydrodynamic lubrication is yielded from the integral of the pressures over the shaft circumference. Moreover, when an external load P is applied the reacting hydrodynamic load W can be resolved to two perpendicular components, as in the following figure:

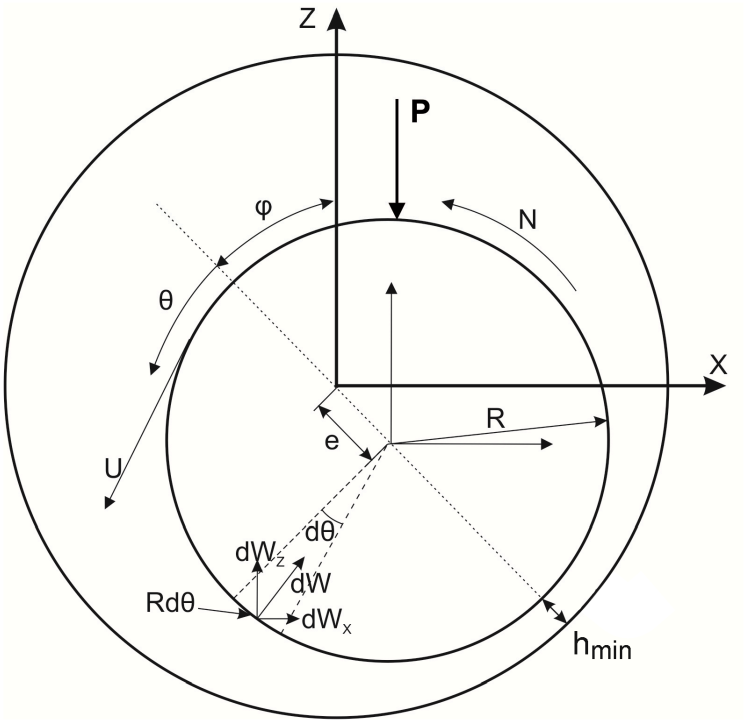

Figure 4: Journal bearing hydrodynamic load components.

Considering a small area of lubricant film $R \cdot dy \cdot d\theta$, where y corresponds to the normal plane of the figure and the direction of the length L of the journal bearing, the corresponding hydrodynamic force is $p \cdot R \cdot dy \cdot d\theta$. The two components of this force are expressed as follows:

$$W_x = \int_0^{2\pi} \int_0^L p \cdot cos(\varphi + \theta - \frac{\pi}{2}) \cdot R \cdot dy \cdot d\theta$$

$$W_z = \int_0^{2\pi} \int_0^L p \cdot sin(\varphi + \theta - \frac{\pi}{2}) \cdot R \cdot dy \cdot d\theta$$

The total load-carrying capacity is acquired from: $W = \sqrt{{W_x}^2 + {W_z}^2}$

2.4.2 Sommerfeld Number

The Sommerfeld number, S constitutes a dimensionless parameter which involves static load but also geometric, operational and lubricant properties. It is defined as follows:

$$S = \frac{\eta N_s DL}{W} \cdot \left(\frac{R}{c}\right)^2$$

Where:

η : lubricant viscosity [Pa·s]
N_s : rotor angular velocity [RPS]
D : journal diameter [m]
L : bearing length [m]
W : applied load [N]
R : journal radius [m]
c : bearing clearance [m]

This very important parameter can be used to compare the behaviour of different bearing designs, or analyse their performance in different operational conditions. Its value and range under different operating conditions can be used as an index of proper operation and sufficient lubrication.

2.4.3 Inlet and Outlet flow rates

Lubricant supply is fundamental in order to achieve proper support to the shafting system. Basic quantities that are used to describe the oil supply are the following:

Inlet flow rate per unit length is:

$$q_x = \int_0^h u \, dz = \left| \left(\frac{z^3}{3} - \frac{z^2 h}{2}\right) \frac{\theta p}{2\eta \theta x} - U_2 \frac{z^2}{2h} + U_2 z \right|_0^h = \left(\frac{h^3}{3} - \frac{h^3}{2}\right) \frac{\theta p}{2\eta \theta x} - U\frac{h}{2} + Uh = -\frac{h^3}{12\eta}\frac{\theta p}{\theta x} + U\frac{h}{2}$$

Thus, inflow at the bearing entrance is calculated with integration over the bearing length as:

$$Q_l = \int_0^L q_x\Big|_{x=0}\, dy = \int_0^L \left(-\frac{h^3}{12\eta}\frac{\theta p}{\theta x} + U\frac{h}{2}\right)\Big|_{x=0}\, dy$$

Outflow rate per unit width is:

$$q_y = \int_0^h v\, dz = \left|\left(\frac{z^3}{3} - \frac{z^2 h}{2}\right)\frac{\theta p}{2\eta\theta y}\right|_0^h = -\frac{h^3}{12\eta}\frac{\theta p}{\theta y}$$

Lubricant side leakage is calculated accordingly with integration over the bearing sides as:

$$Q_L = \int_0^{\pi D} q_y\Big|_{y=0}\, dx + \int_0^{\pi D} q_y\Big|_{y=L}\, dx = \int_0^{\pi D} \left(-\frac{h^3}{12\eta}\frac{\theta p}{\theta y}\right)\Big|_{y=0}\, dx + \int_0^{\pi D} \left(-\frac{h^3}{12\eta}\frac{\theta p}{\theta y}\right)\Big|_{y=L}\, dx$$

It is noted that for normal bearing operation the lubricant supply rate must be equal to the lubricant leakage rate. If that condition is not satisfied the lubricant supply is either abundant or insufficient. In the first case there is no negative effect on the film thickness, while in the second case lubricant starvation occurs which generally leads to smaller values of minimum film thickness than needed and higher values of oil temperature.

2.4.4 Friction Force and Friction Coefficient

The friction force F that is generated over the bearing area can be calculated by integration of the respective component of the shear stress τ_x:

$$F = \int_0^L \int_0^{\pi D} \tau_x dx dy = \int_0^L \int_0^{\pi D} \eta\frac{du}{dz} dx dy$$

As it will be presented in the next chapter:

$$u = \left(\frac{z^2 - zh}{2\eta}\right)\frac{\theta p}{\theta x} + U\frac{z}{h}$$

The final expression for the friction force is obtained by differentiating u with respect to z and substitution:

$$F = \int_0^L \int_0^{\pi D} \left(\frac{2z - h}{2}\frac{\theta p}{\theta x} + \frac{U}{h}\right) dx dy$$

Once the load and friction forces are known, the coefficient of friction, μ, can be calculated as:

$$\mu = \frac{F}{W}$$

2.4.5 Power Loss

The power loss derives from the friction losses and can be calculated as follows:

$$P_{loss} = F \cdot U = W \cdot \mu \cdot \omega \cdot R$$

Where:

F : total friction force
W : total bearing load
μ : friction coefficient
ω : angular speed of the shaft
R : bearing radius

2.4.6 Advanced Film Thickness Geometry

In journal bearing systems, the area between the rotating shaft and the bearing housing is filled with lubricant and corresponds to the parameter defined as film thickness. The lubricant film thickness is geometrically modelled according to constant design parameters of the system (L, R, c) or their representative variables (θ, e, φ). In order to arrive to a solution for the Reynolds Equation, the film thickness h needs to be calculated. Additionally, basic assumptions need to be made concerning: a Newtonian and incompressible fluid, the laminar state of its flow and the neglect of inertia effects, as well as that the heat and thermal conductivity are constants. These assumptions are further explained in the next chapter. The lubricant film thickness can be analysed to the following components:

$$h = h_n + h_{ed} + h_{th} + h_m$$

Where:

h_n : the nominal part of the film thickness
h_{ed} : the elastic deformation of the bearing housing
h_{th} : the thermal deformation of the shaft and the bearing housing
h_m : the misalignment of the shaft and bearing housing

The component of elastic deformation and its contribution to the total value depends on the hydrodynamic pressure applied on the housing and the material it is made of, assuming a rigid shaft. Thermal deformation originates from both the thermal expansion of the shaft and the corresponding deformation of the bearing housing, due to uneven temperature distribution in the bearing solid domain. The importance of this component mainly depends on the operating characteristics of the journal bearings system. Regarding the last component, attributed to misalignment, its magnitude depends on the misalignment angle of the the bearing and the shaft centerlines, which is further analysed in the next paragraph.

2.5 Dynamic Characteristics

In this section, an analysis of the dynamic characteristics of journal bearings is presented based on a range of published studies ([12], [30], [31], [32]). Dynamic coefficients correspond to the stiffness and damping properties of a journal bearing. Their physical essence coincides with changes in the hydrodynamic force of the oil film, which are attributed to the journal motion within the bearing clearance.

Moreover, when a plain cylindrical journal bearing has reached a steady-state position the journal centre O_s is located at a distance $e, (x_0, y_0)$ from the bearing centre O_b as shown in figure 2. The equilibrium condition is described as:

$$\left.\begin{array}{l} f_x = f_{x_0} = 0 \\ f_y = f_{y_0} = W \end{array}\right\} \quad \text{for } x = x_0, y = y_0, \dot{x} = 0, \dot{y} = 0$$

A change in the bearing position will lead to an additional hydrodynamic reaction $(\Delta f_x, \Delta f_y)$ that depends on the journal centre displacement (x_s, y_s) and its velocity $(\dot{x}_s, \dot{y}_s)$. A one-directional displacement (on the x or y axis) generates hydrodynamic force not only in the same direction but also in the perpendicular direction (cross-coupling effects). The first-order Taylor expansion can be used to approximate the total hydrodynamic force for small departures as follows:

$$f_x(x_0 + x_s, y_0 + y_s, \dot{x}_s, \dot{y}_s) = f_x(x_0, y_0, 0, 0) + \frac{\theta f_x}{\theta x_s} \cdot x_s + \frac{\theta f_x}{\theta y_s} \cdot y_s + \frac{\theta f_x}{\theta \dot{x}_s} \cdot \dot{x}_s + \frac{\theta f_x}{\theta \dot{y}_s} \cdot \dot{y}_s$$

$$f_y(x_0 + x_s, y_0 + y_s, \dot{x}_s, \dot{y}_s) = f_y(x_0, y_0, 0, 0) + \frac{\theta f_y}{\theta x_s} \cdot x_s + \frac{\theta f_y}{\theta y_s} \cdot y_s + \frac{\theta f_y}{\theta \dot{x}_s} \cdot \dot{x}_s + \frac{\theta f_y}{\theta \dot{y}_s} \cdot \dot{y}_s$$

$$\text{with } f_x(x_0, y_0, 0, 0) = f_{x_0} = 0 \text{ and } f_y(x_0, y_0, 0, 0) = f_{y_0} = W$$

In matrix form the expressions of the forces are:

$$\begin{bmatrix} \Delta f_x \\ \Delta f_y \end{bmatrix} = \begin{bmatrix} k_{xx} & k_{xy} \\ k_{yx} & k_{yy} \end{bmatrix} \cdot \begin{bmatrix} x_s \\ y_s \end{bmatrix} + \begin{bmatrix} b_{xx} & b_{xy} \\ b_{yx} & b_{yy} \end{bmatrix} \cdot \begin{bmatrix} \dot{x}_s \\ \dot{y}_s \end{bmatrix}$$

The bearing force components are described using the linear bearing stiffness coefficients:

$$k_{xx} = \frac{\theta f_x}{\theta x_s}, \quad k_{xy} = \frac{\theta f_x}{\theta y_s}, \quad k_{yx} = \frac{\theta f_y}{\theta x_s}, \quad k_{yy} = \frac{\theta f_y}{\theta y_s}$$

and the linear bearing damping coefficients:

$$b_{xx} = \frac{\theta f_x}{\theta \dot{x}_s}, \quad b_{xy} = \frac{\theta f_x}{\theta \dot{y}_s}, \quad b_{yx} = \frac{\theta f_y}{\theta \dot{x}_s}, \quad b_{yy} = \frac{\theta f_y}{\theta \dot{y}_s}$$

These coefficients of the oil-film are presented schematically in the next figure [33]:

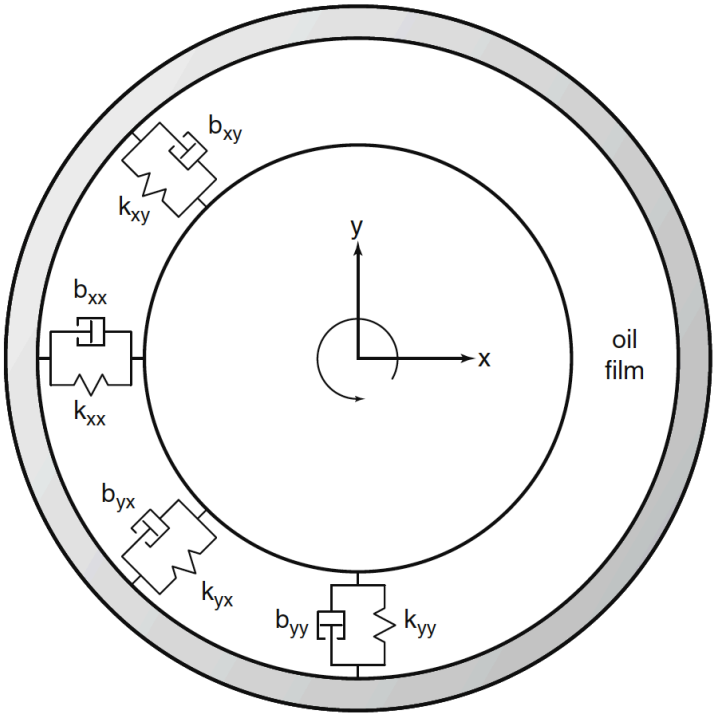

Figure 5: Journal bearing stiffness and damping coefficients illustration.

Furthermore, the indices *xx* and *yy* correspond to direct coefficients of stiffness and damping, which describe changes in the bearing force components resulting from displacement or velocity in the same direction. The indices *xy* and *yx* denote cross-coupling coefficients and describe changes resulting from disruptions in the perpendicular direction.

The dynamic coefficients find key applications in the selection of rotor support systems and definition of the overall rotor-bearing system behaviour. Through calculation of these coefficients the response of the system to imbalance, excitation and its stability in general can be predicted. Both the location of system critical speeds (stiffness value) and its amplitude (damping value) are affected by these coefficients.

2.6 Wear, Misalignment and Elastic deformation

There are multiple possible sources of wear in bearings. Wear, meaning the removal of component surface material, may be caused by adhesive or abrasive practices on an asperity length scale, or observed as spalling and pitting damage on a macroscopic scale. In bearings, as in most types of machinery, there are types and levels of mild wear that allow their effective function but excessive wear leads to improper operation and consequences include deflection, extreme noise and vibration levels and steep rises in torque and temperature. A categorisation of causes of bearing wear types is presented in the following table as well as common examples for each case [34].

Table 3: Causes of wear and examples.

Causes	Possible Sources	Examples
Contamination related wear	Manufacturing process residual particles Foreign material from the outside environment Particles from other worn components Chemical contaminants (e.g. lubricant degradation products) and water-moisture	Denting or bruising damage Initiation of cracks and spalling wear Abrasive wear and excessive polishing effect Rust and corrosion
Inadequate Lubrication related wear	Interruptions of lubricant supply Lubricant loss Degradation of lubricant properties	Softening and yielding of components Degradation of material properties Severe adhesive wear damage Peeling damage
Misuse related wear	Installation with excessive pre-load Operational overload Poor installation and fitting practices Misalignment and high spots Electric current discharge	Cracking, peeling and spalling wear Fretting damage Plastic deformation of components Fluting damage

Most bearing damages are related to wear rather than stress-related material fatigue. Examples of wear types were presented in the previous table, including wear caused by misalignment which constitutes a leading source of faults in journal bearings. Angular misalignment occurs when the journal and bearing centre lines are at an angle to each other. Deflection of the centre lines in the horizontal and vertical planes can also be observed individually or combined with angular misalignment. Definition of proper shafting support and alignment are essential processes for smooth operation of all rotor bearing systems [34].

In the majority of journal bearings in power generation applications, including marine propulsion systems, misalignment angles can be acceptable in certain ranges (usually less than 3 mrad) [3]. Direct effect of bearing misalignment is the alternation of the oil film distribution in both circumferential and axial directions [35]. Excessive misalignment leads to overloaded conditions and causes the bearings to perform poorly or even fail. In general, misalignment can occur due to the following factors individually or combined:

- Manufacturing and assembly errors
- Miscalculated operating conditions
- Irregular and asymmetric bearing loading
- Deformations of the bearing elements and shaft
- Thermal distortions

In the following figure the geometry of a misaligned journal bearing is presented where:

h : oil film thickness
θ : bearing angle
e' : magnitude of the projection of the axis of the journal on the mid-plane
φ_0 : attitude angle between the vertical line and the line of centres
a : misalignment angle

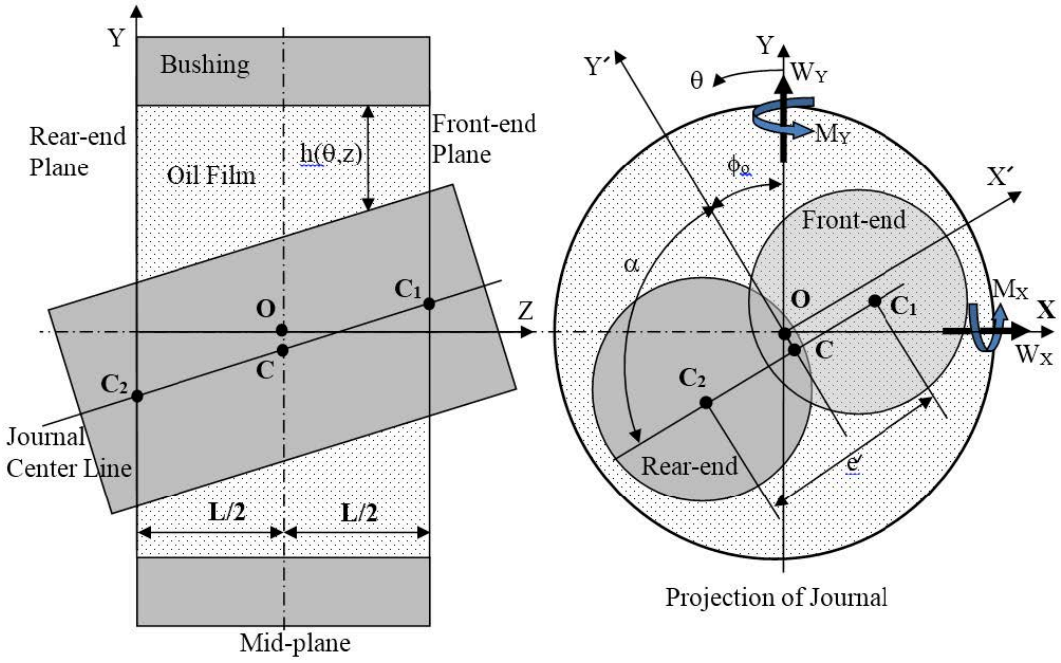

Figure 6: Misaligned journal bearing geometry.

As described, during the operation of the shafting system, wear and damages can be caused that affect the components of the bearings. Another phenomenon occurs, first recorded by Beauchamp Tower whose experimental data were used by Reynolds, as the load of the shaft is supported by the bearing. Their interacting surfaces deform elastically under load and consequently affect the fluid-film geometry and the hydrodynamic pressure profile. The effect of elastic deformation to the pressure profile extends to all the other bearing deformation such as load capacity, friction losses and lubricant flow rate. The developed pressure distribution appears more uniform and relatively more flat with sharp declines at the edges of the bearing, which can lead to augmented vibrational stability [36].

2.6.1 Dufrane wear model

One of the most commonly used wear models is the Dufrane model. Worn steam turbine bearings were studied, inspected and measured to determine the extent and nature of the wear by Dufrane et al [15] and a model was created to simulate the worn regions of the bearings. The Dufrane model is based on a hypothetical abrasive wear model with the worn arc at a radius larger than the journal as shown in the next figure and described by the following equation:

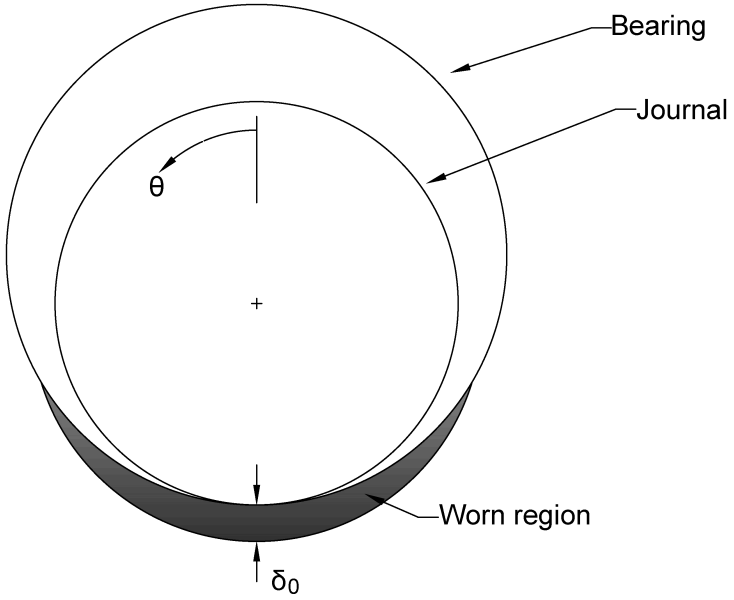

Figure 7: Dufrane uniform wear model of a journal bearing.

$$\frac{\delta}{c} = \frac{\delta_0}{c} - (1 + cos\theta)$$

Where:

δ_0 : maximum wear depth
δ : wear depth at an angle θ
θ : bearing angle
c : bearing clearance

The conclusion of the study is that a limited amount of wear may enhance lubrication, while it predicted that beyond an optimum amount of wear the altered geometry would accelerate wear. More recent studies are in agreement with this analysis.

2.6.2 Winkler elastic deformation model

Different models have been suggested to describe the surface deformation of bearings' shells. An analytical model, used by several authors ([37], [38], [39]), is the Winkler (or column) model. According to the model the elastic deformation of the bearing bush or housing can be calculated as a function of the hydrodynamic pressure, Young's modulus, Poisson's ratio, and the thickness of the bearing bush. The model is expressed from the following equations:

$$\Delta y_i = \delta_{Winkler} = \frac{tP_i}{E} \cdot \frac{(1+v)(1-2v)}{1-v}$$

Where:

$\delta_{Winkler}$: elastic deformation
t : bearing shell thickness
P_i : hydrodynamic pressure at each computational node
E : Young's modulus
v : Poisson's ratio

The geometry of typical journal bearings was described in previous sections of this chapter. The fact that a combination of layers is used was also highlighted, and at this point it is evident that the Winkler model applies to the inner layers. The journal is solid and usually made of steel hence its deflection can be considered negligible, while the effect of the outer layers (made from harder materials) can be regarded as factored into the assembled clearance. The next figure graphically illustrates the Winkler bearing foundation (not in scale):

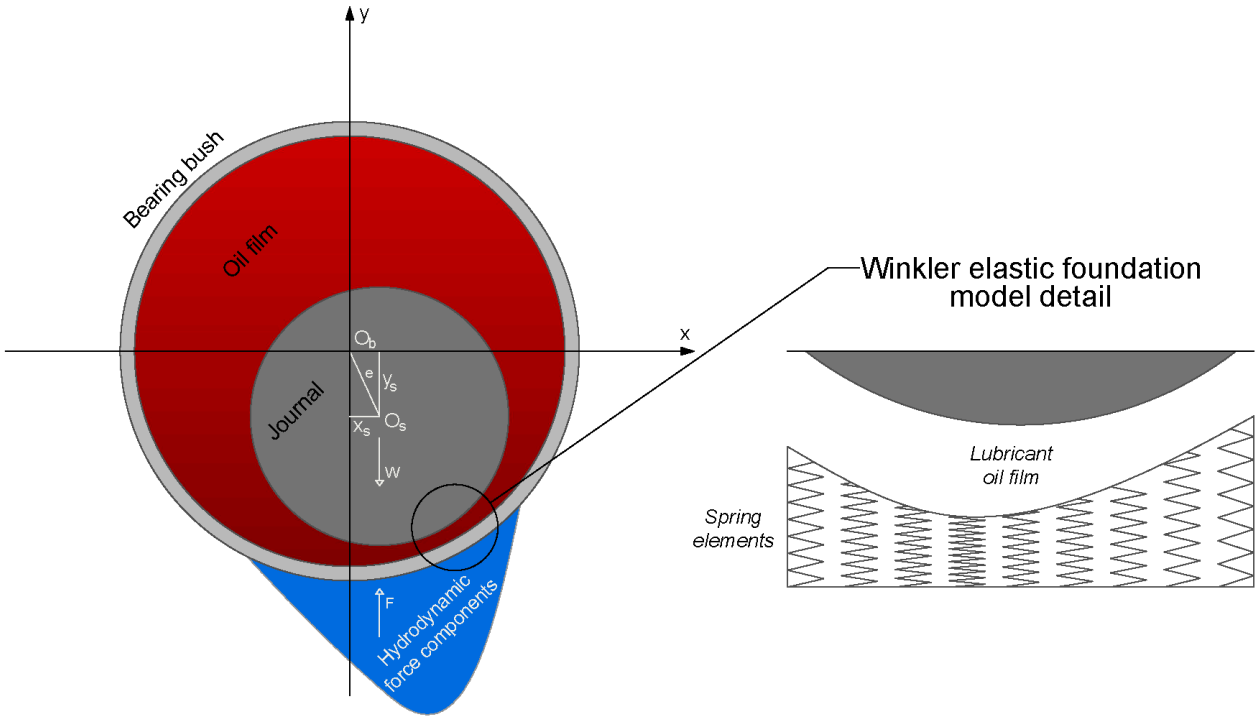

Figure 8: Bearing bush: Winkler elastic foundation.

The deformable object, in this case the bearing bush, is modelled as a set of independent spring-column elements. A plane strain hypothesis is required for the application of the model, meaning that the deformation in each point depends on the pressure at that point, the geometric and material parameters, while the shearing action is neglected.

2.7 Marine Propeller Shaft Bearing Systems Review

Vessel machinery lubrication and sealing requirements arise from the operation of gearboxes, shaft support systems, controllable pitch propeller systems, propeller hub and cap and other systems, as described in previous sections. A more thorough review of typical shafting arrangements in ships and a differentiation between oil and water lubricated bearings are presented in this section.

In marine vessels, the power generated form the main engine is transmitted to the propeller through the shaft and simultaneously axial loads from the propeller are transmitted to the ship's hull. The successful operation of a ship's axial system requires different kinds of bearings. A typical propulsion shaft is comprised of the intermediate, the tube and the propeller shaft. The latter can also be called tailshaft or screwshaft and is the part which the propeller is fitted. The tube shaft passes through the sterntube which is fitted in the shell of the ship at the stern, below the waterline, and can be a section of the propeller shaft. Moreover, the sterntube functions as the housing of the bearing or bearings, ensuring the proper support of the shaft and the propeller, accommodating also the sealing system (of closed systems). While, the intermediate or line-shaft bearings offer additional support to the part of the propulsion shaft inside the vessel. The main engine thrust bearing takes the axial load from the propeller up the propeller shaft to the hull, ensuring the ship's movement.

Sterntube bearings and intermediate bearings are journal bearings, they support radial shaft loads, while axial loads are transmitted through the thrust bearing. As presented in IACS (International Association of Classification Societies) Unified Requirements Z21: Surveys of Propeller Shafts and Tube Shafts [40], journal bearings can be categorized as open or closed loop systems. Closed loop systems use oil or fresh water to lubricate the bearings and are sealed against the environment (such as seawater) by adequate sealing/gland devices. On the other hand, open systems use water to lubricate the bearings and are exposed to environment. The following figure depicts a typical marine propulsion system, comprising from the ship's main engine, propeller, shaft and shafting bearing systems:

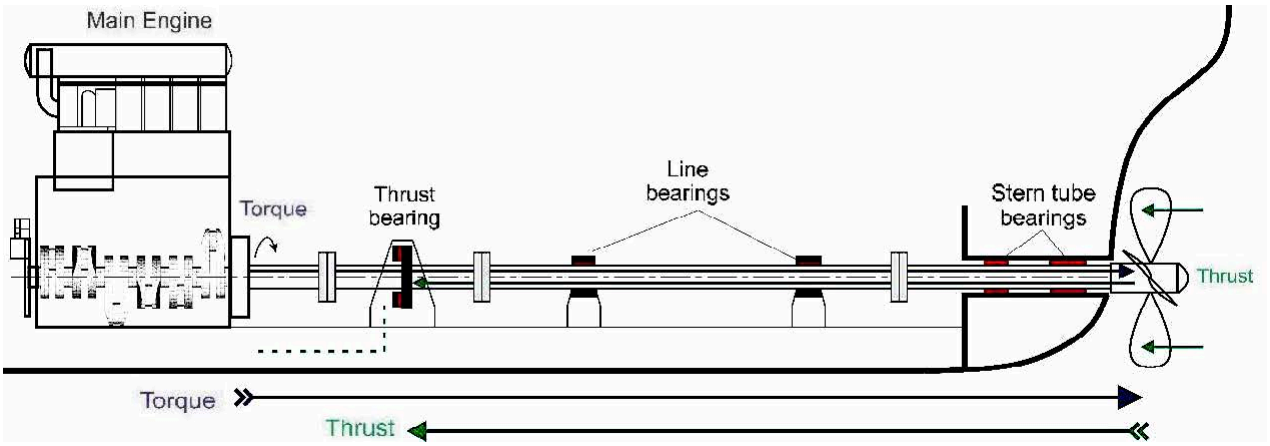

Figure 9: Typical shafting arrangement of a cargo vessel's propulsion system.

2.7.1 Oil Lubricated Journal Bearings

As mentioned above, in marine propulsion shaft configurations sterntube and intermediate line journal bearings are essential, oil bearings are being lubricated and cooled by oil. Sterntube oil bearings found in ships are usually made from cast iron or ductile cast iron housings that are babitted with tin or lead based white metal. Intermediate oil journal bearings are also commonly made from cast iron and lined with white metal. Also composite materials can be used depending on the application and the ship owners' requirements. Bearings can be designed to allow self-lubrication or forced lubrication, giving the optimal running surface for oil lubricants. Most commonly used designs in shaft line bearings are the plain and the split hydrodynamic bearings, with applications that also provide self-aligning design features.

Appropriate and successful design of a radial bearing leads to bearing pressures and hydrodynamic lubrication thickness suitable for the bearing materials and within manufacturers specified limitations. Additionally, as per IACS Unified Requirements M52 [41]: For oil lubricated bearings, which are approved for use as stern bush bearings, the length of the bearing is to be not less than 2.0 times the rule diameter of the shaft in way of the bearing. This requirement is in force for oil bearings of white metal, synthetic rubber, reinforced resin or plastic materials. For the former, the following requirement is also enforced: The length of the bearing may be less provided the normal bearing pressure is not more than 8 bar as determined by static bearing reaction calculation taking into account shaft and propeller weight which is deemed to be exerted solely on the aft bearing divided by the projected area of the shaft. However, the minimum length is to be not less than 1.5 times the actual diameter. Which also stands for bearings of composite materials with a lowered limit of nominal pressure at 6 bar, it is though stated that: Where the material has proven satisfactory testing and operating experience, consideration may be given to an increased bearing pressure. Setting minimum limits for the aft most propeller shaft bearing is of great significance in order to ensure suitable support and damping of possible whirling vibration.

2.7.2 Water Lubricated Journal Bearings

The use of hydrodynamic water-lubricated bearings in ships, although not a new application, has witnessed growing interest in recent years. Increasing ecological awareness and new environmental requirements evidently attribute to this, but water as a lubricant offers more than environmental compatibility.

These types of bearings use water, fresh or salt as the lubricant, rather than oil or grease, to support the rotating shaft and reduce friction and wear. Water-lubricated journal bearings are typically used in applications where oil or grease is not suitable, such as in environments where fire or environmental hazards are a concern, or in applications where water is readily available. They are also commonly used in marine and hydroelectric power applications, where water is abundant. Water-lubricated journal bearings are designed to operate with a thin film of water between the shaft and the bearing surface. The water acts as a lubricant and helps to reduce friction and wear between the shaft and the bearing. In addition, the water can help to dissipate heat generated by the bearing, which can prolong its life and increase its reliability. It is important to note that water-lubricated journal bearings require a clean and consistent supply of water to function properly, and the water must be free of impurities or contaminants that could damage the bearing surface or reduce its performance. Additionally, the design and operation of water-lubricated journal bearings

can be more complex than oil or grease-lubricated bearings, and special design considerations must be taken into account to ensure their proper functioning.

Properly designed water lubricated journal bearings can show improved lubrication performance, reliability, efficiency and solve problems regarding friction, wear, vibration, and noise, compared to conventional oil bearings [24]. These beneficial features are ascribed to the physical properties of water, mainly its low viscosity and high specific heat, and the properties of the bearing materials. Moreover, self-lubricating and anti-corrosion anti-wear tribological properties are optimal characteristics for water-lubricated bearing materials. It is however highlighted that the water's low viscosity causes these bearings to have lower load capacity at the same film thickness ([28], [19]). In other words, under the same conditions to achieve the same load capacity for a water-lubricated, the required film thickness observed is drastically lower, in comparison with an oil bearing. In the corresponding IACS requirement for water lubricated bearings [41], it is stated that the length of the bearing is not to be less than 4.0 times the rule of diameter of the shaft in the way of the bearing, and that for bearings of synthetic material consideration may be given for bearings of shorter length but not less than 2.0 times (requirement similar to the one corresponding to white metal lined oil lubricated bearings). It is also clarified that synthetic materials for application as water lubricated stern tube bearings are to be type approved.

In marine propulsion systems one can come across water-lubricated bearing applications in the propeller shaft support system and the stern rudder. Water lubricated bearings are also common in other machinery used in water-rich environmental conditions, examples are water pumps and hydraulic turbines. As stated, these journal bearings, if designed properly, may function under a hydrodynamic regime in the conditions of typical loads and speeds found in vessel machinery applications. In the respective previous paragraph, categories of bearing materials were concisely analysed. In regard to water-lubricated bearings two main categories are individuated, one including materials with higher elasticity (rubber, polymer and foil) and one with stiffer materials (bronze, ceramic and some composite) [27].

3 Mathematical Foundation of Fluid Lubrication Theory

Following the study and review of lubricants and journal bearings, the mathematical foundation of the fluid film lubrication mechanism is considered an essential part of this study. Fluid lubrication theory expounds the mechanism of separating bodies in contact with a fluid film, according to the physical principle of its motion through a thin gap of separation.

In other words, the relative motion of two pressed bodies leads to friction, fluid lubrication fills the separating gap with a fluid film that develops an elevated pressure to resist the closing force. The fluid lubricant obeys the physical laws of continuum mechanics comprising conservation of mass, momentum, and energy. The ensemble of the three conservation laws of fluid mechanics is attributed to the writings of Navier (1823) and Stokes (1845). Reynolds (1886) [42] first published the thin-film approximation of these equations toward an understanding of the origin of elevated pressure in a lubricating film, which is commonly identified with the theory of fluid-film lubrication.

3.1 Hydrodynamic Lubrication Theory in Journal Bearings

In this paragraph (and based on [36], [26]), it is considered fundamental to discuss the phenomenon of hydrodynamic lubrication and point out the characteristics of elastohydromynamic lubrication. In the following paragraphs, within this context, the foundation of fluid lubrication theory will be further analysed. Hydrodynamic lubrication is the phenomenon in which the formation of a thin lubricating film between two relatively moving, non-parallel surfaces allows their separation (fig. 10). The relative motion and misalignment of the surfaces are essential conditions for the formation of the hydrodynamic field. Between the two surfaces the lubricant oil is also moving. During the motion of this mechanical system a pressure field is generated in the fluid and the pressure gradient causes the fluid velocity profile to bend inwards at the entrance of the wedge and outwards at the exit. The generated pressure field is sufficient for the support of a certain load applied to the slider. It was found by Reynolds and many later researchers that most of the lubricating effect of oil could be explained in terms of its relatively high viscosity. As mentioned in [36] by Stachowiak: All hydrodynamic lubrication can be expressed mathematically in the form of an equation which was originally derived by Reynolds and is commonly known throughout the literature as the □□Reynolds equation. There are several ways of deriving this equation. Since it is a simplification of the Navier-Stokes momentum and continuity equation it can be derived from this basis. It is, however, more often derived by considering the equilibrium of an element of liquid subjected to viscous shear and applying the continuity-of-flow principle. The essential conditions for hydrodynamic lubrication, already mentioned (non-zero relative rotation angle of runner and stator), are also expressed in Reynolds equation. In addition, the influence of the geometry on the spatial rate of pressure change is clearly described [36].

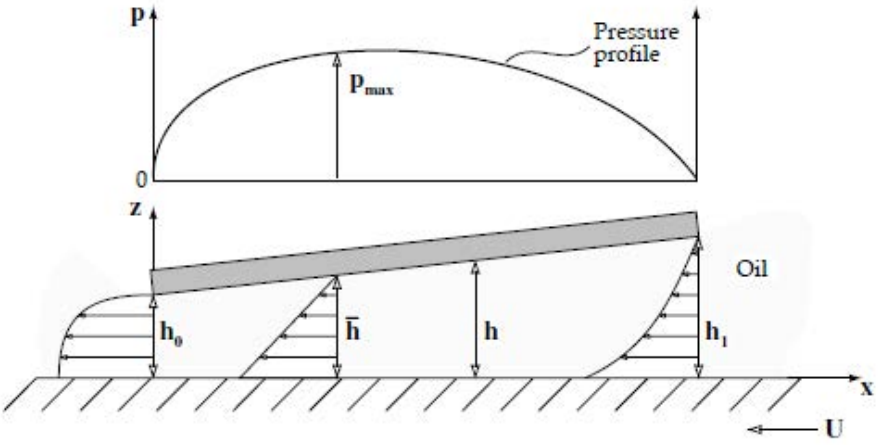

Figure 10: Formation of oil film and hydrodynamic pressure between non-parallel surfaces.

In order to mathematically express the principles of hydrodynamic lubrication a series of basic assumptions need to be true and are listed below:

- Newtonian, viscous, incompressible fluid lubricant
- Negligible lubricant inertia in comparison with the viscous forces
- Negligible gravitational forces
- Bearing inner diameter to bearing clearance ratio is close to infinity
- Steady lubricant flow and spatially constant viscosity

An extension to hydrodynamic lubrication theory is elastohydrodynamic lubrication. In short, this extension addresses the effects of elastic deformation and pressure-sensitive viscosity on the operational characteristics of lubricated surfaces. A review of the available literature on elastohydrodynamic lubrication of bearings indicates that the performance characteristics of journal bearings are affected by the bush bearing flexibility and the consequent deformation.

3.2 Navier-Stokes Equation and Applications in Lubrication

To characterise the motion of a fluid, rigorous mathematical statements of the stresses acting on it and the kinematics describing its motion are required. Newton's second law connects stress and motion, but the equations expressing the principle of conservation of mass and the conservation of linear momentum are fewer in number than the unknowns. The solution is obtained through additional constitutive equations of material characterisation. Thus, the Navier-Stokes equation is derived from the application Newton's law of viscosity, which specifies linear proportionality between stress and deformation. In this paragraph, the logical sequence for defining the Navier-Stokes problem is presented, through its fundamental equations.

3.2.1 Kinematic

Basic quantities and equations need to be defined in order to characterise fluid flow. Moreover, in order to describe the motion of a fluid a differentiation needs to be made between two interconnected types of coordinates. The coordinates of a material point are called its material (Lagrangian) coordinates, $X_i, i = 1, 2, 3$, while the coordinates $x_i, i = 1, 2, 3$, are called spatial (Eulerian) coordinates. Every position of the fluid corresponds to a binary link between all of its material points with spatial points. Observing a fluid moving through physical space equates with different positions, producing a sequence of configurations called motion.

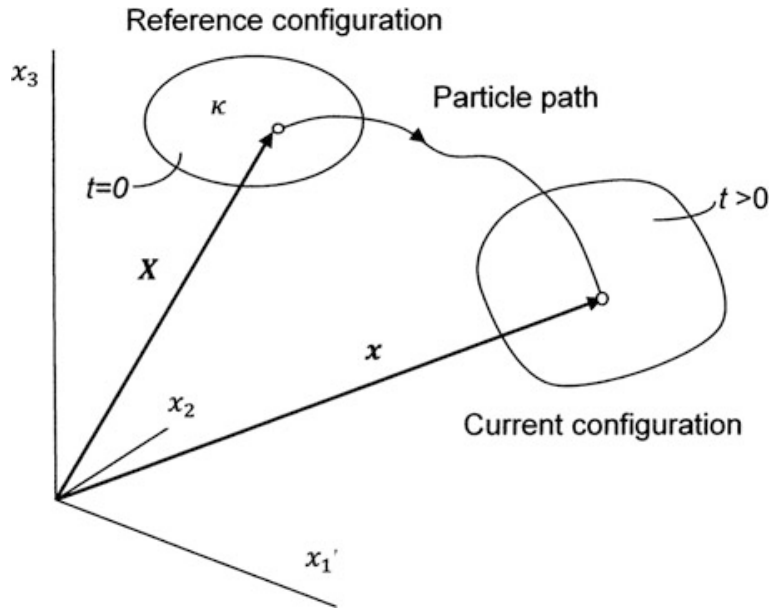

Figure 11: Motion of a Fluid Body

Otherwise stated and as depicted in figure 11, setting a start $t = 0$ and with t increasing, each particle of fluid passes through different spatial coordinates x_i while occupying material positions X_i. It can be expressed as:

$$x = \chi(X, t) \qquad t \geq 0$$

Velocity and acceleration can be described in association with material points as:

$$V(X, t) = \frac{\theta}{\theta t}\chi(X, t), \qquad A(X, t) = \frac{\theta^2}{\theta t^2}\chi(X, t)$$

Particle velocity and acceleration, as all variables, are related to the corresponding spatial quantities through motion:

$$V(X, t) = V[(\chi^{(-1)}(x, t), t] = v(x, t), \qquad a(x, t) = \frac{dv(x, t)}{dt} = \frac{\theta v}{\theta t} + v \cdot \text{grad}v$$

To state the principle of conservation of linear momentum (Newton's second law) the forces that might act on a fluid need to be defined. Forces can be differentiated in two groups: surface forces F_S and body forces F_B , the latter act through the mass centres of the body, while the former act across the bounding surface $S(t)$ of the material volume $V(t)$.

$$F_B = \int_{V(t)} \rho f \, d\theta, \qquad F_S = \oint_{S(t)} t \, ds$$

Where $f(x)$ expresses the body force per unit mass and θ corresponds to a fixed spatial volume (control volume) through which the fluid flow is observed and examined. The surface forces are characterised by applying the stress principle of Cauchy which states: on any imaginary closed surface there is a distribution of stress vectors t , such that the resultant and moment of t are equivalent to the resultant and moment of the actual forces that are exerted by the material outside the surface on the material inside.

The principle of conservation of linear momentum (newton's second law) is stated as: the rate of change of linear momentum of a material volume $V(t)$ equals the resultant force on the volume, $F_B + F_S$. The conservation of mass, also known as the continuity equation, corresponds to the principle that: the mass of a fluid $\mathbb{M}$ in a material volume $V(t)$ does not change by definition, as the latter moves with the fluid. These principles can be formulated, the latter with the use of the transport theorem, with the following equations:

$$\frac{d}{dt}\int_{V(t)} \rho v \, d\theta = \int_{V(t)} \rho f \, d\theta + \oint_{S(t)} t \, ds,$$

$$\frac{d}{dt}\mathbb{M} = \frac{d}{dt}\int_{V(t)} \rho \, d\theta = \int_V \left(\frac{d\rho}{dt} + \rho \, \text{div}v\right) d\theta = 0$$

Concerning the equation of mass conservation, as the limit of the integral is arbitrary, the integrand itself must vanish, leading to the equation of continuity for compressible fluid:

$$\frac{d\rho}{dt} + \rho \, \text{div}v = 0$$

For incompressible fluid, $\rho = constant$ thus:

$$\text{div}v = 0$$

3.2.2 Stress

The stress vector acting on the arbitrary surface at a point is a linear combination of the stress vectors on the coordinate surfaces through the point (Stokes 1845; Serrin 1959). Hence, the stress vector $t$acting at point P on an arbitrary surface with orientation n, can be computed by projecting the stress tensor T onto the surface at P

$$t = n \cdot T$$

or, in component form

$$t_i = n_i \cdot T_{ji}$$

Using the divergence theorem, the transportation and taking into account the conservation of linear momentum of the fluid, Cauchy's equation of motion is derived from the equations of the previous paragraph and is formulated as:

$$\rho \frac{dv}{dt} = \rho f + \mathrm{div} T$$

3.2.3 Constitutive Equations

In order to state the constitutive equations for Newtonian fluids an investigation of relative motion of arbitrary particles is needed. This analysis is necessary as the stress experienced by the fluid particle P depends on the deformation of the neighbourhood of that particle in which particle Q also belongs. By approximating the velocity at Q relative to that at P (figure)and through the needed simplifications and decompositions, the outcome is an equation of velocity that expresses all the motion components of a fluid particle. The mathematical process is rather simple has been presented in existing literature ([36], [43], [33]).

$$v = v_P + dx \cdot D + dx \cdot \Omega$$

While:

$$\mathrm{grad} v = \frac{1}{2}\left(\nabla v + \nabla v^T\right) + \frac{1}{2}\left(\nabla v - \nabla v^T\right) = D + \Omega$$

The equation can be written as:

$$v = v_P + \mathrm{grad}\left(\frac{1}{2}\mathcal{D}\right) + \frac{1}{2}\omega \times dx$$

Through this equation of relative velocity of two particles, the motion of the fluid is described as an arbitrary instantaneous motion v, is the superposition of a uniform velocity of translation, v_P, a dilatation along three mutually perpendicular axes, $grad\left(\frac{1}{2}\mathcal{D}\right)$, and a rigid body rotation of these axes, $\frac{1}{2}\omega \times dx$.

To formulate the stress a liquid is experiencing a mathematical process described extensively in literature is needed. This process leads to the constitutive equation for a compressible Newtonian fluid:

$$T = (-p + \lambda\theta)I + 2\mu D$$

Where p is the thermodynamic pressure and μ and λ are scalar functions of the thermodynamic state.

For an incompressible Newtonian fluid, $\Theta = 0$ and:

$$T = -pI + 2\mu D$$

Where p now is a fundamental dynamic variable and μ is a scalar function of temperature.

3.2.4 Boundary Conditions

The boundary conditions concerning velocity include no-slip for incompressible fluids (also for compressible but under conditions); while there are no boundary conditions on pressure, as it is induced by the flow or might be imposed externally.

3.2.5 Navier-Stokes Equation

Using the equations formulated in previous paragraphs the Navier-Stokes equation can be easily derived. In particular, substituting the stress formulation into Cauchy's equation of motion results in the Navier-Stokes equations for a compressible Newtonian fluid, and expressed as:

$$\rho\frac{dv}{dt} = \text{grad}(-p + \lambda\Theta) + \text{div}(2\mu D) + \rho f$$

In orthogonal Cartesian coordinates the component equations are:

$$\rho\left(\frac{\theta u}{\theta t} + u\frac{\theta u}{\theta x} + v\frac{\theta u}{\theta y} + w\frac{\theta u}{\theta z}\right) = \frac{\theta}{\theta x}\left[-p + \lambda\left(\frac{\theta u}{\theta x} + \frac{\theta v}{\theta y} + \frac{\theta w}{\theta z}\right) + 2\mu\frac{\theta u}{\theta x}\right] + \frac{\theta}{\theta y}\left[\mu\left(\frac{\theta u}{\theta y} + \frac{\theta v}{\theta x}\right)\right] + \frac{\theta}{\theta z}\left[\mu\left(\frac{\theta u}{\theta z} + \frac{\theta w}{\theta x}\right)\right] + \rho f_x,$$

$$\rho\left(\frac{\theta v}{\theta t} + u\frac{\theta v}{\theta x} + v\frac{\theta v}{\theta y} + w\frac{\theta v}{\theta z}\right) = \frac{\theta}{\theta y}\left[-p + \lambda\left(\frac{\theta u}{\theta x} + \frac{\theta v}{\theta y} + \frac{\theta w}{\theta z}\right) + 2\mu\frac{\theta v}{\theta y}\right] + \frac{\theta}{\theta x}\left[\mu\left(\frac{\theta u}{\theta y} + \frac{\theta v}{\theta x}\right)\right] + \frac{\theta}{\theta z}\left[\mu\left(\frac{\theta v}{\theta z} + \frac{\theta w}{\theta y}\right)\right] + \rho f_y,$$

$$\rho\left(\frac{\theta w}{\theta t} + u\frac{\theta w}{\theta x} + v\frac{\theta w}{\theta y} + w\frac{\theta w}{\theta z}\right) = \frac{\theta}{\theta z}\left[-p + \lambda\left(\frac{\theta u}{\theta x} + \frac{\theta v}{\theta y} + \frac{\theta w}{\theta z}\right) + 2\mu\frac{\theta w}{\theta z}\right] + \frac{\theta}{\theta x}\left[\mu\left(\frac{\theta u}{\theta z} + \frac{\theta w}{\theta x}\right)\right] + \frac{\theta}{\theta y}\left[\mu\left(\frac{\theta v}{\theta z} + \frac{\theta w}{\theta y}\right)\right] + \rho f_z.$$

For an incompressible fluid the Navier-Stokes equation can be obtained from the equations above by substituting $\Theta = 0$.

The Navier-Stokes problem consists of the equation of continuity, the three equations of motion presented above, and, for compressible fluids, the equation of state. For the more extensive and general mathematical examination of the equations formulated in this chapter the reader is referred to the literature cited and specifically to the publications by Stachowiak [36] and Szeri [43]. The equations stated in this section constitute the mathematical basis for describing the motion Newtonian fluids. The Navier-Stokes equation, together with the equation of conservation of mass and the boundary conditions on velocity and pressure (the latter, only where appropriate) constitute the mathematical characterisation of fluid flow. Last but not least, these equations are also employed in characterising the behaviour of lubricating films, but usually after simplifications provided by the geometry of typical lubricated contacts, such simplifications result in the Reynolds equation of lubrication which is examined in the next section.

3.3 Reynolds Equation and Applications

The process of finding solutions of the full Navier-Stoke equations can be simplified by introducing assumptions and adding boundary conditions, depending on the application that is studied. The Navier-Stokes momentum and continuity equation were employed by Reynolds to express the theory of lubrication. Through appropriate assumptions the Reynolds equation is derived and it constitutes the governing equation that describes the pressure distribution in a hydrodynamic film. This equation and its derivations are fundamental to the study of fluid-film bearings, as the evaluation of the pressure lubrication profile in a bearing with an arbitrary film shape, allows the determination of bearing performance parameters.

3.3.1 Basic Assumptions

The key assumptions that need to be introduced in order to derive the Reynolds equation are:

a. Newtonian fluid: Depends on the kind of the examined fluid.

b. Negligible inertia and body forces: Inertia can be neglected in conditions of high load and/or low rotational speeds, body forces are neglected since no outside field of forces acts on the fluid.

c. Laminar flow: This assumption is valid for relatively small bearings (large turbine bearings constitute an exception).

d. No slip at the fluid-solid edges-Negligible curvature effects: This assumption is valid since the velocity of the oil layer adjacent to the boundary is considered equal to the velocity of the boundary.

e. Negligible pressure gradient across the film thickness: This assumption is valid as the pressure remains usually constant, since film thickness varies in the range of micrometers (elastic films are an exception).

Some of these assumptions can be relaxed as a means of extending the derivation to more generalised forms. In other cases, assumptions and boundary conditions can be added in order to employ the equation to applications with specified conditions. Solution of the equation enables one to determine the pressure distribution on the bearing surfaces with an arbitrary film shape.

3.3.2 Reynolds Equation

The Reynolds equation combines the equations that govern the conservation of momentum and conservation of mass into a single equation where the unknown is pressure. The process of producing this equation begins with assuming an element of fluid from a hydrodynamic film and the equations describing its equilibrium as shown in figure 12:

For the forces acting on the x, y and z directions the condition is:

$$\frac{\theta\tau_x}{\theta z} = \frac{\theta}{\theta z}\left(\eta\frac{\theta u}{\theta z}\right) = \frac{\theta p}{\theta x}, \qquad \frac{\theta\tau_y}{\theta z} = \frac{\theta}{\theta z}\left(\eta\frac{\theta v}{\theta z}\right) = \frac{\theta p}{\theta y}$$

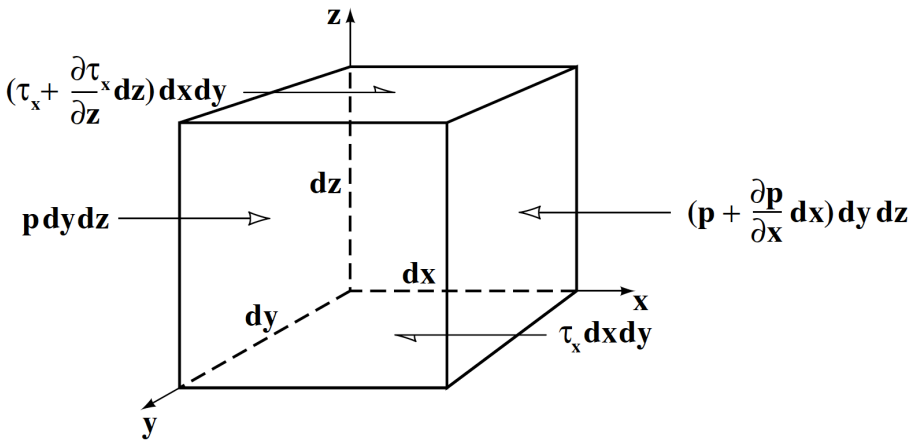

Figure 12: Equilibrium of an element of fluid from a hydrodynamic film.

and

$$\frac{\theta p}{\theta z} = 0, \text{since the pressure is constant through the film.}$$

Where:

$\tau_{x,y}$: is the shear stress acting in the x, y directions

p : is the pressure

η : represents the viscosity of the lubricant film

u, v : denote the flow velocity in the x and y directions respectively

The equation of balance of the forces acting in the x direction can be integrated, assuming a constant viscosity throughout the film, and the variables can be separated as follows:

$$\theta\left(\eta \frac{\theta u}{\theta z}\right) = \frac{\theta p}{\theta x} \theta z$$

integration and a following separation of values yield the next equations respectively:

$$\eta \frac{\theta u}{\theta z} = \frac{\theta p}{\theta x} z + C_1 \quad \text{or} \quad \eta \theta u = \left(\frac{\theta p}{\theta x} z + C_1\right) \theta z$$

another integration gives:

$$\eta u = \frac{\theta p}{\theta x} \frac{z^2}{2} + C_1 z + C_2$$

As shown in the coordinate system in figure 13 the boundaries of the wedge are defined in $z = 0$ and $z = h$:

And the conditions are: $u = U_1$ at $z = h$ and $u = U_2$ at $z = 0$, after the boundary conditions are defined, the constants C_1 and C_2 are calculated as:

$$C_1 = \frac{\eta}{h}(U_1 - U_2) - \frac{\theta p}{\theta x} \frac{h}{2}$$

$$C_2 = \eta U_2$$

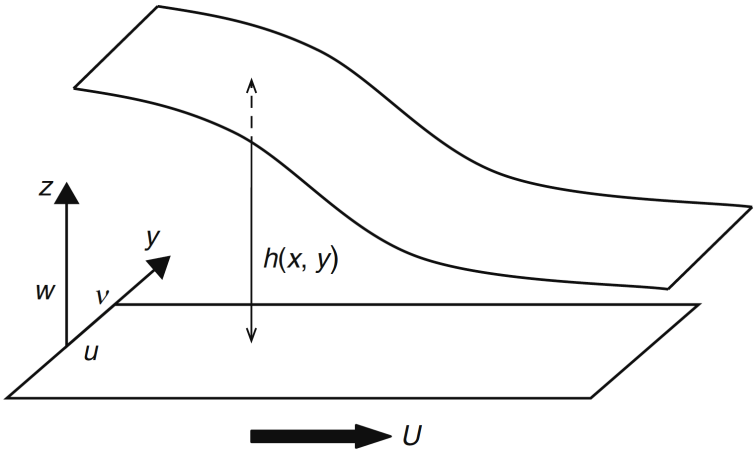

Figure 13: Coordinate system for the Reynolds Equation

The following equation is produced by substitution of the above constants.

$$\eta u = \frac{\theta p}{\theta x}\frac{z^2}{2} + \left(\frac{\eta}{h}(U_1 - U_2) - \frac{\theta p}{\theta x}\frac{h}{2}\right)z + \eta U_2$$

Solving for the unknown flow velocity u in the x direction yields:

$$u = \left(\frac{z^2 - zh}{2\eta}\right)\frac{\theta p}{\theta x} + (U_1 - U_2)\frac{z}{h} + U_2$$

Following the same process the equation for the flow velocity v in the y direction is calculated as:

$$v = \left(\frac{z^2 - zh}{2\eta}\right)\frac{\theta p}{\theta y} + (V_1 - V_2)\frac{z}{h} + V_2$$

The three terms in each of the two velocity equations represent the velocity profiles across the fluid film as explained in [36] and they are schematically shown in figure 14:

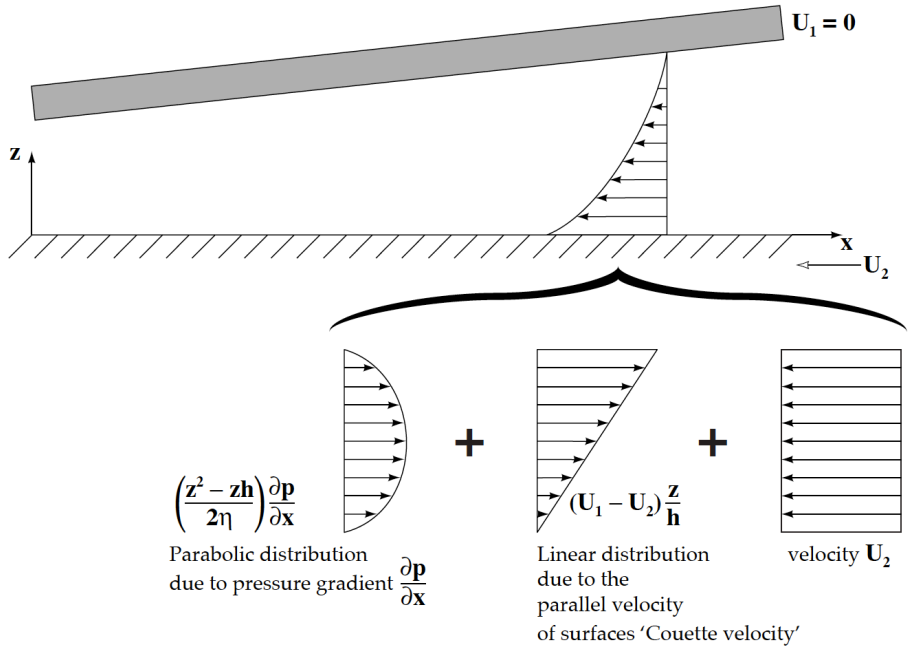

Figure 14: Velocity profiles at the entry of the hydrodynamic film.

In order to write the conservation of mass equation for a compressible fluid the rates of flow of the lubricant in the x, y, z directions need to be expressed. The difference between the influx and efflux rate is equal to the lubricant mass accumulation rate (continuity of flow), thus:

$$\frac{\theta\rho}{\theta t}dxdydz = \rho udydz + \rho vdxdz + \rho wdxdy - \left(\rho u + \frac{\theta(\rho u)}{\theta x}\right)dydz - \left(\rho v + \frac{\theta(\rho v)}{\theta y}\right)dxdz - \left(\rho w + \frac{\theta(\rho w)}{\theta z}\right)dxdy$$

After simplifications the conservation of mass equation is given as:

$$\frac{\theta\rho}{\theta t} + \frac{\theta(\rho u)}{\theta x} + \frac{\theta(\rho v)}{\theta y} + \frac{\theta(\rho w)}{\theta z} = 0$$

Where ρ is is the density and w is the velocity component across the gap along the z direction. The Reynolds equation is obtained by substituting u and v and integrating across the film thickness, h. The integration of each term is presented below:

$$\int_0^h \frac{\theta\rho}{\theta t}\,dz \overset{Leibniz}{=} \frac{\theta}{\theta t}\int_0^h \rho\,dz - \rho\frac{\theta h}{\theta t} = \frac{\theta(\rho h)}{\theta t} - \rho\frac{\theta h}{\theta t}$$

$$\int_0^h \frac{\theta(\rho u)}{\theta x}\,dz \overset{Leibniz}{=} \frac{\theta}{\theta x}\int_0^h \rho u\,dz - \rho u_h\frac{\theta h}{\theta x}$$

An equivalent equation results for the third term. After the required integrations and the replacement of velocity values, as calculated above, are taken into account, the resulting values of the second and third term are:

$$\int_0^h \frac{\theta(\rho u)}{\theta x}\,dz = \frac{\theta}{\theta x}\left(-\rho\frac{h^3}{12\eta}\frac{\theta p}{\theta x} + \rho h\frac{U_1+U_2}{2}\right) - \rho U_1\frac{\theta h}{\theta x}$$

$$\int_0^h \frac{\theta(\rho v)}{\theta y}\,dz = \frac{\theta}{\theta y}\left(-\rho\frac{h^3}{12\eta}\frac{\theta p}{\theta y} + \rho h\frac{V_1+V_2}{2}\right) - \rho V_1\frac{\theta h}{\theta y}$$

and the final term:

$$\int_0^h \frac{\theta(\rho w)}{\theta z}\, dz = \rho(w_h - w_0)$$

Assuming that the surfaces are impermeable and neglecting terms involving physical stretch, density wedge, and local expansion, the following simplified Reynolds equation, for an incompressible fluid, is derived with the substitution of the above integrated terms:

$$\frac{\theta}{\theta x}\left(\frac{\rho h^3}{\eta}\frac{\theta p}{\theta x}\right) + \frac{\theta}{\theta y}\left(\frac{\rho h^3}{\eta}\frac{\theta p}{\theta y}\right) = 6\left(U\frac{\theta \rho h}{\theta x} + V\frac{\theta \rho h}{\theta y}\right) + 12\rho(w_h - w_0)$$

3.3.3 Simplifications to the Reynolds Equation and Derivations

The Reynolds equation can be used for a series of different engineering applications and it can be modified and simplified in accordance to the specified requirements. The most common simplifications adopted in studies are the following:

Unidirectional Velocity: The coordinate system configuration (axis direction) can be chosen so that one of the velocities is nullified. Such a coordinate system is used in the examination of journal bearings, where the hydrodynamic film is generated by the angular motion of the shaft, without any axial motion ($V = 0$). The resulting equation is:

$$\frac{\theta}{\theta x}\left(\frac{\rho h^3}{\eta}\frac{\theta p}{\theta x}\right) + \frac{\theta}{\theta y}\left(\frac{\rho h^3}{\eta}\frac{\theta p}{\theta y}\right) = 6U\frac{\theta \rho h}{\theta x} + 12\rho(w_h - w_0)$$

Steady Film Thickness Condition: Assuming no vertical flow across the film translates to a steady film thickness and a constant distance between the two surfaces ($w_h - w_0 = 0$). This assumption, for example, leads to the neglect of any vibration of bearings and any other type of motion of surfaces known as a squeeze film effect. The Reynolds equation with this assumption taken into account is written as:

$$\frac{\theta}{\theta x}\left(\frac{\rho h^3}{\eta}\frac{\theta p}{\theta x}\right) + \frac{\theta}{\theta y}\left(\frac{\rho h^3}{\eta}\frac{\theta p}{\theta y}\right) = 6U\frac{\theta \rho h}{\theta x}$$

Isoviscous Condition: Applying the assumption that the lubricant viscosity is constant over the film ($\eta = constant$) is known in literature as the isoviscous model. It is used in many engineering models where the the thermal effects in hydrodynamic films are neglected.

$$\frac{\theta}{\theta x}\left(\rho h^3\frac{\theta p}{\theta x}\right) + \frac{\theta}{\theta y}\left(\rho h^3\frac{\theta p}{\theta y}\right) = 6\eta\left(U\frac{\theta \rho h}{\theta x} + V\frac{\theta \rho h}{\theta y}\right) + 12\rho\eta(w_h - w_0)$$

Constant Density: In the region of the bearing where positive pressures exist (active zones), lubricant density can be assumed constant ($\rho = constant$) as the lubricant is a non-compressible fluid. The

Reynolds equation can be simplified to:

$$\frac{\theta}{\theta x}\left(h^3\frac{\theta p}{\theta x}\right)+\frac{\theta}{\theta y}\left(h^3\frac{\theta p}{\theta y}\right)=6\eta\left(U\frac{\theta h}{\theta x}+V\frac{\theta h}{\theta y}\right)+12\eta(w_h-w_0)$$

Other simplifications can be applied depending on the type of each study and its requirements. For simple engineering analyses the pressure gradient acting along an axis (X or Y in the coordinate system defined in Fig. 13) can be neglected. In journal bearing analysis, this assumption corresponds to the long bearing approximation or the narrow bearing approximation depending on which pressure gradient is considered negligibly small compared to the other. It is evident that the simplifications described above can be combined and create other forms of the Reynolds equation. The unidirectional velocity approximation is used in most studies examining journal bearings, while the use of the other simplifications listed varies depending on the goal of each study.

3.3.4 Boundary Conditions

For a solution of the Reynolds to be achieved a set of boundary conditions is required. Historically, in past studies the most predominant sets of boundary conditions are the following:

Full-Sommerfeld condition: Is expressed by the assumption of pressure equal to zero at the edges of the unwrapped journal bearing geometry. According to this assumption, negative pressure is formed in the diverging region which is the mirror image (equal and opposite) of the pressure distribution in the converging region [36]. Consequentially, the total pressure is equal to zero making this condition unrealistic and thus rarely used.

Half Sommerfeld condition: Is expressed by the assumption of positive pressure distribution in the converging section identical to the corresponding distribution of the full Sommerfeld condition. While, negative pressure in the diverging region is considered constant and equal to zero. This set of boundary conditions is quite simple and easy to apply but its physical basis is erroneous, since it leads to discontinuity of flow between the two regions [36].

Reynolds condition: This boundary conditions set also suggests that the negative pressure in the diverging region can be considered equal to zero as it cannot be sustained. And in the boundary region between zero and non-zero pressure the following condition should apply: $p=\frac{dp}{dx}=0$. The results of calculations when this set of boundary conditions is applied are more accurate than with the two previous sets [36], and it is used for the pressure calculations of the present study.

4 Computational Approach for Hydrodynamic Lubrication Problems in Journal Bearings

As the mathematical foundation of the fluid film lubrication mechanism in journal bearings was established in the previous chapter, a presentation of the resolution method for the Reynolds equation, employed in this study, follows. For bearings of finite length numerical methods as finite differences, finite elements and finite volumes can be applied in order to acquire a satisfactory solution.

4.1 Finite Difference Method for Fluid Film Bearings

Reynolds equation is a partial differential equation (PDE) and an approach for its resolution, for the calculation of pressure distribution, is through the finite difference method (FDM). Furthermore, as defined in [44] FDM is a numerical procedure applied for the solution of differential equations, where derivatives are approximated by linear functions using finite differences equations. In other words, the basis of the method is the replacement of differential equations with equivalent finite differences extracted from the Taylor series expansion.

Journal bearing geometry is studied in the unwrapped domain and a numerical solution for a pressure distribution at this domain can be achieved using FDM. The calculation of pressure for each of the nodal points of the grid covering the domain (fig. 15) requires the replacement of the continuous differential terms with the linear finite difference approximations [44]. The unwrapped journal

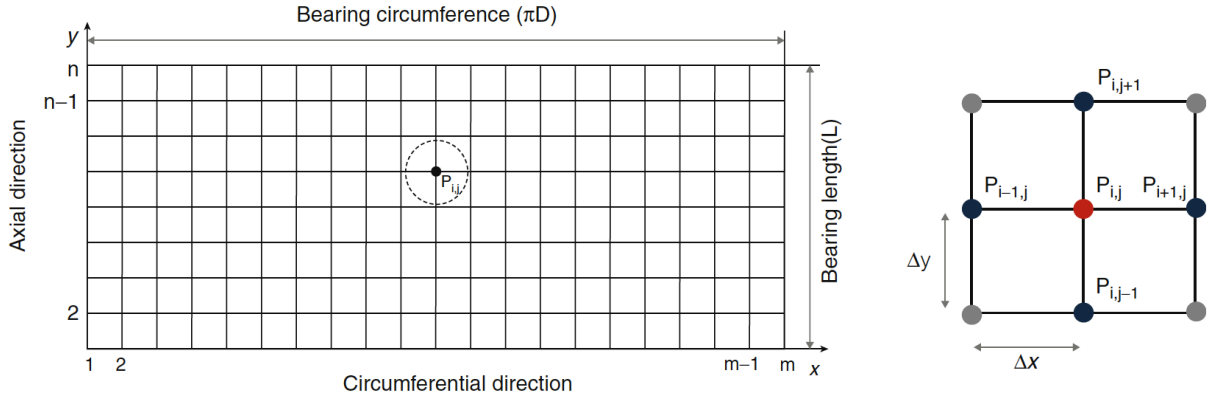

Figure 15: Journal bearing grid for finite difference solution of Reynolds equation.

bearing grid is formed by a finite number of divisions along the length and the circumference of the bearing. Creating a set of points each one identified by i, j indices and with four neighbouring nodes (except for the boundary nodes). The first and second order pressure derivatives of the Reynolds equation are replaced by linear functions as they result from central difference approximations as follows:

$$f_{i+1,j} = f_{i,j} + \Delta x \left(\frac{\theta u}{\theta x}\right)_{i,j} + \frac{\Delta x^2}{2!}\left(\frac{\theta^2 u}{\theta x^2}\right)_{i,j} + \frac{\Delta x^3}{3!}\left(\frac{\theta^3 u}{\theta x^3}\right)_{i,j} + \frac{\Delta x^4}{4!}\left(\frac{\theta^4 u}{\theta x^4}\right)_{i,j} + \dots$$

$$f_{i-1,j} = f_{i,j} - \Delta x \left(\frac{\theta u}{\theta x}\right)_{i,j} + \frac{\Delta x^2}{2!}\left(\frac{\theta^2 u}{\theta x^2}\right)_{i,j} - \frac{\Delta x^3}{3!}\left(\frac{\theta^3 u}{\theta x^3}\right)_{i,j} + \frac{\Delta x^4}{4!}\left(\frac{\theta^4 u}{\theta x^4}\right)_{i,j} + \dots$$

With smaller increments (Δx) faster convergence can be achieved and the higher order terms can be neglected, therefore the derivatives can be written as:

$$\left(\frac{\theta f}{\theta x}\right)_{i,j} = \frac{f_{i+1,j} - f_{i-1,j}}{2\Delta x}$$

$$\left(\frac{\theta^2 f}{\theta x^2}\right)_{i,j} = \frac{f_{i+1,j} - 2f_{i,j} + f_{i-1,j}}{\Delta x^2}$$

For the extended Finite Difference Method the reader is referred to existing literature ([44], [36]). In the following paragraphs the FDM solution algorithm used in this study is further analysed.

4.2 Reynolds Equation in Journal Bearings

Hydrodynamic lubrication problems have been approached with different methods and several algorithms have been proposed for their solutions. The most accurate, and at first glance straightforward, method would be to express and solve the Navier Stokes momentum and continuity equation. But, to follow this method is a computation intensive task. As it has already been analysed, several simplifications and the derivation of the Reynolds equation allow for a more computationally efficient solution method.

4.2.1 Solution Algorithm

In this section, an algorithm introduced by Raptis in [45] and used in this study will be presented. This solver for the Reynolds equation has been developed at the NTUA section of Marine Engineering. At the start of this algorithm, all the necessary geometric and operational characteristics of the journal bearing (L, D, c, speed etc.), the solver parameters (grid details, solver selection, convergence criteria, points per cycle, etc.) and the applied bearing loads in the x-and y-directions are read from an input file. Then, the unwrapped journal bearing is been discretised into small divisions.

The next step involves initial assumptions for eccentricity e_0 and attitude angle φ_0 and an initial calculation for the film thickness geometry h_0. Using the Gauss-Seidel iterative method, solution of the Reynolds is achieved numerically and the pressure field is calculated. The hydrodynamic force components in axis z, x are derived by integration of the pressure field on the bearing surface. Force equilibrium is attained if the initial assumptions for eccentricity for eccentricity e_0 and attitude angle φ_0 are correct. Usually that is not the case, and proper values of e_0, φ_0 need to be re-estimated by means of a Newton-Raphson method for two variables, until force equilibrium is achieved. At the end, all the bearing operational parameters of interest are calculated and printed to an output file for further processing. For the application of the algorithm described above, as well as its extension presented in the next paragraph, the programming language C++ is used.

4.2.2 Elastic Deformation in Journal Bearings - Algorithm Extension

As mentioned in previous paragraphs, elastic deformation of the bearing bush affects the pressure distribution and the operational characteristics of the bearing in general. An extension to the algorithm discussed in the previous paragraph can be made with the application of the Winkler elastic deformation model analysed in paragraph 2.6.2. Furthermore, by applying a deformation model to the inner layers of a journal bearing, a numerical model that investigates the effect of lining compliance can be developed. Even though, the Winkler or column model can be considered rather simple to its expression, it constitutes a useful way for modelling elastic deformation without the requirement for an enormous amount of calculating power.

The algorithm extension requires a series of steps based on the expression of elastic deformation which is:

$$h_{ed} = \Delta y_i = \delta_{Winkler} = \frac{tP_{i,j}}{E} \cdot \frac{(1+v)(1-2v)}{1-v}$$

Where:

$\delta_{Winkler}, h_{ed}$: elastic deformation
t : bearing shell thickness
$P_{i,j}$: hydrodynamic pressure at each computational node
E : Young's modulus
v : Poisson's ratio

At the start of this extended algorithm, the input file created must also contain some additional geometrical and operational characteristics (bearing shell thickness, Young's modulus, Poisson's ratio) an initial value for the elastic deformation. Then the value of elastic deformation is added as a factor of the oil film thickness. The algorithm continues, as described in this previous paragraph, and the pressure field is calculated allowing the calculation of a new value for the elastic deformation thickness component. This sequence is shown schematically in figure 16.

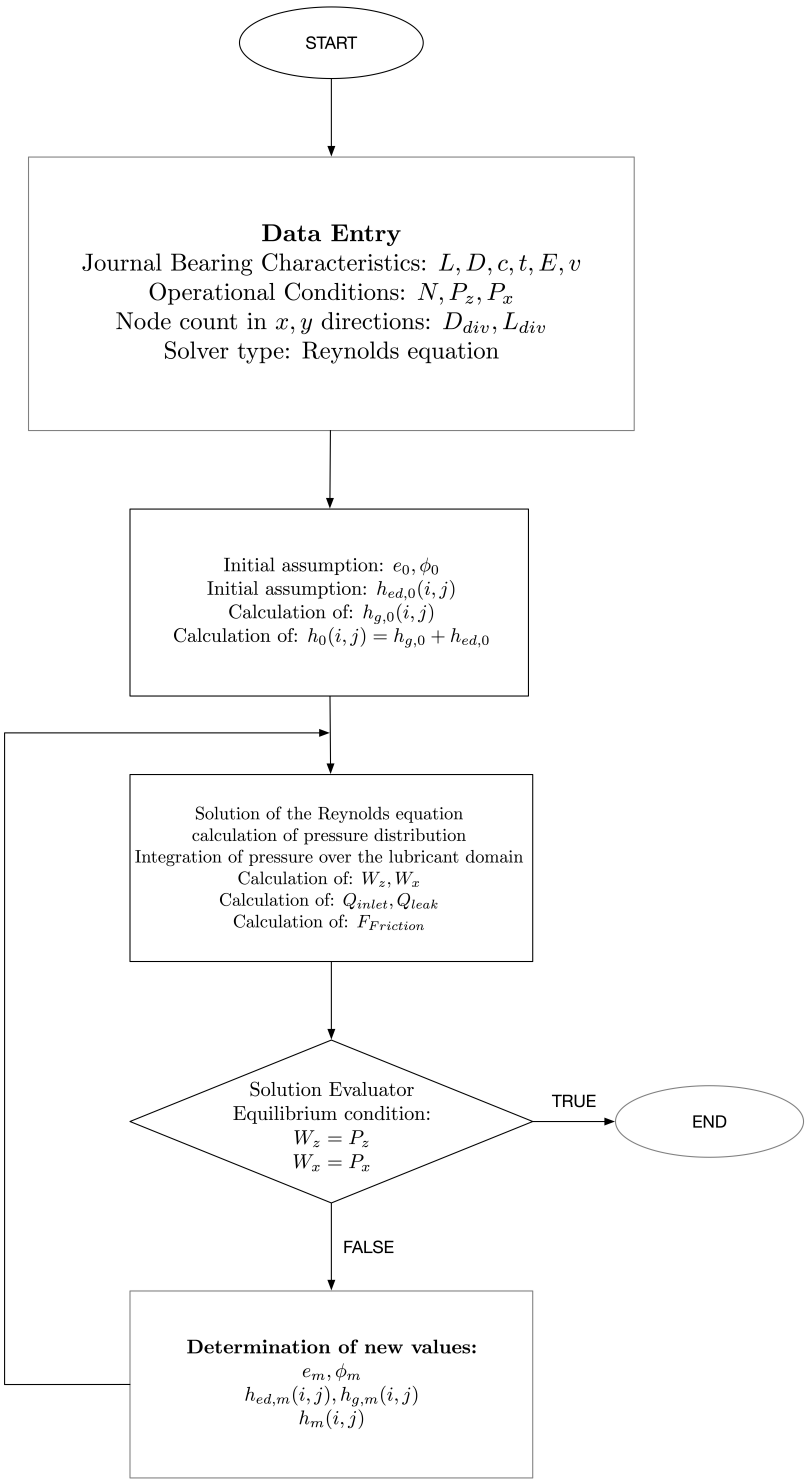

Figure 16: Reynolds equation solution flowchart, with elastic deformation extension.

5 Elastohydrodynamic Model Extension Validation and Study

In the present section, the Finite Difference Model presented above is validated for both oil and water lubricated journal bearings. Suitable simulations are carried out and the results, yielded from the proposed solution for the Reynolds equation extended with the Winkler model, are compared with results published in literature.

Additionally, appropriate simulations are completed, in order to highlight the effect the extension, which considers the elastic deformation of the bearing liner, has on the results. This is achieved by comparing these results with the corresponding output, obtained from the original solution algorithm.

5.1 Validation of Compliant Journal Bearing Bush Liner Model

In order to investigate the applicability of the integration of the Winkler-plane stress hypothesis model to the solution algorithm, data derived from validated studies are needed. As analysed in the previous paragraphs, this model is used to predict the deformation of the compliant bearing liner. With its implementation this model will have an effect on the pressure profiles produced by the solution of the Reynolds equation, as explained in the relative flowchart, presented in the previous section.

As described in the preceding chapters, journal bearings operation is based on the developed hydrodynamic pressure fields. The calculation of this operational characteristic is conducive to the prediction of smooth bearing function. It also allows one to perceive the synergy of the lubricant and of all the machine elements, or to detect possible anomalies. The validation simulations will be carried out for both water and oil lubricated journal bearings. Taking that into consideration, the studies used for the objective of validating the model, focus on obtaining precise results for the pressure profiles developed in plain journal bearings, yielded from the relative simulations. The results are illustrated in proper diagrams and presented in tables, which are followed by corresponding analyses.

5.1.1 Oil Lubricated Bearings Validation Cases

In order to validate the solution algorithm the results obtained are compared against results from an experimental analysis of plain journal bearings performance characteristics, presented by Bouyer and Fillon et all in [46] and in [47]. The test apparatus used in this study has been used and presented in more studies by the authors, its main features are noted for the purposes of the present study.

Moreover, the journal is made of steel, while the bush is made of bronze, also the main design characteristics of the journal bearing, operating conditions of the tests and lubricant characteristics are presented in the following table [46], [47]:

Table 4: Oil lubricated journal bearing design characteristics and operating conditions.

Quantity	Nomenclature	Value	Units
Bearing diameter	D	100	mm
Bearing length	L	80	mm
Radial clearance	C	0.11	mm
Bush Outer Diameter	d	200	mm
Liner Wall Thickness	t	50	mm
Length/Diameter	L/D	0.8	-
Liner Young's modulus	E	130	GPa
Liner Poisson's ratio	v	0.34	-
Rotational Speed	N	1500, 2000, 3000, 4000	RPM
Vertical Load	W	3000, 9000	N
Lubricant type	-	ISO VG 32	-
Density	ρ	870	kg/m^3
Specific heat capacity	c_f	2000	J/kg·K
Thermal conductivity	k	0.132	W/m·K
Oil viscosity at 35 ^oC	μ_{35}	0.0358	Pa·s

The corresponding parameters necessary for the simulations are naturally identical to the ones of the experimental tests. Additional input parameters concerning the model of the unwrapped journal bearing are presented in the next table.

Table 5: Oil lubricated journal bearing validation models input parameters.

Quantity	Nomenclature	Value
Mesh axial divisions	L_{div}	81
Mesh circumferential divisions	D_{div}	101
Solution type	-	Steady
Thermal analysis	-	Isothermal

A comparison of the pressure profiles in the journal bearing mid-plane, calculated with the elasto-hydrodynamic model and measured experimentally, is presented in figure 17. The tested case shaft rotational speed is 2000 RPM and a static load of 3000 N is exerted. Additionally, cases with shaft rotational speeds 1500, 2000, 3000, 4000 RPM and a load of 9000 N are simulated and the derived maximum pressure values of the lubrication film are set against the corresponding experimental, also the difference is calculated and presented in figure 18.

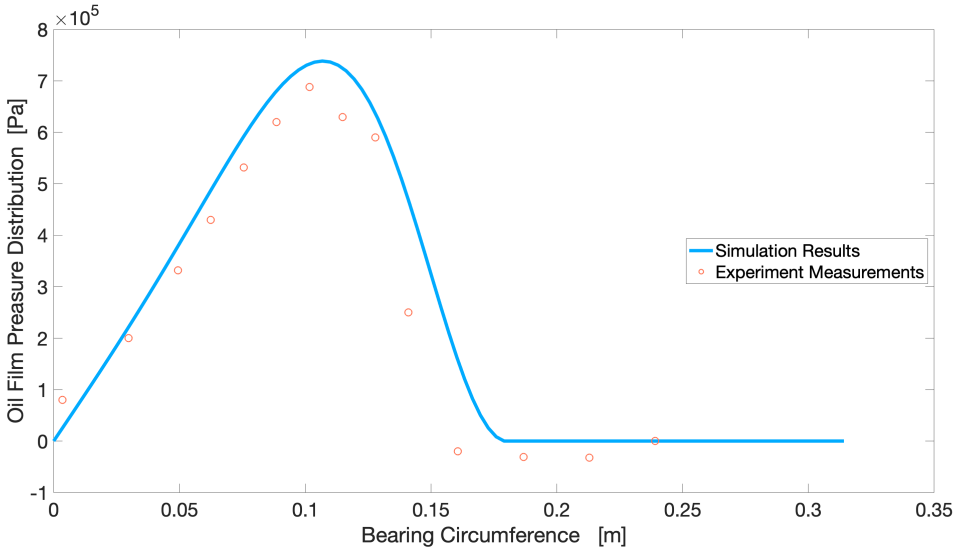

Figure 17: Mid-plane pressure distributions from measured and calculated results.

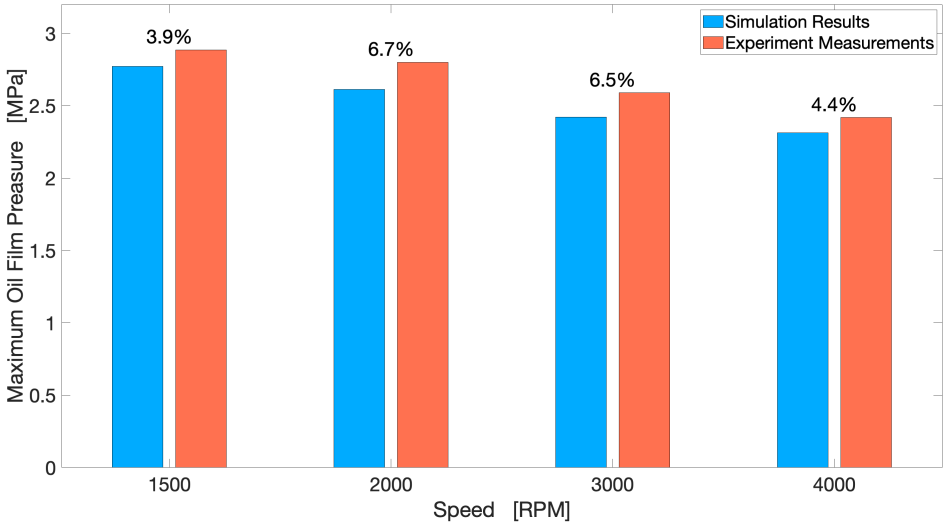

Figure 18: Mid-plane maximum pressure values from measured and calculated results.

Numerical simulation results show good agreement with the experimental measurements. Moreover, the pressure profile's maximum value is calculated with an 6.84 % difference from the experimental results. In the next set of simulations the maximum difference between the calculated and measured values is 6.70%. The deviation in the experimental and the calculated results can be attributed to the fixed values of oil temperature and viscosity, as well as the values of liner material properties. Additionally the small difference in the spatial distribution of the oil film reformation and the pressure profile can be justified, in large part, by the influence of the location and the pressure of the supply groove, as described analytically in one of the reference papers [47]. Last but not least, a relative

margin of error is accepted for the experimental results, as described by the authors, due to the imperfect shape of the bush and the operation of the test rig, as well as for the simulation results.

5.1.2 Water Lubricated Bearings Validation Cases

An equivalent process, with the one presented above, needs to be carried out for water lubricated journal bearings. A study published by Litwin [48] is used for this purpose. In this article, measurements are conducted on water lubricated shaft bearings using a single bearing test stand, which has been presented and employed in a series of studies, including [49] and [50]. As described by the author in the paper, the test bearing is set and sealed in a steel sleeve and fitted with a bush of composite polymer material, external load can be exerted on the bearing by a lever force. A detailed presentation of the test bearing set up and the experimental conditions follows in the next table.

Table 6: Water lubricated journal bearing design characteristics and operating conditions.

Quantity	Nomenclature	Value	Units
Bearing diameter	D	100	mm
Bearing length	L	300	mm
Radial clearance	C	0.1	mm
Bush Outer Diameter	d	124	mm
Liner Wall Thickness	t	12	mm
Length/Diameter	L/D	3	-
Liner Young's modulus	E	4.5	GPa
Liner Poisson's ratio	v	0.45	-
Rotational Speed	N	180, 420, 660	RPM
Vertical Load	W	6000 0.2	N MPa
Lubricant type	-	Fresh water	-
Density	ρ	1000	kg/m^3
Specific heat capacity	c_f	4182	J/kg·K
Thermal conductivity	k	0.6071	W/m·K
Water viscosity at 25 °C	μ_{25}	1.0016	mPa·s
Water viscosity at 5 °C	μ_5	1.55	mPa·s

As presented in the previous paragraph for the oil lubricated bearing, the additional input parameters concerning the model of the unwrapped water lubricated journal bearing are presented in the next table.

Table 7: Water lubricated journal bearing validation models input parameters.

Quantity	Nomenclature	Value
Mesh axial divisions	L_{div}	301
Mesh circumferential divisions	D_{div}	101
Solution type	-	Steady
Thermal analysis	-	Isothermal

In the next two figures, first (fig. 19) a comparison of the pressure profiles in the mid-plane is presented and a comparison of the pressure maximum values follows (fig. 20). The pressure measured in the water film for a test of 180 RPM and a load of 6000 N is used to validate the mid-plane pressure results of the model. Furthermore tests of the same load, executed with shaft rotational speeds of 180, 420, 660 RPM are used to compare the maximum pressure values derived from the model.

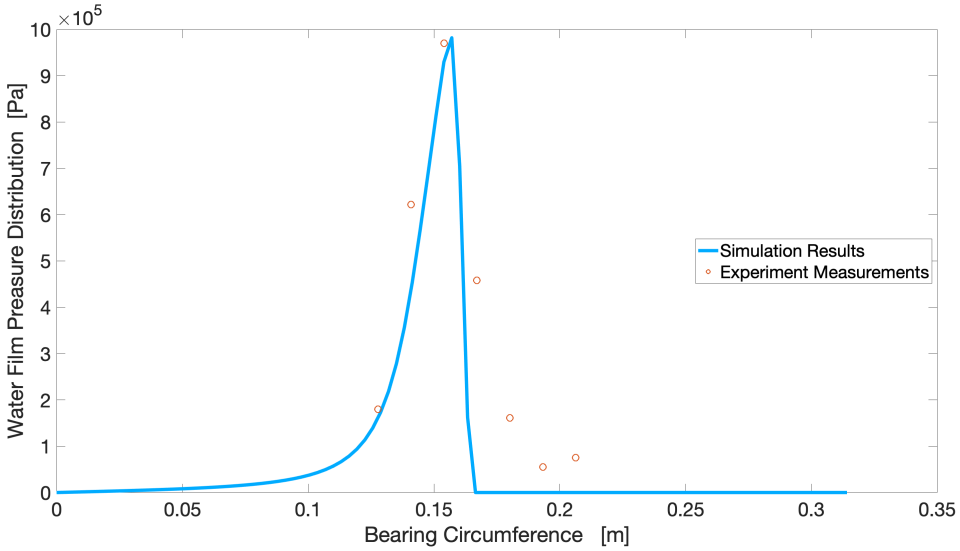

Figure 19: Mid-plane pressure distributions from measured and calculated results.

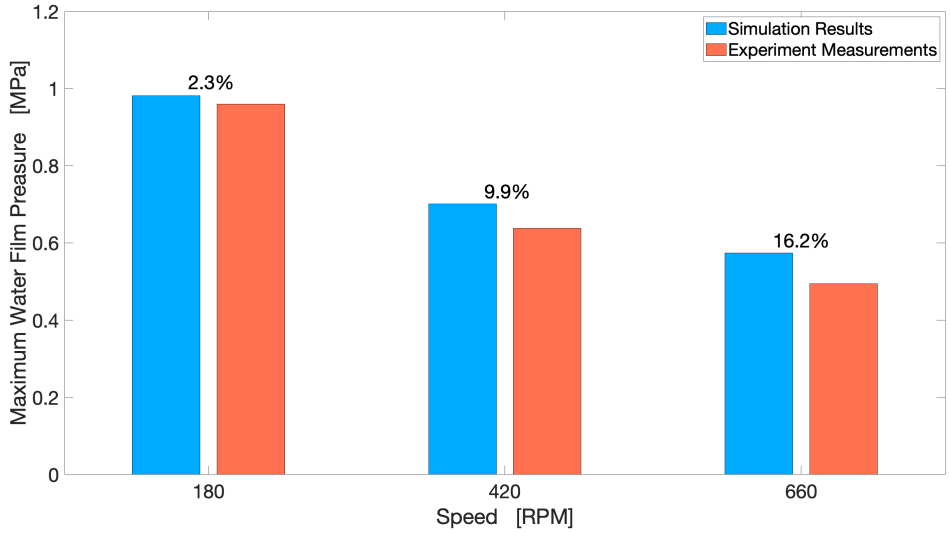

Figure 20: Mid-plane maximum pressure values from measured and calculated results.

The form of the calculated pressure profile shows good agreement with the profile developed in the test rig. Similarly to the oil lubricated journal bearing validation cases, the deviation of the results can be attributed to a margin of error loaded in the experimental and the simulation models, and to assumptions as is the constant temperature, water viscosity, liner material elastic properties, the imperfect and swelled shape of the bush, as well as the configurations of the supply groove and pressure sensors. In the first simulation, the pressure profile's maximum value is calculated with a 2.28 % difference from the experimental results. rising the shaft rotational speed causes an increase to the difference which reaches 16.16 % at 660 RPM.

It is also noted that in this set of simulations, which are carried out to validate the model for water lubricated bearings, the calculated maximum pressures are higher than the measured ones. While in the validation cases of oil lubricated bearings, presented before, the calculation results demonstrate higher values. This is an indication to the influence of different operational parameters, mainly the physical properties of the lubricant but also others like the exerted load and the shaft rotational speed, on the application of the plane strain hypothesis model. Similar comparisons, with an emphasis on the influence of a series of design and operating characteristics, are presented in the following chapter.

5.2 Investigation of the Effect of Bush Liner Compliance

Since the applicability of the Winkler-plane stress hypothesis model in journal bearings was investigated and confirmed in the previous paragraph, the next step concerns the investigation of its effect when adapted in the solution algorithm. Moreover, the purpose of this section and the presented simulations is to showcase the influence of the compliant lining on journal bearing behavior and performance. This is achieved through the completion of appropriate comparative simulations, using models with and without the bush bearing deformation extension algorithm.

In order to demonstrate the practicality and the advantage of applying numerical solutions, which incorporate the computation of the bush deformation, an array of design and operating characteristics is used. An appropriate analysis is performed for both oil and water lubricated journal bearings.

5.2.1 Bush Liner Compliance Effect in Oil Lubricated Bearings

Conducive to the aim of understanding the usefulness of the extended algorithm is the completion of suitable simulations. Equally important is the presentation and the analysis of the corresponding results. In the following table the design characteristics and operating conditions of the oil lubricated journal bearing, investigated in this section, are presented, and in the one following more parameters are presented, particular to the simulation model. Three different bush-liner designs were adopted and tested, one equipped with white metal liner material and two with elastomeric material and different thickness.

Table 8: Oil lubricated journal bearing design characteristics and operating conditions.

Quantity	Nomenclature	Value	Units
Bearing diameter	D	100	mm
Bearing length	L	200	mm
Radial clearance	C	0.15	mm
Length/Diameter	L/D	2	-
Rotational Speed	N	100, 200, 300, 400	RPM
Vertical Load	W	5000	N
Lubricant type	-	ISO VG 32	-
Density	ρ	870	kg/m^3
Specific heat capacity	c_f	2000	J/kg·K
Thermal conductivity	k	0.132	W/m·K
Oil viscosity at 35 ^{o}C	μ_{35}	0.0358	Pa·s

Table 9: Oil lubricated journal bearing models input parameters.

Quantity	Nomenclature	Value
Mesh axial divisions	L_{div}	101
Mesh circumferential divisions	D_{div}	51
Solution type	-	Steady
Thermal analysis	-	Isothermal

The material properties of the white metal bush liner are as presented next:

Table 10: White metal-lead based bush liner properties.

Quantity	Nomenclature	Value	Units
Young's modulus	E	18	GPa
Poisson's ratio	v	0.42	-
Wall Thickness	t	5	mm

The relative elastomeric liner properties necessary for carrying out the simulations are as follows:

Table 11: Elastomeric bush liner properties.

Quantity	Nomenclature	Value	Units
Young's modulus	E	0.925	GPa
Poisson's ratio	v	0.45	-
Wall Liner Thickness	t	4, 8	mm

First, a table with the maximum pressure values for each bearing of different liner configuration is presented. The percentage change between the simulations accounting for liner deformation and rigid liners is also presented.

Table 12: Maximum pressures with different liner configurations and rotational speeds.

Speed	Maximum pressure [Pa]			
[RPM]	100	200	300	400
Rigid liner	688354	560432	508283	482652
White Metal liner 5 mm	685866 -0.36%	559734 -0.125%	507915 -0.072%	482365 -0.059%
Elastomeric liner 8 mm	663093 -3.81%	549662 -1.96%	502476 -1.16%	478138 -0.94%
Elastomeric liner 4 mm	646016 -6.55%	539260 -3.93%	496602.00 -2.35%	473532 -1.93%

Next is a diagram of the pressure distributions in the mid plane of the simulations presented above.

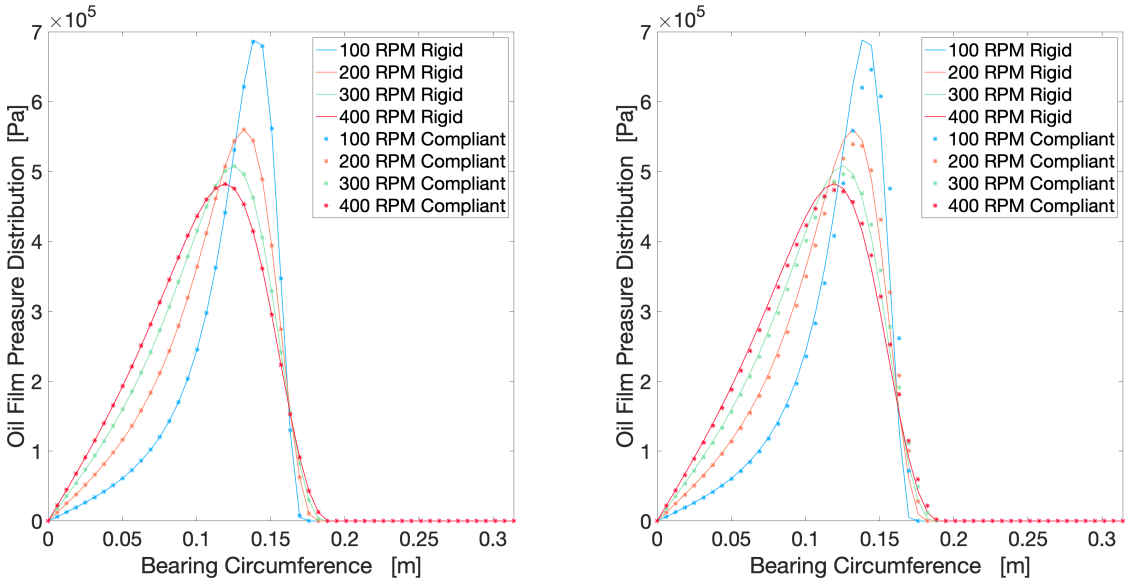

(a) White Metal liner 5 mm

(b) Elastomeric liner 8 mm

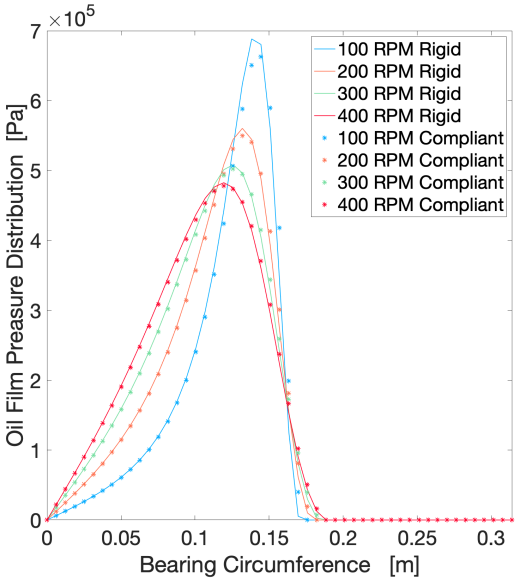

(c) Elastomeric liner 4 mm

Figure 21: Mid-plane pressure distributions for oil lubricated bearings under different shaft rotational speeds.

5.2.2 Bush Liner Compliance Effect in Water Lubricated Bearings

An equivalent process with the one presented in the previous paragraph is carried out for water lubricated bearings. Moreover, a design configuration is chosen for a water lubricated journal bearing

and for an array of operational parameters simulations are completed. The aim is to highlight the effect liner deformation has on the simulation model results. In the next table the design and operating characteristics of the bearing are presented, and in the one following more parameters are presented, particular to the simulation model. As in the previous paragraph, three different bush-liner designs were adopted and tested, one equipped with a liner of a plastic material used in mechanical and bearing applications, cast polyamide 6, and two with elastomeric material and different thickness.

Table 13: Water lubricated journal bearing design characteristics and operating conditions.

Quantity	Nomenclature	Value	Units
Bearing diameter	D	160	mm
Bearing length	L	400	mm
Radial clearance	C	0.18	mm
Length/Diameter	L/D	2.5	-
Rotational Speed	N	200, 400, 600, 800	RPM
Vertical Load	W	8000	N
Lubricant type	-	Fresh water	-
Density	ρ	1025	kg/m^3
Specific heat capacity	c_f	4182	J/kg·K
Thermal conductivity	k	0.6071	W/m·K
Oil viscosity at 25 °C	μ_{25}	1.0016	Pa·s
Oil viscosity at 5 °C	μ_5	1.55	Pa·s

Table 14: Water lubricated journal bearing models input parameters.

Quantity	Nomenclature	Value
Mesh axial divisions	L_{div}	141
Mesh circumferential divisions	D_{div}	71
Solution type	-	Steady
Thermal analysis	-	Isothermal

The material properties of the composite PA6C (cast polyamide 6) material bush liner are as presented next:

Table 15: Composite PA6C (cast polyamide 6) bush liner properties.

Quantity	Nomenclature	Value	Units
Young's modulus	E	2.9	GPa
Poisson's ratio	v	0.42	-
Wall Thickness	t	8	mm

The relative elastomeric liner properties necessary for carrying out the simulations are as follows:

Table 16: Elastomeric bush liner properties.

Quantity	Nomenclature	Value	Units
Young's modulus	E	0.85	GPa
Poisson's ratio	v	0.45	-
Wall Thickness	t	3, 9	mm

Following is a table with the maximum pressure values for each water lubricated bearing of different liner configuration. In addition, the percentage change between the simulations accounting for liner deformation and rigid liners is also presented.

Table 17: Maximum pressures with different liner configurations and rotational speeds.

Speed	Maximum pressure [Pa]			
[RPM]	200	400	600	800
Rigid liner	1212970	904388	768886	686683
Elastomeric liner 8 mm	998468 -21.48%	817973 -10.57%	730119 -5.31%	657230 -4.48%
Elastomeric liner 3 mm	1020260 -18.88%	814881 -10.98%	719320 -6.89%	652674 -5.21%
Elastomeric liner 9 mm	1062050 -14.21%	788999 -14.62%	682321 -12.69%	617467 -11.21%

The next diagram presents the pressure distributions in the mid plane of the simulations described above.

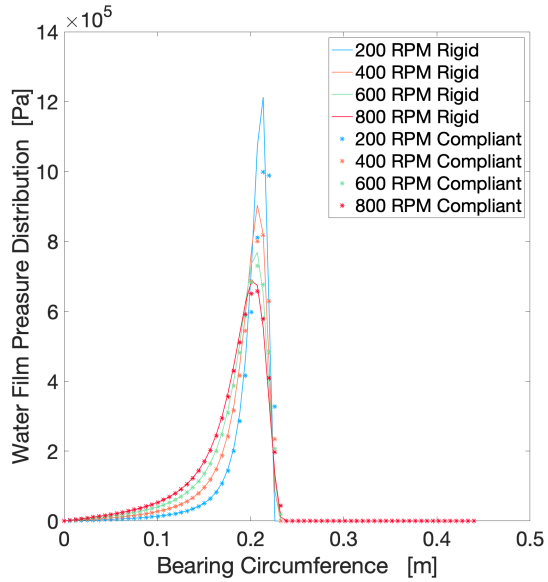

(a) White Metal liner 5 mm

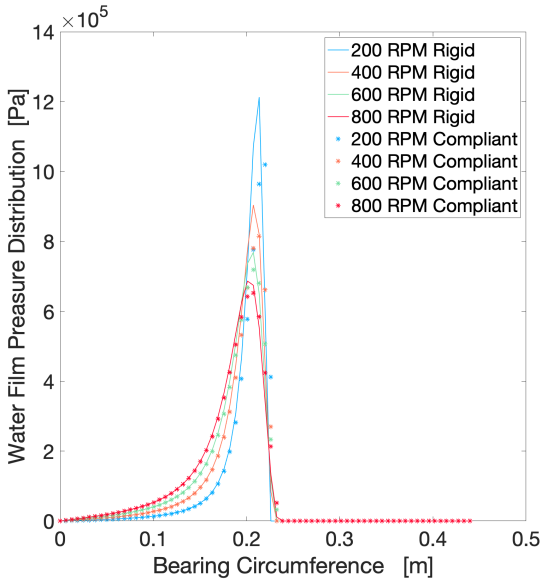

(b) Elastomeric liner 9 mm

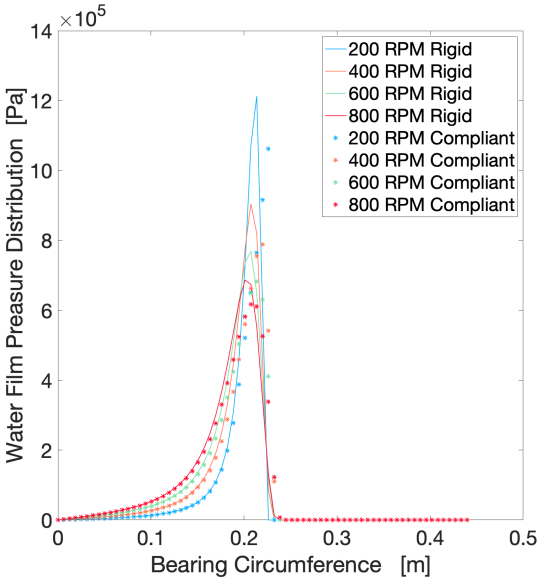

(c) Elastomeric liner 3 mm

Figure 22: Mid-plane pressure distributions for water lubricated bearings under different shaft rotational speeds.

6 Marine Stern Tube Bearing System: Comparative Case Study

In the previous chapters of this thesis a framework has been set around the study of hydrodynamic journal bearings. This was achieved with the presentation of vital information and the application of numerical models to several design and operational cases of oil and water lubricated journal bearings. In this chapter focus is added on the investigation of an integral part of marine shaft systems, the stern tube bearing system. The previous chapters contain an analytical review of this system and the requirements concerning its installation, operation and survey procedures.

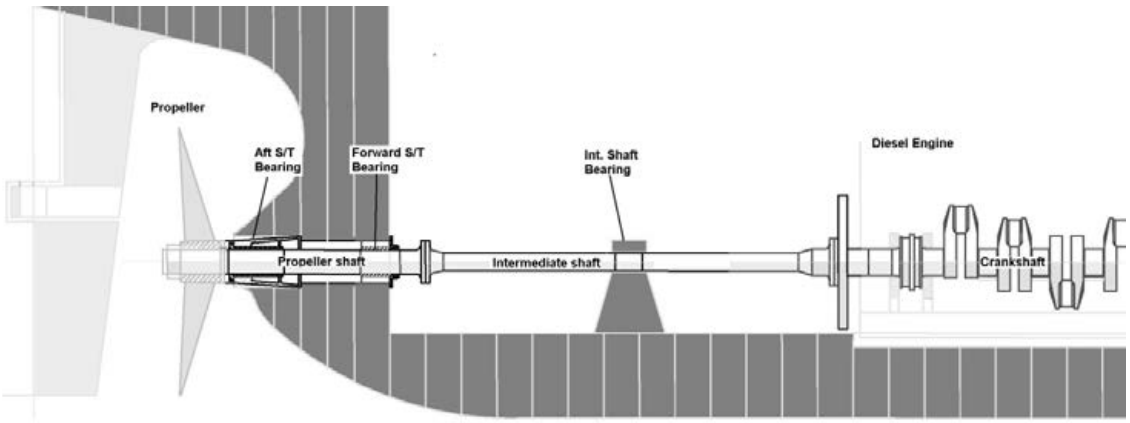

Figure 23: Typical shafting arrangement of a marine vessel.

Similarly to the figure [40] presented above, a widespread configuration for the stern tube bearing system involves two bearings, one in the aft end closer to the propeller and one forward. Exploring the options for marine stern tube bearings, one can easily find out that there is a plethora of choices, depending on the size of the shaft, the desired lubricant options, the material of the bearing and its' liner and other technical and budgetary factors. A fundamental differentiation is made between water and oil lubricated systems, with the evident difference being the lubricant of choice and one more being the bearing bush liner materials.

This chapter aims to compare and highlight the different operational behaviors of water and oil lubricated systems through the analysis of a case study for a marine vessel. Such a comparison can offer great insight during the design process of the propulsion system of a ship, or later on in the life of the ship when a replacement or repair of the stern tube bearings is needed or considered. For the purposes of this study theoretical design characteristics and operational conditions are chosen for two journal bearings, one aft and one forward comprising a stern tube bearing system.

In order to test and investigate adequately the performance characteristics of the stern tube bearing system, simulations are carried out with the chosen nominal design and operating characteristics but also with cases of variable conditions. Furthermore, these parameters are determined through the application of the proper regulations and requirements, based on actual ships and engineering manuals of commercial makers. The designs and operating conditions chosen correspond to configurations used in ships like small cargo vessels, product, chemical and small to medium-sized tankers, ferries, passenger, RO-RO vessels, coasters, large fishing vessels, tugs, workboats, and supply vessels. The power demands of these vessels can be covered with a range of solutions, including four

stroke engines coupled with gearboxes and more recently with hybrid propulsion systems of diesel engines and electric motors. Also these vessels can be equipped with two shafts and propellers, where the energy output is distributed leading to shafts and bearings of smaller sizes in relation to configurations of one propeller.

The results for the water and the oil lubricated bearings are presented side by side in order to display the relative differences and similarities in the behaviors of the two systems. The aft bearing is presented in the first section and the forward in the second, aiming at offering a thorough and complete analysis for the present case study

6.1 Aft Stern Tube Bearing Analysis

The stern tube or pipe is fitted in the hull of the ship, below the waterline. It functions as the housing for the two bearings (aft and fore) of the aftermost part of the propeller or tube shaft, facilitating the rotation of the shaft with less frictional resistance [40]. In this section an aft stern tube bearing is investigated, it is designed to satisfy relative requirements and regulations. Additionally, data required for its design and operation correspond to commercial applications as described above, and at the same time this configuration corresponds to the range of the models used for the validation of the algorithm applied. Its main characteristics are derived from the formula presented in IACS Unified Requirements M68: Dimensions of propulsion shafts and their permissible torsional vibration stresses, and the applied load corresponds to a bearing pressure of 4 kg/cm^2 (bar). Bearing pressures are typically designed with values of this range [51], which is also consistent with data of actual ships from the section of Marine Engineering of NTUA. The following table presents the main design parameters of the bearing and its nominal operation characteristics, these are common for the oil and the water lubricated bearings.

Table 18: Aft stern tube journal bearings design characteristics and operating conditions.

Quantity	Nomenclature	Value	Units
Bearing diameter	D	300	mm
Bearing length	L	600	mm
Length/Diameter	L/D	2	-
Rotational Speed	N	200	RPM
Vertical Load	W	-70600	N

As described simulations are carried out for both the water and the oil lubricated designs chosen and the results are compared, in order to gain insight on the different responses of these systems. It is consider useful to present the results of these bearings for the chosen nominal conditions in this paragraph and organise the next paragraphs according to the variable parameter (shaft rotational speed, misalignment angle and load condition). Water lubricated stern tube bearings are fitted, on a large scale, with liners of composite materials, while oil lubricated bearings are respectively fitted with white metal liners. This and other design and operating parameters that differentiate the simulations for the two different kinds of bearings are presented next. First, the data concerning the oil lubricated bearing are presented.

Table 19: Oil lubricated aft stern tube journal bearings simulation parameters.

Quantity	Nomenclature	Value	Units
Lubricant type	-	SAE 30	-
Density	ρ	870	kg/m^3
Specific heat capacity	c_f	2000	J/kg·K
Thermal conductivity	k	0.132	W/m·K
Oil viscosity at 40 °C	μ_{40}	0.07	Pa·s
Liner Material	-	White metal	-
Liner Young's modulus	E	50	GPa
Liner Poisson's ratio	v	0.35	-
Radial clearance	C	0.15	mm
Liner Wall Thickness	t	4	mm
Mesh axial divisions	L_{div}	61	-
Mesh circumferential divisions	D_{div}	31	-
Solution type	-	Steady	-
Thermal analysis	-	Isothermal	-

The parameters' table concerning the water lubricated bearing are presented next.

Table 20: Water lubricated aft stern tube journal bearings simulation parameters.

Quantity	Nomenclature	Value	Units
Lubricant type	-	Seawater	-
Density	ρ	1025	kg/m^3
Specific heat capacity	c_f	4007	J/kg·K
Thermal conductivity	k	0.6	W/m·K
Oil viscosity at 25 °C	μ_{25}	0.959	mPa·s
Liner Material	-	Elastomeric	-
Liner Young's modulus	E	2.5	GPa
Liner Poisson's ratio	v	0.42	-
Radial clearance	C	0.2	mm
Liner Wall Thickness	t	8	mm
Mesh axial divisions	L_{div}	61	-
Mesh circumferential divisions	D_{div}	31	-
Solution type	-	Steady	-
Thermal analysis	-	Isothermal	-

The model results for the spatial pressure and film thickness distribution are presented next.

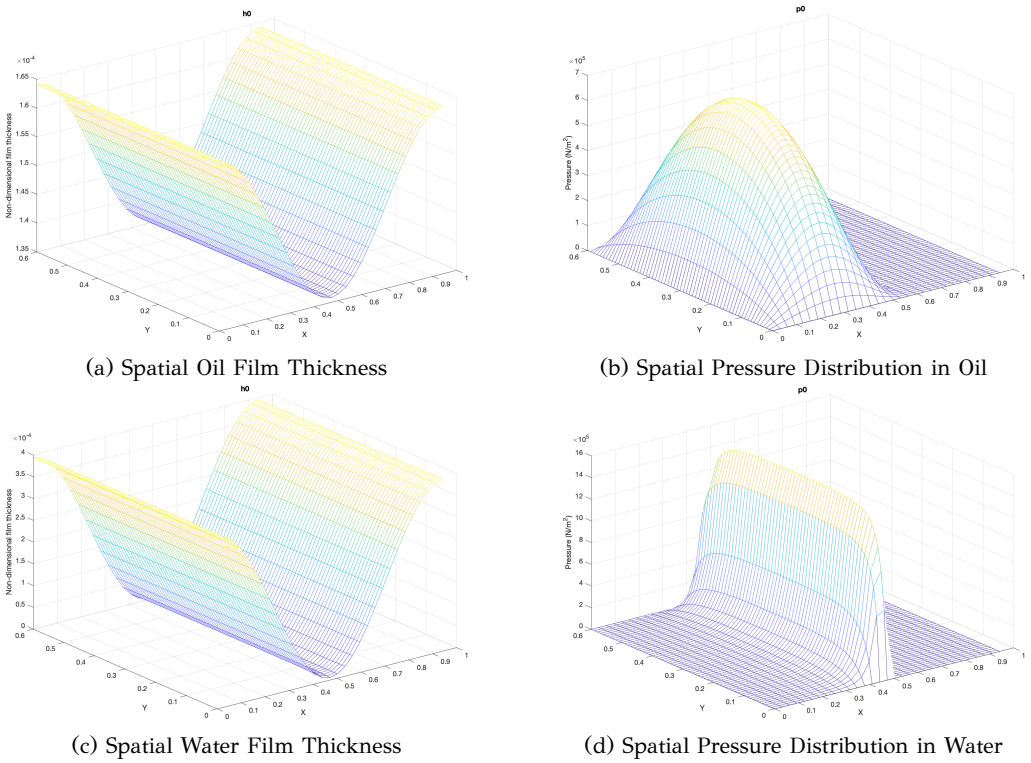

(a) Spatial Oil Film Thickness

(b) Spatial Pressure Distribution in Oil

(c) Spatial Water Film Thickness

(d) Spatial Pressure Distribution in Water

Figure 24: Film thickness and pressure distribution of oil and water lubricated aft stern tube bearings.

The maximum pressure and the minimum film thickness values are presented in the next table as a reference.

Table 21: Aft stern tube oil and water lubricated bearings performance parameters.

Speed	Maximum pressure [Pa]		Minimum film thickness [μm]	
RPM	Oil	Water	Oil	Water
200	689019	1546930	135.82	5.49

6.1.1 Shaft Rotational Speed Effect on Aft Bearing

In this paragraph, changes on the shaft rotational speed are applied and simulations are carried out. The aim of these simulations is to investigate the influence of this operational parameter on the performance characteristics of the aft stern tube journal bearing. The different shaft rotational speed values are presented in the next table.

Table 22: Aft stern tube journal bearings shaft rotational speeds.

Shaft rotational speed	Value [RPM]
Slow steaming-1	160
Slow steaming-2	180
Nominal	200
Increased	220

The values for this analysis are theoretical but correspond to actual operating scenarios. For example, a marine vessel can travel with reduced speed, corresponding to lower requested power from the main engine and subsequently to lower engine and propeller speeds [52]. These speed conditions are described as slow steaming and are applied by the global merchant shipping industry in order to cut fuel costs, reduce capacity and reduce the emissions to the atmosphere resulting from usage of fossil fuels. In a similar way, increased shaft rotational speeds result from increased vessel speed and power needs, which may result from a variety of reasons like avoiding weather phenomena.

The operational parameters investigated and presented in this paragraph are the pressure distribution on the mid-plane, the minimum film thickness developed on the bearing and the power loss resulting from its operation.

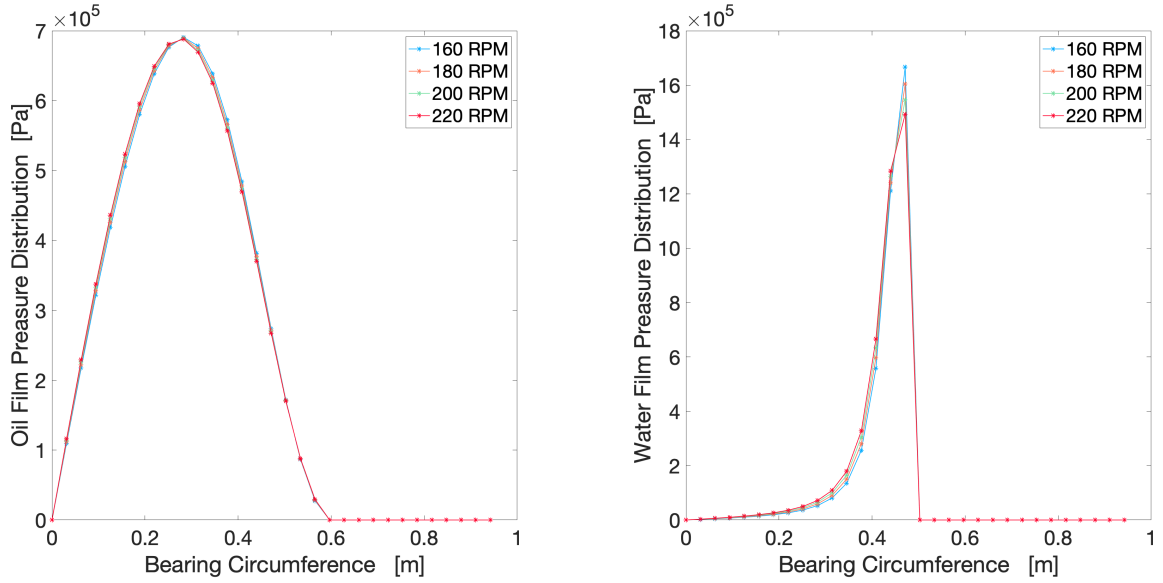

(a) Oil Lubricated Aft Bearing.

(b) Water Lubricated Aft Bearing.

Figure 25: Mid-plane pressure distributions of oil and water bearings for different shaft rotational speeds.

In connection to the figures presented above, the maximum pressure values developed in the oil and water films are presented in the next table, along with the corresponding percentage change.

Table 23: Aft stern tube bearings maximum pressure for different rotational speeds.

Speed	Maximum pressure [Pa]			
RPM	Oil	%	Water	%
160	690726	+0.25	1666710	+7.74
180	689852	+0.12	1604420	+3.72
200	689019	-	1546930	-
220	688250	-0.11	1493550	-3.45

Following are the diagrams for the minimum film thickness developed in the bearings and the power loss resulting from their operation.

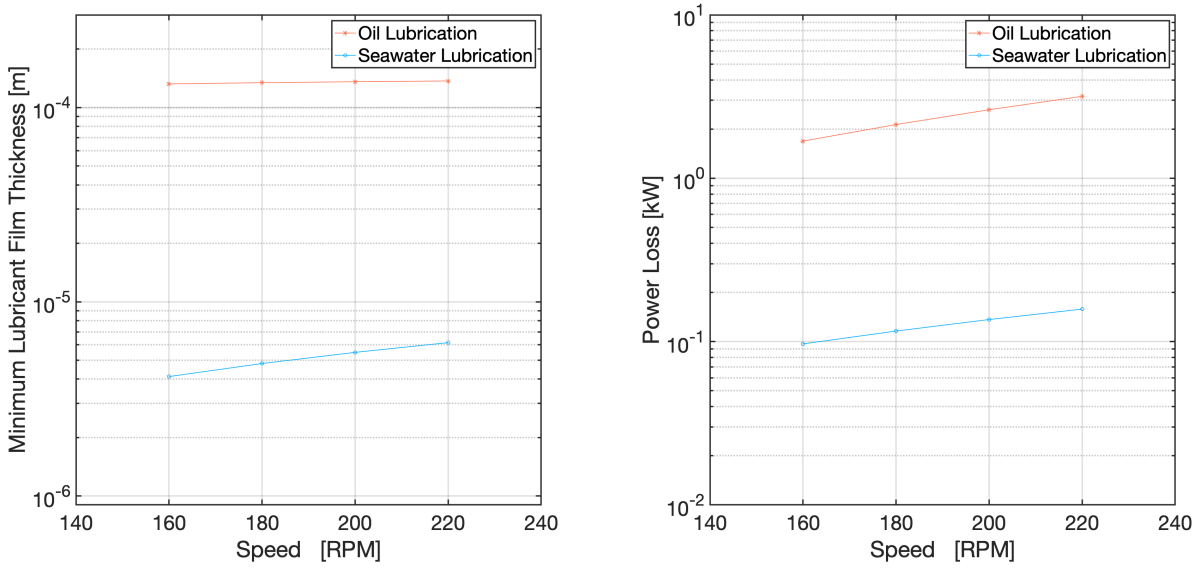

(a) Minimum film thickness.

(b) Power loss.

Figure 26: Minimum film thickness and power loss of oil and water bearings for different rotational speeds.

In order to add some context to the figures presented above, the relative values and the percentage change are presented in the next tables, for both the oil and the water lubricated bearings.

Table 24: Aft stern tube bearings minimum film thickness for different rotational speeds.

Speed	Minimum film thickness [μm]			
RPM	Oil	%	Water	%
160	132.37	-2.54	4.12	-24.95
180	134.28	-1.13	4.81	-12.38
200	135.82	-	5.49	-
220	137.09	+0.93	6.16	+12.20

Table 25: Aft stern tube bearings power loss for different rotational speeds.

Speed	Power loss [kW]			
RPM	Oil	%	Water	%
160	1.68835	-35.71	0.09679	-29.03
180	2.13119	-18.84	0.11596	-14.98
200	2.62608	-	0.13638	-
220	3.17305	+20.83	0.15800	+15.85

6.1.2 Misalignment Effect on Aft Bearing

In a like manner to the one presented above, in this paragraph the influence misaligned operation has on the bearing behavior is investigated. Misalignment in journal bearings has been explained and presented in previous paragraphs and the present case studies aim at offering practical examples for its effect. Misalignment angles in the axial direction are applied to the models with an applied load of 3 bar and the obtained results are presented in appropriate diagrams. The values of the angles are presented in the following table.

Table 26: Aft stern tube journal bearings misalignment angles.

Misalignment angle	Value
Angle 1	0.01
Angle 2	0.02
Angle 3	0.03
Angle 4	0.04

The results obtained from the simulations for the pressure distribution, the minimum film thickness and the power loss are presented next. The pressure distribution is presented both in the mid-plane circumferential direction, as well as in the axial direction at the angle where the maximum value develops. Similarly to the previous simulations the results for the oil and the water lubricated aft stern tube bearings are presented side by side.

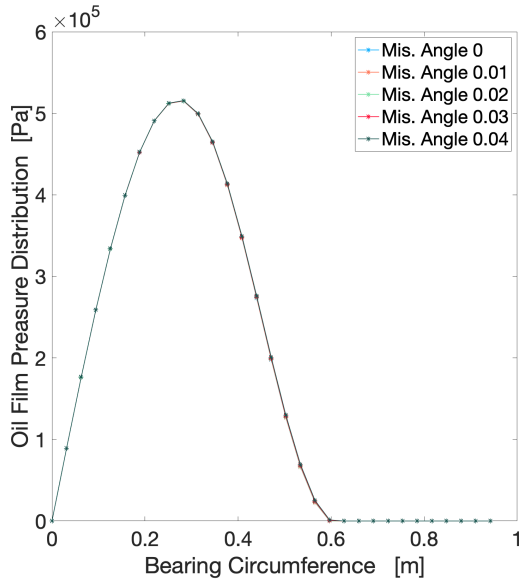

(a) Oil Lubricated Aft Bearing.

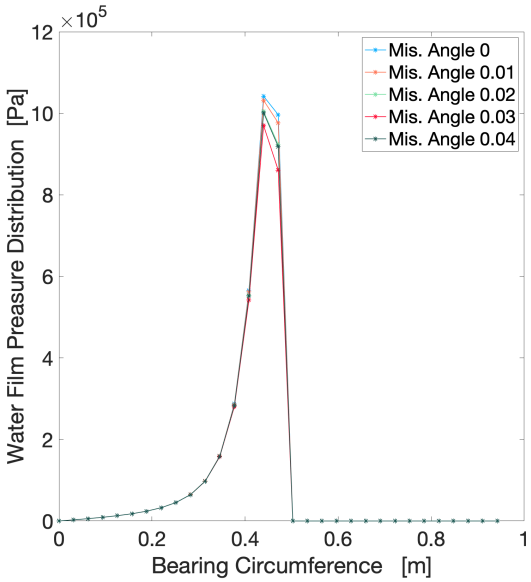

(b) Water Lubricated Aft Bearing.

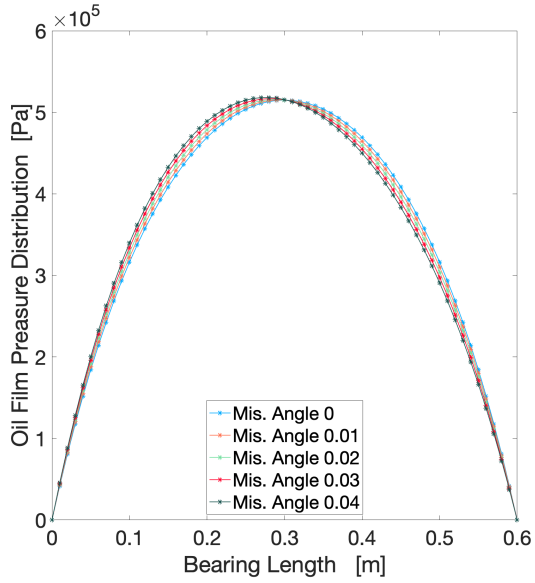

(c) Oil Lubricated Aft Bearing.

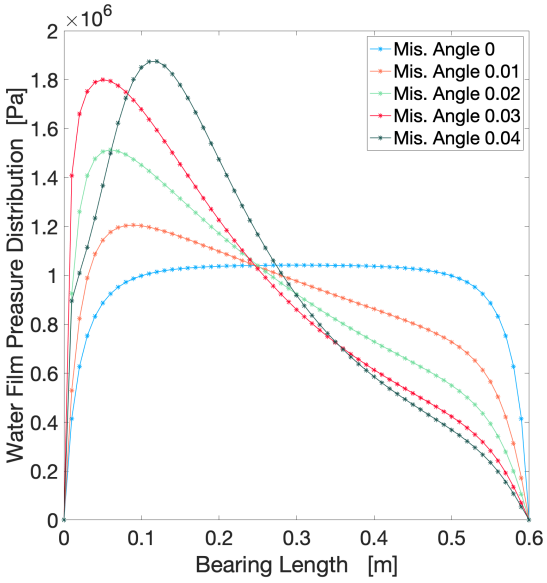

(d) Water Lubricated Aft Bearing.

Figure 27: Mid and axial planes pressure distributions of oil and water bearings with misalignment angles.

The next table is presented as a reference to the diagrams presented above. It contains the maximum pressure values as well as the percentage change for the oil and water films.

Table 27: Aft stern tube bearings maximum pressure with misalignment angles.

Angle	Maximum pressure [Pa]			
	Oil	%	Water	%
0.0	515048	-	1041980	-
0.01	515160	+0.02	1205580	+15.07
0.02	515781	+0.14	1513700	+45.27
0.03	516817	+0.34	1800220	+72.77
0.04	518220	+0.62	1874890	+79.94

The diagrams corresponding to the the minimum film thickness developed in the bearings and the power loss resulting from their operation with misalignment are presented next.

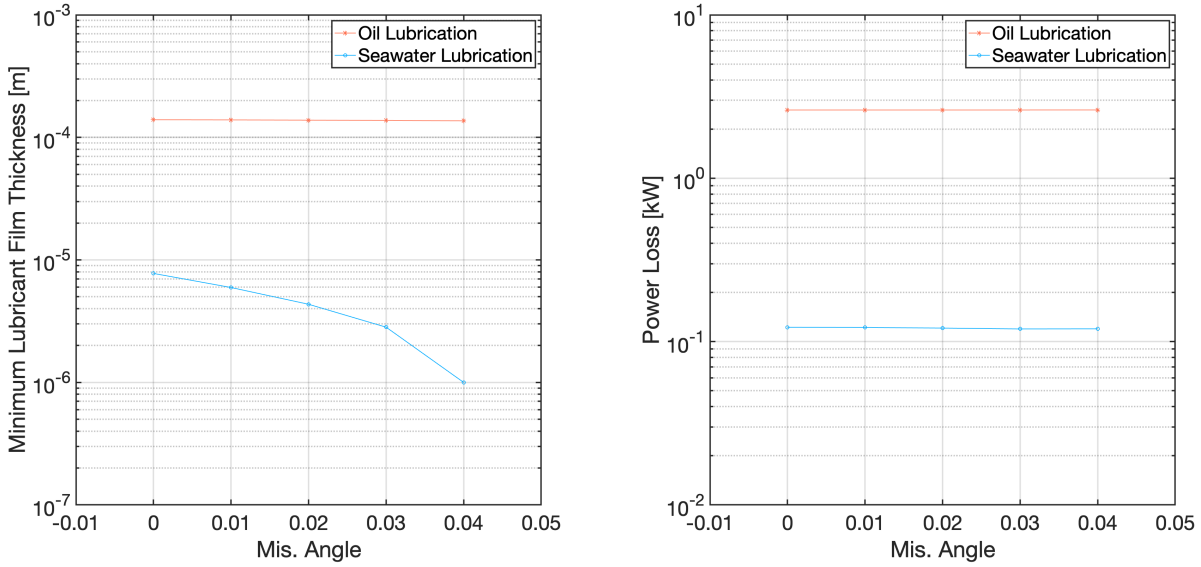

(a) Minimum film thickness.

(b) Power loss.

Figure 28: Minimum film thickness and power loss of oil and water bearings with misalignment angles.

In addition, the relative tables presenting the values and the percentage changes follow.

Table 28: Aft stern tube bearings minimum film thickness with misalignment angles.

Angle	Minimum film thickness [μm]			
	Oil	%	Water	%
0.0	139.32	-	7.75	-
0.01	138.91	-0.29	5.95	-23.24
0.02	138.26	-0.76	4.34	-43.99
0.03	137.49	-1.32	2.82	-63.59
0.04	136.55	-1.99	1.00	-87.10

Table 29: Aft stern tube bearings power loss with misalignment angles.

Angle	Power loss [kW]			
	Oil	%	Water	%
0.0	2.61672	-	0.12230	-
0.01	2.61677	+0.002	0.12195	-0.29
0.02	2.61693	+0.008	0.12092	-1.13
0.03	2.61720	+0.018	0.11944	-2.34
0.04	2.61758	+0.032	0.11968	-2.15

6.1.3 Load Effect on Aft Bearing

In the previous paragraphs the influence of shaft rotational speed and of misalignment angle was investigated, this paragraph focuses on the applied vertical load. This load corresponds to the weight of the propeller and the subsequent pressure developed from its support by the bearing. Different draughts and cargo conditions results to different loads. Additionally, to the primary tested load two different load conditions are simulated, one increased (+50%) and one decreased (-50%), in order to verify and investigate hydrodynamic lubrication in all operating conditions. In the following pages, the alternative load conditions are presented and the corresponding simulation results are presented in diagrams and comparative tables, regarding the water and the oil lubricated bearings.

Table 30: Aft stern tube journal bearings load conditions.

Load [N]	Value
Decreased load	-35300
Primary load	-70600
Increased load	-105900

First, the pressure distributions on the midplane are presented for both the oil and the water lubricated aft bearings in appropriate diagrams, as well as in an appropriate table.

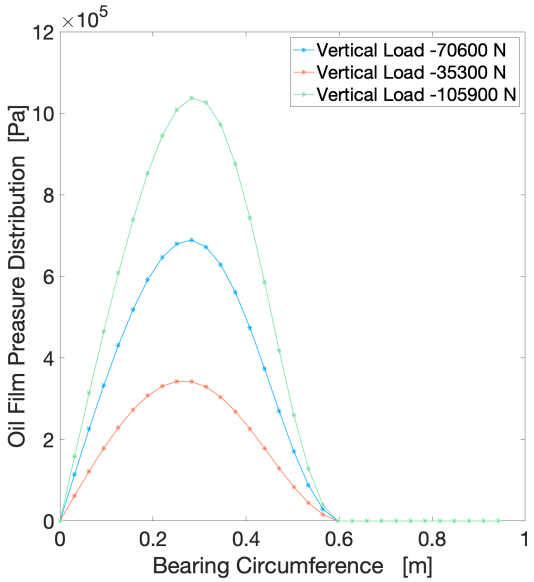

(a) Oil Lubricated Aft Bearing.

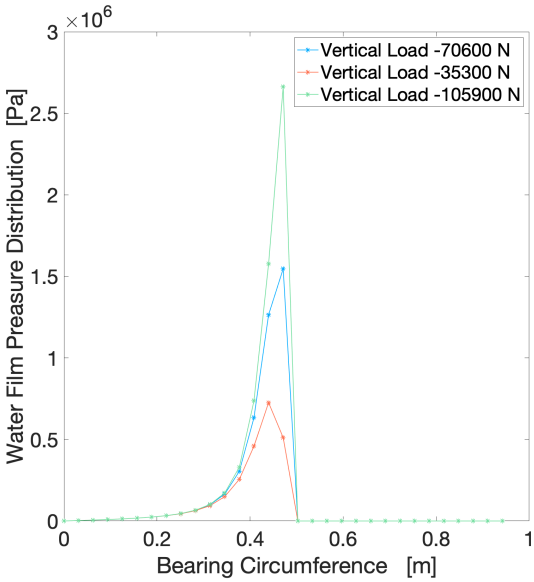

(b) Water Lubricated Aft Bearing.

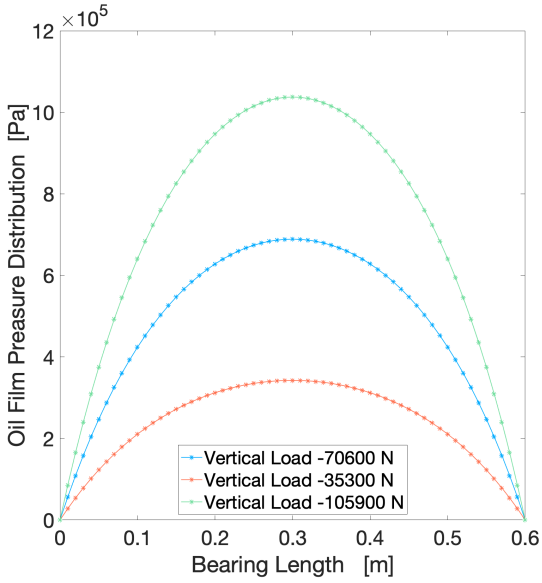

(c) Oil Lubricated Aft Bearing.

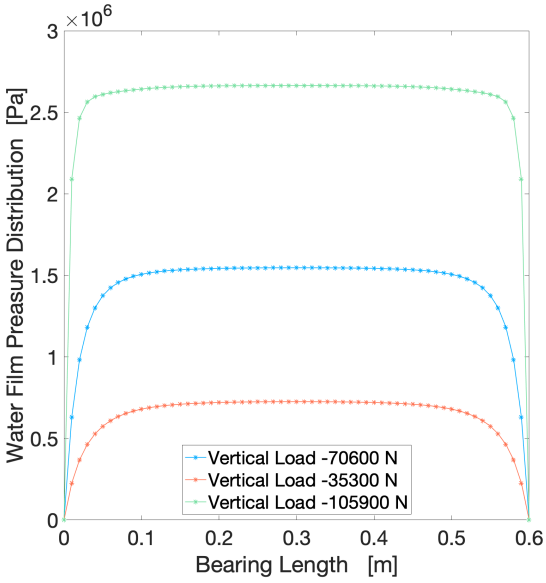

(d) Water Lubricated Aft Bearing.

Figure 29: Mid and axial planes pressure distributions of oil and water bearings under different load conditions.

Next is a table presenting the maximum pressure valuew as a reference to the above diagrams.

Table 31: Aft stern tube bearings maximum pressure for different load conditions.

Load	Maximum pressure [Pa]			
N	Oil	%	Water	%
-35300	342510	-50.29	725892	-53.07
-70600	689019	-	1546930	-
-105900	1037610	+50.59	2664630	+72.25

Following are the relative diagrams for the minimum film thickness and the power loss in the aft bearings.

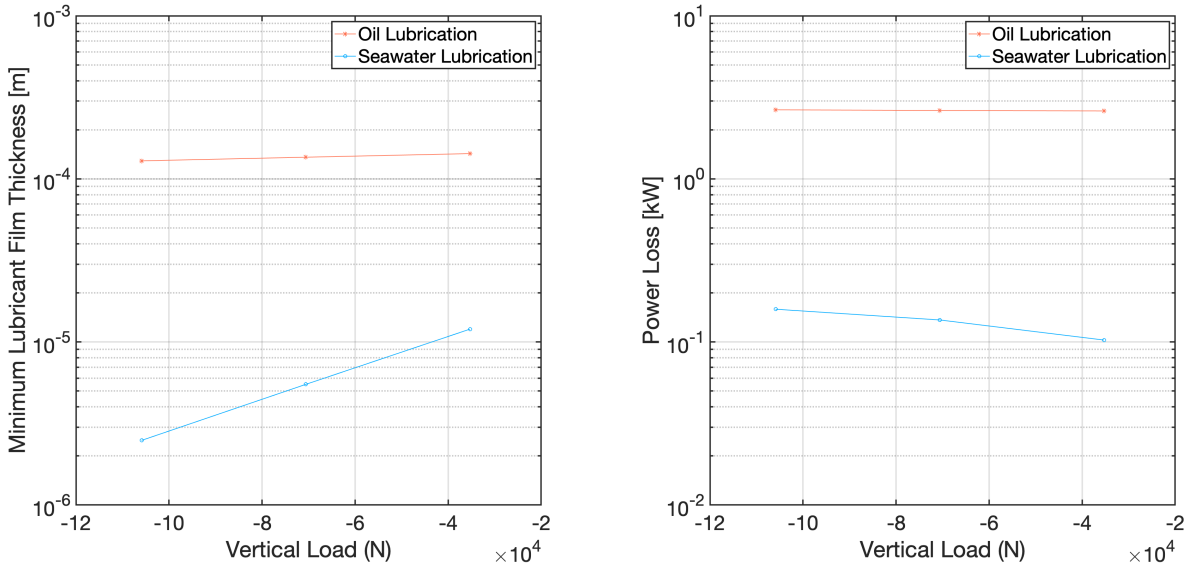

(a) Minimum film thickness.

(b) Power loss.

Figure 30: Minimum film thickness and power loss of oil and water bearings under different loads.

The next tables present the values for the minimum film thickness and the power loss as a reference to the diagrams presented above.

Table 32: Aft stern tube bearings minimum film thickness for different load conditions.

Load	Minimum film thickness [μm]			
N	Oil	%	Water	%
-35300	142.85	+5.17	11.98	+118.14
-70600	135.82	-	5.49	-
-105900	128.97	-5.05	2.49	-54.67

Table 33: Aft stern tube bearings power loss for different load conditions.

Load	Power loss [kW]			
N	Oil	%	Water	%
-35300	2.60996	-0.61	0.10270	-24.69
-70600	2.62608	-	0.13638	-
-105900	2.65234	+1.00	0.15872	+16.38

6.2 Forward Stern Tube Bearing Analysis

As explained and analysed in the beginning of this chapter and in the previous section, the stern tube bearing system is often comprised of two bearings, the aft and the fore. In this section, the forward stern tube bearing, corresponding to the aft bearing presented before, is analysed. The fundamental design difference between the aft and the forward bearing is their length to diameter ratio. It is also highlighted that limits for this ratio are described in regulations mentioned in this study but only regarding the aft bearing. Usually the fore bearing is shorter in length than the aft and this type of combination is also investigated in the present study. The following table presents in detail the main design parameters of the forward bearing and its nominal operation characteristics.

Table 34: Forward stern tube journal bearings design characteristics and operating conditions.

Quantity	Nomenclature	Value	Units
Bearing diameter	D	300	mm
Bearing length	L	300	mm
Length/Diameter	L/D	1	-
Rotational Speed	N	200	RPM
Vertical Load	W	-17650	N

The data and results of the forward bearing analysis follow the same format as in the previous section. The simulations are carried out for both oil and water lubricated bearings. The different characteristics of these bearings are presented in the next tables. The oil lubricated forward stern tube bearing is presented first.

Table 35: Oil lubricated forward stern tube journal bearings simulation parameters.

Quantity	Nomenclature	Value	Units
Lubricant type	-	SAE 30	-
Density	ρ	870	kg/m^3
Specific heat capacity	c_f	2000	J/kg·K
Thermal conductivity	k	0.132	W/m·K
Oil viscosity at 40 °C	μ_{40}	0.07	Pa·s
Liner Material	-	White metal	-
Liner Young's modulus	E	50	GPa
Liner Poisson's ratio	v	0.35	-
Radial clearance	C	0.15	mm
Liner Wall Thickness	t	4	mm
Mesh axial divisions	L_{div}	61	-
Mesh circumferential divisions	D_{div}	31	-
Solution type	-	Steady	-
Thermal analysis	-	Isothermal	-

The corresponding forward water lubricated bearing parameters' table and results are presented next.

Table 36: Water lubricated forward stern tube journal bearings simulation parameters.

Quantity	Nomenclature	Value	Units
Lubricant type	-	Seawater	-
Density	ρ	1025	kg/m^3
Specific heat capacity	c_f	4007	J/kg·K
Thermal conductivity	k	0.6	W/m·K
Oil viscosity at 25 °C	μ_{25}	0.959	mPa·s
Liner Material	-	Elastomeric	-
Liner Young's modulus	E	2.5	GPa
Liner Poisson's ratio	v	0.42	-
Radial clearance	C	0.2	mm
Liner Wall Thickness	t	8	mm
Mesh axial divisions	L_{div}	61	-
Mesh circumferential divisions	D_{div}	31	-
Solution type	-	Steady	-
Thermal analysis	-	Isothermal	-

The model results for the spatial pressure and film thickness distribution are presented next.

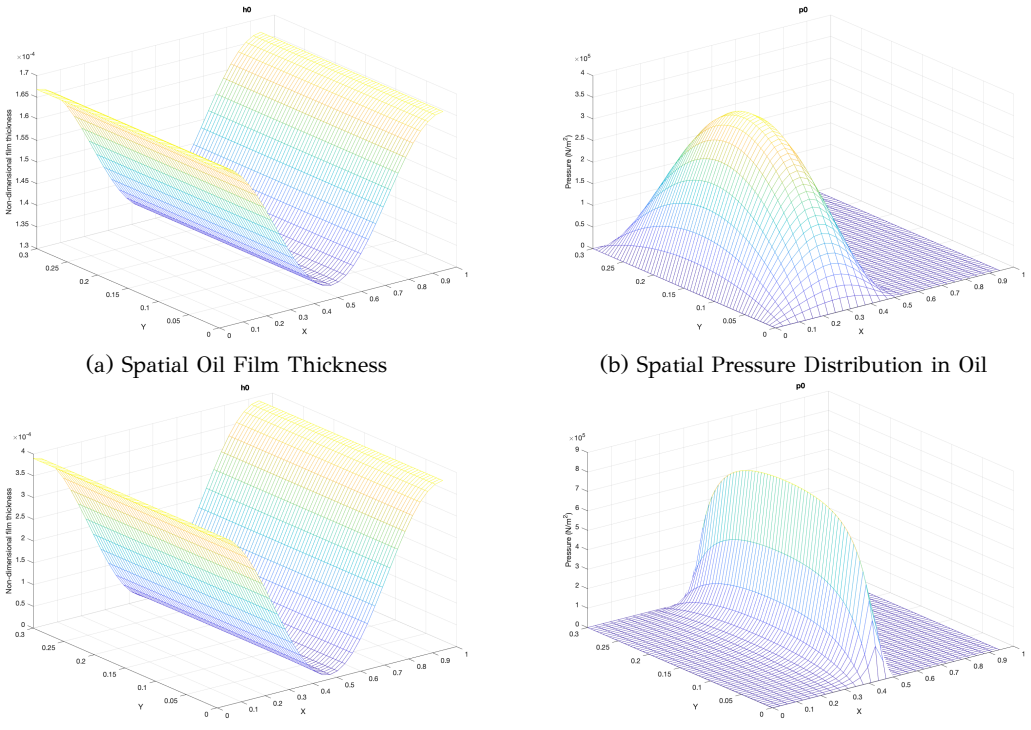

(a) Spatial Oil Film Thickness

(b) Spatial Pressure Distribution in Oil

(c) Spatial Water Film Thickness

(d) Spatial Pressure Distribution in Water

Figure 31: Film thickness and pressure distribution of oil and water lubricated aft stern tube bearings.

The maximum pressure and the minimum film thickness values are presented in the next table.

Table 37: Forward stern tube oil and water lubricated bearings performance parameters.

Speed	Maximum pressure [Pa]		Minimum film thickness [μm]	
RPM	Oil	Water	Oil	Water
200	363503	820953	133.21	10.03

6.2.1 Shaft Rotational Speed Effect on Forward Bearing

The first variable operating parameter investigated is the shaft rotational speed. As in the previous section of the aft bearing, different speeds are applied and simulations are carried out for the forward stern tube bearing. The different shaft rotational speed values are the same as before and are presented in the next table.

Table 38: Forward stern tube journal bearings shaft rotational speeds.

Shaft rotational speed	Value [RPM]
Slow steaming-1	160
Slow steaming-2	180
Nominal	200
Increased	220

The reader is reminded that the values for this analysis are theoretical but correspond to actual operating scenarios. The operational parameters investigated and presented in this paragraph are the pressure distribution on the mid-plane, the minimum film thickness developed on the bearing and the power loss resulting from its operation.

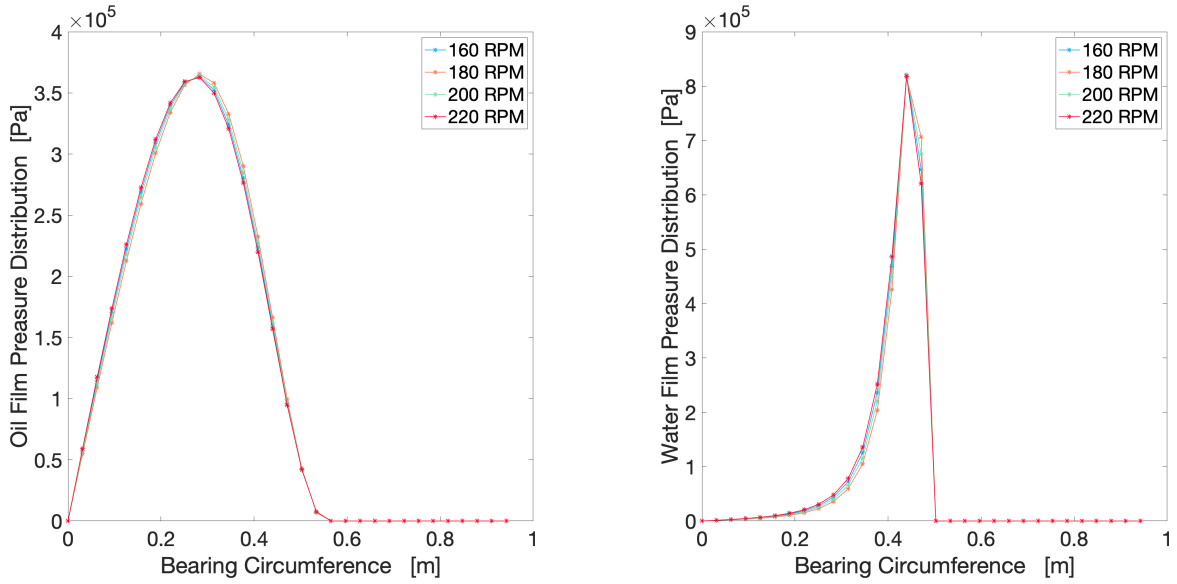

(a) Oil Lubricated Forward Bearing.

(b) Water Lubricated Forward Bearing.

Figure 32: Mid-plane pressure distributions of oil and water bearings for different shaft rotational speeds.

The date presented in the next table correspond to the maximum pressure values presented in the previous diagrams.

Table 39: Forward stern tube bearings maximum pressure for different rotational speeds.

Speed	Maximum pressure [Pa]			
RPM	Oil	%	Water	%
160	365513	+0.55	817142	-0.46
180	364479	+0.227	820695	+0.03
200	363503	-	820953	-
220	362605	-0.25	818792	-0.26

Next are the diagrams of the minimum film thickness and the power loss generated in the forward bearings under different shaft rotational speeds.

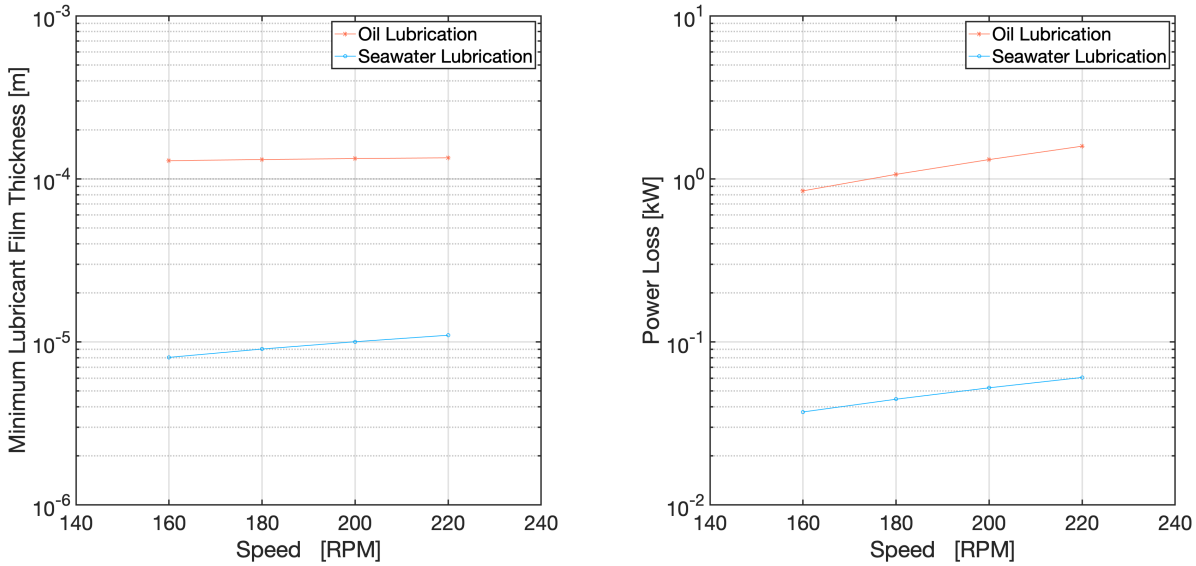

(a) Minimum film thickness.

(b) Power loss.

Figure 33: Minimum film thickness and power loss of oil and water bearings for different shaft rotational speeds.

Also following are two tables with the corresponding values.

Table 40: Forward stern tube bearings minimum film thickness for different rotational speeds.

Speed	Minimum film thickness [μm]			
RPM	Oil	%	Water	%
160	129.25	-2.97	8.04	-19.83
180	131.43	-1.33	9.05	-9.80
200	133.21	-	10.03	-
220	134.67	+1.10	11.00	+9.60

Table 41: Forward stern tube bearings power loss for different rotational speeds.

Speed	Power loss [kW]			
RPM	Oil	%	Water	%
160	0.84447	-35.71	0.03721	-28.89
180	1.06596	-18.84	0.04454	-14.88
200	1.31347	-	0.05233	-
220	1.58700	+20.83	0.06056	+15.72

6.2.2 Misalignment Effect on Forward Bearing

In this paragraph the influence misaligned operation has on the forward stern tube bearing behavior is investigated. Misalignment angles in the axial direction are applied to the models and the obtained results are presented in appropriate diagrams. The values of the angles are the same with the ones applied on the aft bearing simulations, for the sake of completeness they are presented in the following table.

Table 42: Forward stern tube journal bearings misalignment angles.

Misalignment angle	Value
Angle 1	0.01
Angle 2	0.02
Angle 3	0.03
Angle 4	0.04

The results obtained from the simulations for the pressure distribution, the minimum film thickness and the power loss are presented next. The pressure distribution is presented both in the mid-plane circumferential direction, as well as in the axial direction at the angle where the maximum value develops. Similarly to the previous simulations the results for the oil and the water lubricated forward stern tube bearings are presented side by side.

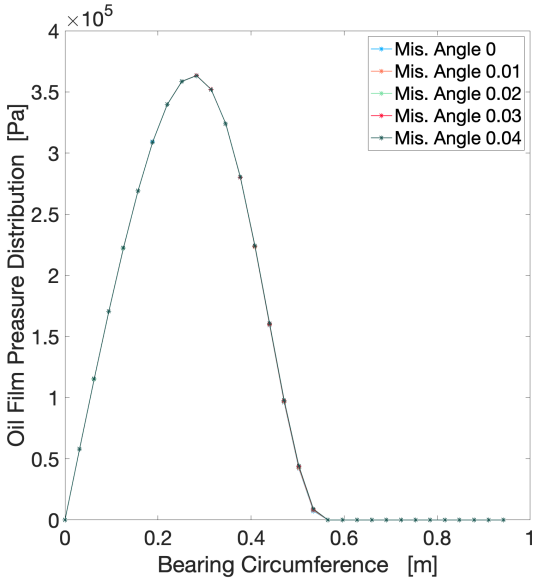

(a) Oil Lubricated Forward Bearing.

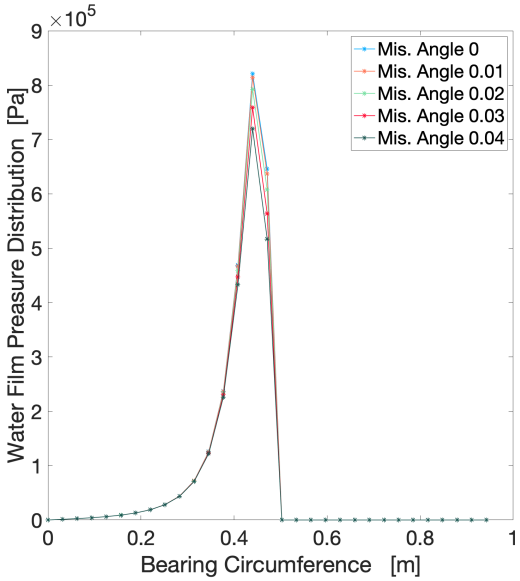

(b) Water Lubricated Forward Bearing.

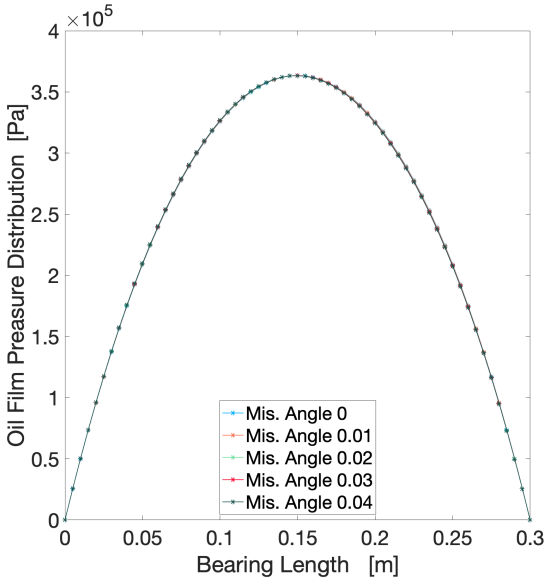

(c) Oil Lubricated Forward Bearing.

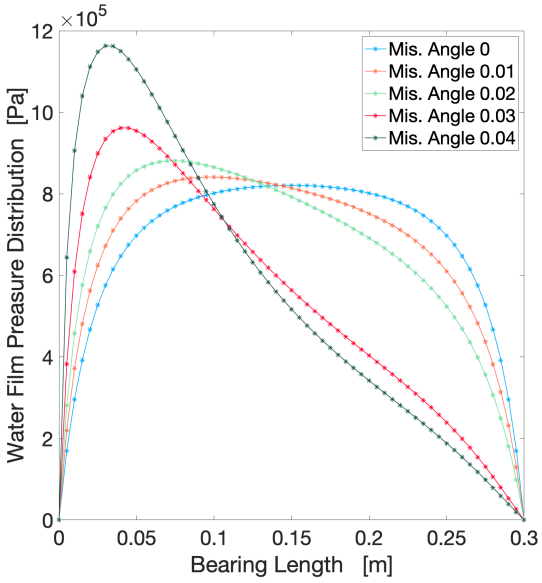

(d) Water Lubricated Forward Bearing.

Figure 34: Mid and axial planes pressure distributions of oil and water bearings with misalignment angles.

The next table presents the relative maximum pressure values as a reference to the above diagrams.

Table 43: Forward stern tube bearings maximum pressure with misalignment angles.

Angle	Maximum pressure [Pa]			
	Oil	%	Water	%
0.0	363503	-	820953	-
0.01	363485	-0.005	841182	+2.46
0.02	363454	-0.013	881209	+7.34
0.03	363412	-0.025	962066	+17.19
0.04	363348	-0.042	1163250	+41.70

The relative diagrams for the minimum film thickness developed in the bearings and the power loss caused from their operation with misalignment are presented next. As a reference to the diagrams appropriate tables follow.

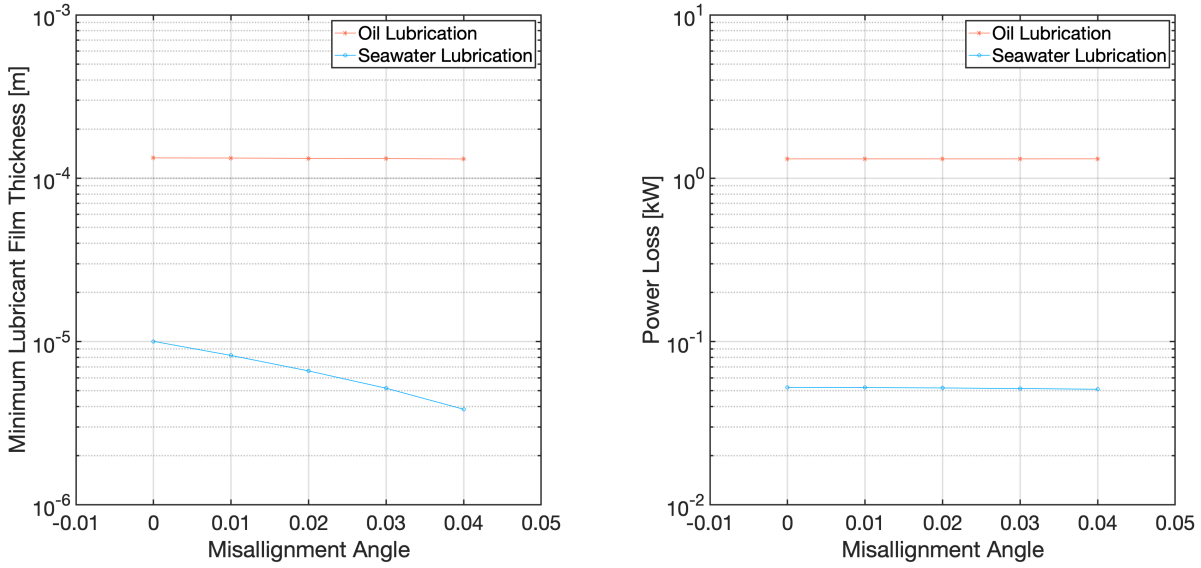

(a) Minimum film thickness.

(b) Power loss.

Figure 35: Minimum film thickness and power loss of oil and water bearings with misalignment angles.

Table 44: Forward stern tube bearings minimum film thickness with misalignment angles.

Angle	Minimum film thickness [μm]			
	Oil	%	Water	%
0.0	133.21	-	10.03	-
0.01	132.92	-0.22	8.22	-18.07
0.02	132.39	-0.61	6.61	-34.12
0.03	131.80	-1.10	5.18	-48.34
0.04	131.19	-1.52	3.85	-61.65

Table 45: Forward stern tube bearings power loss with misalignment angles.

Angle	Power loss [kW]			
	Oil	%	Water	%
0.0	1.31347	-	0.05233	-
0.01	1.31349	+0.002	0.05226	-0.131
0.02	1.31356	+0.007	0.05200	-0.637
0.03	1.31368	+0.015	0.05155	-1.497
0.04	1.31385	+0.029	0.05105	-2.453

6.2.3 Load Effect on Forward Bearing

Following the same pattern as in the aft stern tube bearing analysis, this paragraph focuses on the applied load. The results of the chosen primary load are compared with results from a model with increased load and one with decreased. The corresponding simulation results are presented in diagrams and comparative tables, regarding the water and the oil lubricated bearings.

Table 46: Forward stern tube journal bearings load conditions.

Load [N]	Value
Decreased load	-8825
Primary load	-17650
Increased load	-26475

In the first set of diagrams the pressure distributions on the mind plane are presented.

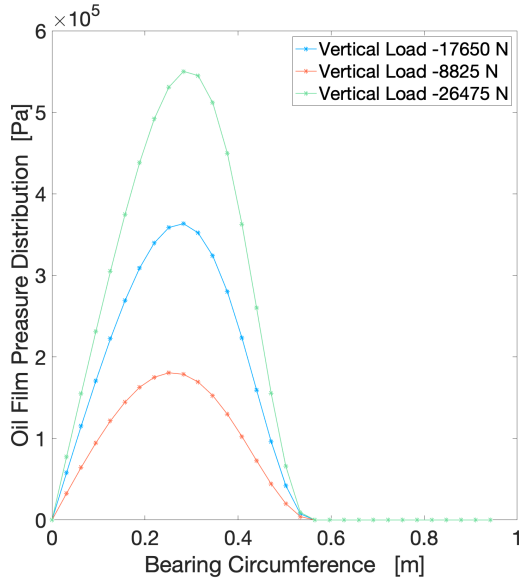

(a) Oil Lubricated Aft Bearing.

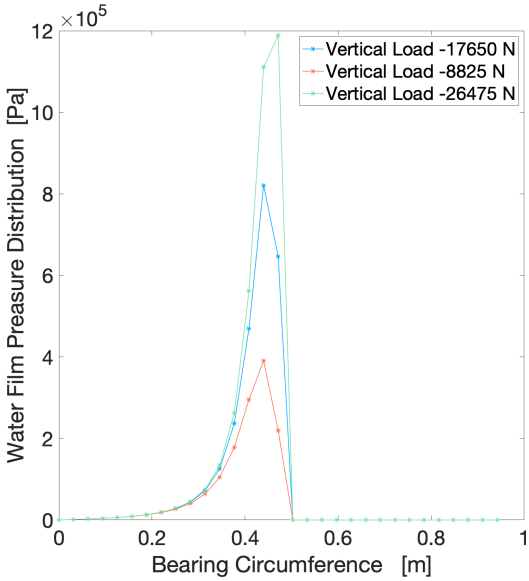

(b) Water Lubricated Aft Bearing.

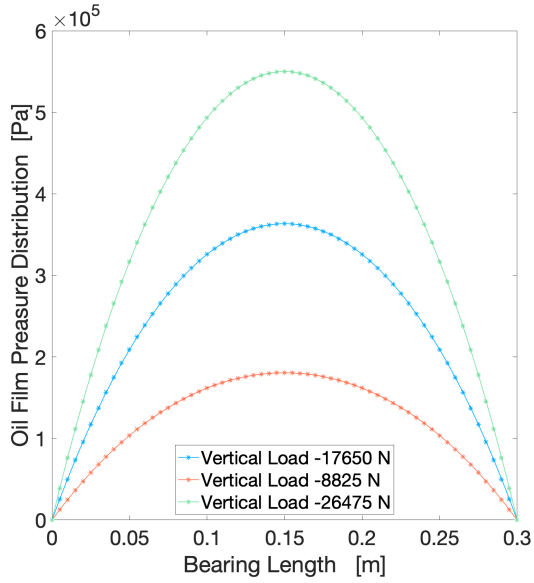

(c) Oil Lubricated Aft Bearing.

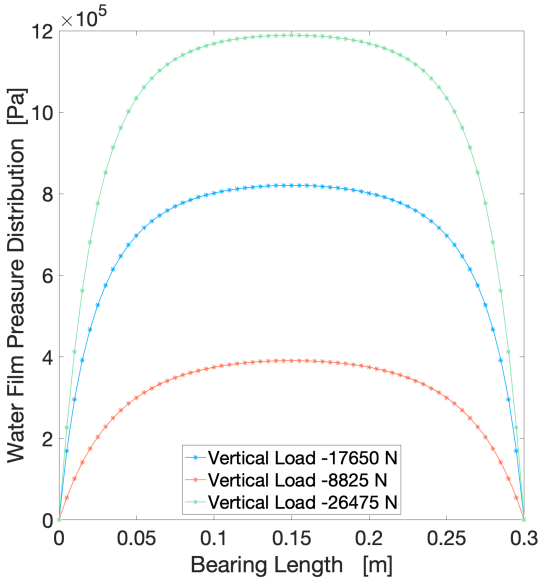

(d) Water Lubricated Aft Bearing.

Figure 36: Mid and axial planes pressure distributions of oil and water bearings under different load conditions.

The relative table of ,aximum pressure values is presented next.

Table 47: Forward stern tube bearings maximum pressure for different load conditions.

Load	Maximum pressure [Pa]			
N	Oil	%	Water	%
-8825	180577	-50.32	390964	-52.38
-17650	363503	-	820953	-
-26475	550256	+51.38	1189220	+44.86

Following are the diagrams presenting the change in the minimum film thickness and power loss under different loads.

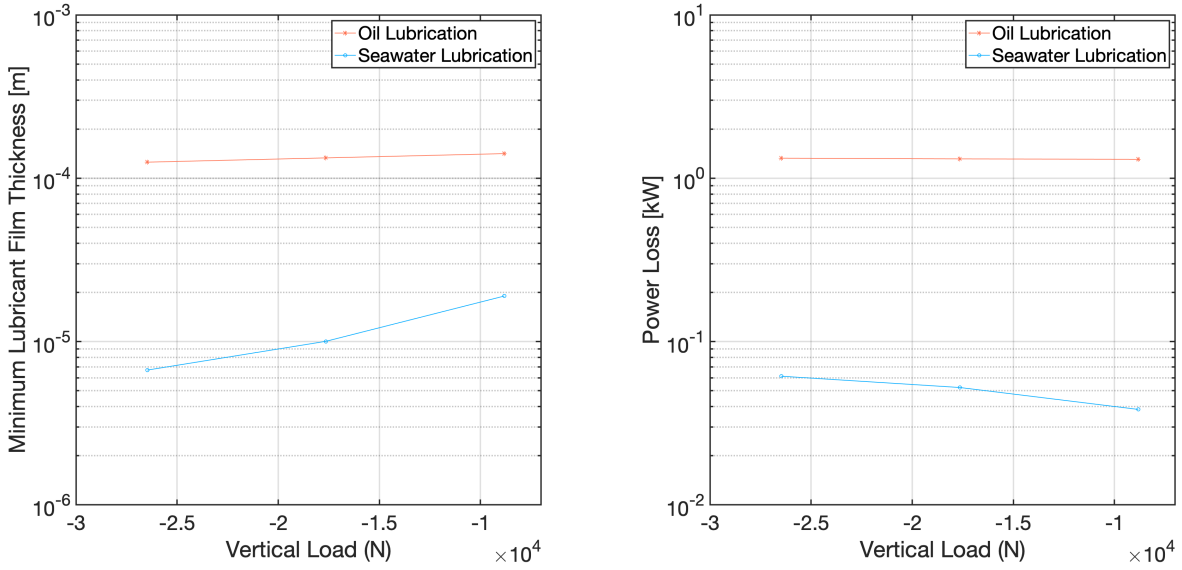

(a) Minimum film thickness.

(b) Power loss.

Figure 37: Minimum film thickness and power loss of oil and water bearings under different loads.

Finally, next are two tables presenting the relative data for the quantities presented in the above diagrams.

Table 48: Forward stern tube bearings minimum film thickness for different load conditions.

Load	Minimum film thickness [μm]			
N	Oil	%	Water	%
-8825	141.45	+6.19	18.99	+89.37
-17650	133.21	-	10.03	-
-105900	125.42	-5.84	6.69	-33.31

Table 49: Forward stern tube bearings power loss for different load conditions.

Load	Power loss [kW]			
N	Oil	%	Water	%
-8825	1.30514	-0.63	0.03841	-26.59
-17650	1.31347	-	0.05233	-
-26475	1.32657	+1.00	0.06134	17.23

6.3 Complete stern tube bearing system results and discussion

In this section, the results of the simulations carried out with variable operating parameters for both oil and water lubricated bearings are discussed. The main and relatively easier to distinguish differences between the oil and water lubricated bearings come from the investigation of the developed pressure field. Also, the film thickness field is directly correlated to the pressure. In the next table, results for the maximum pressure and the minimum film thickness, for the initial designs and nominal operational conditions of both the aft and forward bearings are presented alongside.

Table 50: Aft and Forward stern tube oil and water lubricated bearings results.

Oil lubricated bearings					
Maximum pressure [Pa]		Minimum film thickness [μm]		Power loss [kW]	
Aft	Forward	Aft	Forward	Aft	Forward
689019	363503	135.82	133.21	2.62608	1.31347
Water lubricated bearings					
Maximum pressure [Pa]		Minimum film thickness [μm]		Power loss [kW]	
Aft	Forward	Aft	Forward	Aft	Forward
1546930	820953	5.49	10.03	0.13639	0.05233

It is evident that the pressure fields developed in the water lubricated bearings are greater in absolute values than the ones in the oil lubricated. While the corresponding minimum film thicknesses show a great difference, as the water films are much more thin than the oil films. In addition, the pressure fields in the water lubricated bearings are presented with a more steep increase and decrease in the circumferential sections than those of the oil lubricated bearings. On the other hand, the corresponding forms of pressure distributions in the axial section are more uniform in the water lubricated bearings than the oil bearings. Also, the power losses caused by the operation of the water lubricated bearings are much smaller than the ones in oil bearings. These results are consistent with findings in research papers referenced in the present study.

Differences between water and oil lubricated bearings are also found in the investigation of the parametric simulations. The first parameter investigated was the shaft rotational speed. From the results and the relative diagrams, it is evident that the water lubricated are influenced relatively more. Moreover, the pressure distributions of the water bearings is decreased relatively more, while the minimum film thickness increases with a faster rate and the power loss change rates are at comparable levels. These observations are true for both the aft and the forward bearings.

Differences are also observed in the simulations corresponding to misaligned operation. It is easily observed that the small misalignment angles imposed on the bearings, influence the water lubricated stern tube bearings operation in a greater way than the oil lubricated bearings. Furthermore, the pressure distribution profiles in the axial plane show a rapid increase and shift towards one end of the bearing, these changes are much greater in the water lubricated bearings. It is evident from relative studies that, in order to produce similar results in oil lubricated bearings larger misalignment angles need to be imposed on the models. The minimum film thickness of the water lubricated bearings is also affected by the misaligned operation decreasing with a faster rate than the on the oil bearings. In regards to the power loss change rate, as the misalignment value increases a small change is shown in water lubricated bearings and a smaller one in the oil lubricated bearings, these changes can be considered almost negligible, especially in comparison to the changes of the pressure profiles and the minimum film thicknesses.

The last parameter of this comparative study involved the applied load. The difference in results for the alternative load conditions is evident in both the oil and the water lubricated bearings. Through the diagrams and the values presented in the relative tables it is evident that the maximum pressure is affected in a proportionate manner in the two kinds of bearings. The other other two main parameters investigated show differences in the operational behaviour of the two different kinds of bearings. The minimum film thickness in the oil lubricated aft and forward bearings is affected in a very limited way while the results of the water lubricated bearings show that the film thickness is greatly affected by the applied load. Again, in the oil lubricated bearings the effect on the power loss levels was limited, while in the water lubricated the changes are considered significant.

In the following last chapter of this study the conclusion is made and suggestions for future work are presented.

Conclusion and Future Work

The present Diploma Thesis constitutes a study of oil and water lubricated marine journal bearings. The necessary theoretical framework has been established through proper investigation of prevalent literature, corroborated studies and contemporary published research. The subsequent tribological analysis and comparative study was accomplished through the application of tools developed at the Machine Elements and Tribology Lab at NTUA. To achieve the goals of this thesis, proper bearing simulations have been performed. The pressure distributions developed in journal bearing models was calculated by solving the Reynolds equation, with the application of the Reynolds boundary conditions on the unwrapped bearing geometries. The Reynolds equation has been solved with the finite difference method, whereas the Winkler elastic deformation model has been successfully added to the solution algorithm, in order to account for the bearing liner deformation.

The extension of the algorithm with the plane strain hypothesis model was utilized to account for the effect of the liner deformation on the operational characteristics of the bearings. This extension is significant, since it allows to increase the accuracy of simulation results for oil lubricated journal bearings, but more importantly for water lubricated journal bearings, where the liner deformation is substantially more important. The first step was to validate the extended model and this was achieved with the use of experimental data from published studies. Conclusive simulations were carried out, and the results verified that the model can be used to produce simulations of bearing operational characteristics with sufficient accuracy. Following the validation of the model, several simulations have been performed for highlighting the effect of liner thickness and elasticity on bearing performance. Appropriate operational and design parameters were chosen for both oil and water lubricated bearings with different liner configurations, and comparisons of the pressure fields developed were illustrated. Through this analysis, it was showcased that the operation and the performance of journal bearings is substantially affected by the design of the bush liner, especially in cases of highly loaded bearings. The next step of this study was initiated following the validation and investigation of the extended model and its effects. The solution algorithm was applied to a stern tube bearing system, and an analysis was conducted on two pairs of journal bearings. These pairs included one pair of oil lubricated bearings and one pair of water lubricated bearings, each constituting the aft and forward bearings of a ship. The system design and operational parameters were determined in accordance with relevant regulations, requirements, engineering manuals of commercial makers, and actual ships. Additionally, simulations were performed for various operating conditions to obtain a comprehensive understanding of the performance of the two systems.

Probable future work may include direct extensions to the algorithm, development of tools coupled with the present models and the execution of experiments to broaden the scope of work. For example, a more expansive array of liner configurations and lubricants can be tested, coupled with a wear model to account for wear varying from small imperfections on the liner surface to extensive cracking and peeling. Another example is an extension which would assess the effect of shaft coating, when applicable, to the performance of the shafting system. Finally, completion of experimental measurements and implementation of optimization analyses could be exploited to establish optimum bearing configurations.

References

[1] J. F. Booker. Dynamically-loaded journal bearings: Numerical application of the mobility method. Journal of Lubrication Technology, 93(1):168–174, 1971.

[2] K. P. Oh and P. K. Goenka. The elastohydrodynamic solution of journal bearings under dynamic loading. Journal of Tribology, 107(3):389–394, 1985.

[3] Pantelis G. Nikolakopoulos, Christos I. Papadopoulos, and Lambros Kaiktsis. Elastohydrodynamic analysis and pareto optimization of intact, worn and misaligned journal bearings. Meccanica, 46(1):577–588, 2011.

[4] Anstassios Charitopoulos, Michel Fillon, and Christos I. Papadopoulos. Numerical investigation of parallel and quasi-parallel slider bearings operating under thermoelastohydrodynamic (tehd) regime. Tribology International, 149, 2020. 45th Leeds-Lyon Symposium on Tribology â□□Smart Tribology Systems.

[5] Evgeny Kuznetsov, Sergei Glavatskih, and Michel Fillon. Thd analysis of compliant journal bearings considering liner deformation. Tribology International, 44(1):1629–1641, 2011.

[6] Georgios N. Rossopoulos, Christos I. Papadopoulos, and Chris Leontopoulos. Tribological comparison of an optimum single and double slope design of the stern tube bearing, case study for a marine vessel. Tribology International, 150, 2020.

[7] J. W. Lund. Review of the concept of dynamic coefficients for fluid film journal bearings. Journal of Tribology, 109(1):37–41, 1987.

[8] J. W. Lund. Dynamic Coefficients for Fluid Film Journal Bearings. NATO ASI Series-Springer US, 1990.

[9] Gregory J. Kostrzewsky and Ronald D. Flack. Accuracy evaluation of experimentally derived dynamic coefficients of fluid film bearings part ii: Case studies. Tribology Transactions, 33(1):115–121, 1990.

[10] G. H. Jang, S. H. Lee, and H. W. Kim. Finite element analysis of the coupled journal and thrust bearing in a computer hard disk drive. Journal of Tribology, 128(2):335–340, 2006.

[11] J. W. Lund and K. K. Thomsen. A calculation method and data for the dynamic coefficients of oil-lubricated journal bearings. Topics in Fluid Film Bearing and Rotor Bearing System Design and Optimization, 1978.

[12] Omidreza Ebrat, Zissimos P. Mourelatos, Nickolas Vlahopoulos, and Kumar Vaidyanathank. Calculation of journal bearing dynamic characteristics including journal misalignment and bearing structural deformation. Tribology Transactions.

[13] Theotokis A. Pafelias and Czeslaw A. Broniarek. Bearing-system dynamic with general misalignment in the journal bearings. A S L E Transactions, 24(3):379–386, 1981.

[14] Pantelis G. Nikolakopoulos and Chris A. Papadopoulos. A study of friction in worn misaligned journal bearings under severe hydrodynamic lubrication. Tribology International, 41(6):461–472, 2008.

[15] K. F. Dufrane, J. W. Kannel, and R. D. Stockwell. Wear of steam-turbine journal bearings at low operating speeds. 1982.

[16] Pantelis G. Nikolakopoulos and Chris A. Papadopoulos. Wear model evaluation in misaligned journal bearings. 2009.

[17] A. Michael G. Papanikolaou, Michael G. Farmakopoulos, and Chris A. Papadopoulos. Alternation of the dynamic coefficients of short journal bearings due to wear. International Journal of Structural Integrity, 6(5):649–664, 2015.

[18] Wojciech Litwin and Artur Olszewski. Water-lubricated sintered bronze journal bearings-theoretical and experimental research. Tribology Transactions, 57:114–122, 2014.

[19] Xiuli Zhang, Zhongwei Yin, Dan Jiang, and Gengyuan Gao. Comparison of the lubrication performances of water-lubricated and oil-lubricated plain journal bearings. Applied Mechanics and Materials, 711:27–32, 2015.

[20] Gwidon W. Stachowiak and Andrew W. Batchelor. 2 - physical properties of lubricants and 3 - lubricants and their composition. In Gwidon W. Stachowiak and Andrew W. Batchelor, editors, Engineering Tribology (Third Edition), pages 11–50. Butterworth-Heinemann, third edition edition, 2006.

[21] Theo Mang. Rheology of Lubricants, chapter 3, pages 23–33. John Wiley & Sons, Ltd, 2006.

[22] Carter B.H. and Green D. Marine Lubricants. Springer, Dordrecht, 2010.

[23] Q. Jane Wang and Yip-Wah Chung, editors. Marine Engine Oils. Springer US, 2013.

[24] Phil Cumberlidge. Lubricant Types and Performance in Marine Propulsion Systems. John Wiley & Sons, 2018.

[25] Ryan Albert and Brian Rappoli. Environmentally Acceptable Lubricants. United States Environmental Protection Agency, Office of Wastewater Management Washington, DC 20460, 2011.

[26] Michael M. Khonsari E. and Richard Booser. Journal Bearings. John Wiley & Sons, Ltd, 2008.

[27] Q. Jane Wang and Yip-Wah Chung, editors. Fluid Film Bearing Materials. Springer US, 2013.

[28] Madan Pal, Ian Kerr, and John Harrison. Plain Bearings in Marine Applications. John Wiley & Sons, 2018.

[29] Q. Jane Wang and Yip-Wah Chung, editors. Hydrodynamic Bearings. Springer US, Boston, MA, 2013.

[30] Q. Jane Wang and Yip-Wah Chung, editors. Dynamic Characteristics of Fluid Film Bearings. Springer US, 2013.

[31] Lambros Kaiktsis, Christos I. Papadopoulos, and Pantelis G. Nikolakopoulos. Characterization of stiffness and damping in textured sector pad micro thrust bearings using computational fluid dynamics. Journal of Engineering for Gas Turbines and Power, 134(11), 2012.

[32] R. L. Campbell. Fluid film bearing dynamic coefficients and their application to structural finite element models. 2003.

[33] Q. Jane Wang and Yip-Wah Chung, editors. Mathematical Foundation of Fluid Lubrication Theory. Springer US, 2013.

[34] Q. Jane Wang and Yip-Wah Chung, editors. Bearing Wear. Springer US, Boston, MA, 2013.

[35] Joon Young Jang and Michael M. Khonsari. On the characteristics of misaligned journal bearings. Lubricants, 3(1):27–53, 2015.

[36] Gwidon W. Stachowiak and Andrew W. Batchelor. 4 - hydrodynamic lubrication. In Gwidon W. Stachowiak and Andrew W. Batchelor, editors, Engineering Tribology (Third Edition), pages 103–204. Butterworth-Heinemann, third edition edition, 2006.

[37] C. R. Lin and Jr. H. G. Rylander. Performance characteristics of compliant journal bearings. Journal of Tribology, 113(3):639–644, 1991.

[38] S. B. Glavatskih and Michel Fillon. Tehd analysis of thrust bearings with ptfe-faced pads. ASME/STLE 2004 International Joint Tribology Conference, pages 603–613.

[39] Matthew Cha, Evgeny Kuznetsov, and Sergei Glavatskih. A comparative linear and nonlinear dynamic analysis of compliant cylindrical journal bearings. Mechanism and Machine Theory, 64:80–92, 2013.

[40] International Association of Classification Societies. Surveys of Propeller Shafts and Tube Shafts, Unified Requirements Z21. 2015.

[41] International Association of Classification Societies. Length of aft stern bush bearing, Unified Requirements M52. 2019.

[42] Osborne Reynolds. On the theory of lubrication and its application to mr. beauchamp towerâ□□s experiments, including an experimental determination of the viscosity of olive oil. Phil. Trans. R. Soc., 177:157–234, 1886.

[43] Andras Z. Szeri. Fluid Film Lubrication Theory and Design. Cambridge University Press, 2010.

[44] Q. Jane Wang and Yip-Wah Chung, editors. Finite Difference Method fo Fluid-Film Bearings. Springer US, 2013.

[45] Leonidas Raptis. Software development for the solution of hydrodynamic lubrication problems in main bearings of marine diesel engines. Diploma Thesis, NTUA, 2014.

[46] J. Bouyer and M. Fillon. An experimental analysis of misalignment effects in hydrodynamic plain journal bearing performances. Journal of Tribology, 124, 2002.

[47] L. Costa, M. Fillon, and A. An experimental investigation of the effect of groove location and supply pressure on the thd performance of a steadily loaded journal bearing. Journal of Tribology, 122, 2000.

[48] Wojciech Litwin. Water lubricated stern tube bearings: Attempt at estimating hydrodynamic capacity. Proceedings of the ASME/STLE 2009 International Joint Tribology Conference, pages 179–181, 2009.

[49] Wojciech Litwin. Water lubricated polymer hydrodynamic bearing with full and grooved bearing bushing. ASME International Mechanical Engineering Congress and Exposition, pages 49–57, 2005.

[50] Wojciech Litwin. Influence of main design parameters of ship propeller shaft water lubricated bearings on their properties. Polish Maritime research, pages 39–45, 2010.

[51] Wartsila UK LTD. Water Lubricated Propeller Bearings Design and Procedures Maunal. 2016.

[52] Andreas Wiesman. Slow-steaming: a viable long term option? Wartsila Technical Journal, pages 49–55, 2010.